# Thermal Energy Recovery from Drinking Water Distribution Systems

## A study into microbial water quality and potential energy

Ahmad, J.I.

**DOI**
10.4233/uuid:7ba47471-dea5-43e8-a69d-6db07162bd70

**Publication date**
2022

**Document Version**
Final published version

**Citation (APA)**
Ahmad, J. I. (2022). *Thermal Energy Recovery from Drinking Water Distribution Systems: A study into microbial water quality and potential energy*. [Dissertation (TU Delft), Delft University of Technology]. https://doi.org/10.4233/uuid:7ba47471-dea5-43e8-a69d-6db07162bd70

**Important note**
To cite this publication, please use the final published version (if applicable).
Please check the document version above.

# Thermal Energy Recovery from Drinking Water Distribution Systems

A study into microbial water quality and potential energy

# Thermal Energy Recovery from Drinking Water Distribution Systems

## A study into microbial water quality and potential energy

**Proefschrift**

ter verkrijging van de graad van doctor
aan de Technische Universiteit Delft,
op gezag van de Rector Magnificus Prof.dr.ir. T.H.J.J. van der Hagen,
voorzitter van het College voor Promoties,
in het openbaar te verdedigen op
14 December 2022 om 10:00 uur

door

Jawairia Imtiaz AHMAD

Master of Science in Environmental Sciences, NUST, Pakistan

geboren te Rawalpindi, Pakistan

This dissertation has been approved by the promotors.

Composition of the doctoral committee:

| | |
|---|---|
| Rector Magnificus | Voorzitter |
| Prof. dr. ir. Jan Peter van der Hoek | Delft University of Technology, promotor |
| Prof. dr. Gertjan Medema | Delft University of Technology, promotor |
| Prof. dr. Gang Liu | Chinese Academy of Sciences, co-promotor |

Independent members:

| | |
|---|---|
| Prof. dr. Johannes S. Vrouwenvelder | KAUST, Saudi Arabia |
| Prof. dr. ir. Doris van Halem | Delft University of Technology |
| Dr. Frederik Hammes | Eawag, Switzerland |
| Dr. Emmanuelle Prest | PWNT, The Netherlands |

Reserve member:

| | |
|---|---|
| Prof. dr. ir. L.C. Rietveld | Delft University of Technology |

The work presented in this thesis has been carried out at the Delft University of Technology and was supported by Topsector Water TKI Water Technology Program (grant nr. 2015TUD003) of the Dutch Ministry of Economic Affairs and Climate Change and water utility Waternet.

Printing: Gildeprint Enschede, gildeprint.nl
Layout and design: Anna Bleeker, persoonlijkproefschrift.nl
ISBN: 978-94-6419-666-5


E-mail: jawairiaimtiaz@live.com

*To my Mother and my late Father*

## Summary

Drinking water distribution systems (DWDSs) are intended to supply hygienically safe and biostable water for human consumption. To supply aesthetically pleasant drinking water at the customers tap, water treatment and supply requires energy for production and distribution purposes (e.g. overall between 0.47 kWh/$m^3$ in the Netherlands). On the other hand, DWDSs also contain thermal energy as a surplus of cold or heat. Depending on the drinking water temperature within the distribution network, thermal energy can either be used for heating or cooling purposes. Thermal energy recovery potential from drinking water has been explored recently. Cold thermal energy recovery from drinking water (TED) can provide cooling for buildings and spaces with high cooling requirements as an alternative for traditional cooling and thus TED helps reduce in greenhouse gas (GHG) emissions.

The effects of increased water temperature induced by TED on the drinking water quality and biofilm development within DWDSs are not yet known. Hence this thesis was initiated with the objective to investigate the effects of TED on microbial water quality and biofilm development within DWDSs. The first part of this thesis investigated the impacts of TED at 25 °C on microbiological drinking water quality, using pilot distribution systems. The first study revealed that the water temperature increased to 25°C in a pilot distribution system as a result of cold recovery does not affect the bacterial water quality in the drinking water phase. However, it does affect the concentration and community composition of biofilms (Chapter 2). Hence, in the second part of this thesis, the effect of TED on biofilm was investigated extensively. In pilot scale distribution systems, both water and biofilm phases were studied with water temperatures increased to 25 °C and 30 °C after TED. It was concluded that the timeline for biofilm microbial development was influenced by temperature: the higher the temperature, the faster the microbial development of a biofilm took place. Simultaneously, higher biomass activity (ATP and cell concentration) was also observed in the water phase. In the biofilm phase, the initial faster microbial development did not lead to differences in microbial diversity and composition at the end of the experimental period (Chapter 3).

Similarly, biofilm development after TED at 25 °C followed for a long period of time, 99 weeks, showed that instantaneous increase in water temperature influenced the early stages of biofilm development. High temperature initiates faster growth of primary colonizers (*Betaproteobacteriales*, *Sphingomonadaceae*) (Chapter 4). Both studies univocally showed that as a result of constantly stable increased water temperature after TED, biofilms reached to a steady phase faster when compared to fluctuating drinking water temperatures in reference and control systems (Chapter 3 and 4).

After studying the microbial water quality in unchlorinated drinking water distribution systems for both water and biofilm phases, initial investigation of TED application within chlorinated networks was also performed. Compared with unchlorinated DWDSs, here chlorine dramatically reduced the biofilm biomass growth, and raised the relative abundances of the chlorine-resistant genera (i.e. *Pseudomonas* and *Sphingomonas*) in bacterial communities. As a result of TED, no

significant effects were observed on chlorine decay, microbial water quality and biofilm composition during the experimental period (Chapter 5).

After extensively studying the changes in the microbial drinking water quality as a result of TED, the last part of this thesis was carried out to determine what raising the maximum temperature limit ($T_{max}$) after recovery of cold would entail in terms of energy savings, GHG emission reduction and water temperature dynamics during water transport. A full-scale TED system was used as a benchmark, where $T_{max}$ is currently set at 15 °C. By raising $T_{max}$ to 20, 25 and 30 °C, the retrievable cooling energy and GHG emission reduction could be increased by 250, 425 and 600%, respectively. The drinking water temperature model predicted that within a distance of 4 km after TED, water temperature resembles that of the surrounding subsurface soil. Hence, a higher $T_{max}$ will substantially increase the TED potential of DWDSs while keeping the same comfort level at the customer's tap (Chapter 6).

All of these observations indicate that increasing $T_{max}$ up to 25-30 °C in TED can be safe in terms of microbiological drinking water quality. However, this is specifically the case for unchlorinated DWDSs with microbiologically stable water (AOC <10 ug C/L). More insight is required in terms of microbiological assessment of TED to further explore the potential within chlorinated systems. Further research on the effects of cold recovery on DWDSs already in operation is highly recommended. In order to get better insight on response of already developed biofilm towards increase in temperature after TED. Moreover, specific opportunistic pathogens that are sensitive to temperature increase, should be investigated thoroughly in order to provide hygienically safe water after recovery of cold from both chlorinated and unchlorinated drinking water distribution systems.

# Table of content

Chapter 1

# Introduction

## 1.1 Climate change and greenhouse gas emissions

Climate change is raising the temperature of the planet earth and results in changes in the global temperature, and consequently has impacts on global weather patterns (Pachauri and Reisinger, 2008; Solomon, 2007). In the past centuries, the exponential growth in human population and utilization of non-renewable resources and energy, led to environmental degradation (Stocker et al., 2013). In 19$^{th}$ and 20$^{th}$ century, the fossil fuels were excessively utilized to achieve economic growth and development, which caused emission of greenhouse gases (GHG) into the atmosphere. In late 20$^{th}$ century, concerns were raised for global climate change as a result of GHG emissions from anthropogenic activities. Climate change has caused huge loss and damage to both built and natural environments (Karlsson-Vinkhuyzen et al., 2017; Wesselink and Deng, 2009). There are even impacts which cannot be reversed, like extinction of animal and plant species, loss of animals and natural habitats (Solomon, 2007; Stocker et al., 2013). Now, mankind is trying to stop these catastrophes, by taking sustainable actions and mitigation measures that can help to maintain an equilibrium where both nature and mankind can survive together and to slow down the global rise in temperature.

For this reason, in 2015 the United Nations General Assembly adopted the sustainable development agenda. It contains seventeen specific Sustainable Development Goals (SDGs) to be achieved by the year 2030. The seventeen SDGs are addressing a broad range of topics, among which climate action and sustainable cities are also included (United Nations, 2019). Also in 2015, the Paris Climate Agreement was signed by the UN member countries, for limiting the global temperature rise well below 2$^{o}$C by the year 2030 (Karlsson-Vinkhuyzen et al., 2018). In accordance with the Paris Climate Agreement the signatory countries set their own national commitments to reduce the national GHG emissions. Furthermore, at the end of 2019 the European Union (EU) has set its own action plan, in the form of the European Green Deal, to combat climate change and to achieve a more sustainable and energy efficient EU with zero net GHG emissions by the end of 2050 (Sikora, 2021).

To achieve the objectives of above mentioned agreements and deals (Table 1.1), many countries have set and implemented their national level targets and policies and made action plans to combat climate change and integrate sustainable solutions to achieve the goal of GHG emission reductions (Blok et al., 2020; Wesselink and Deng, 2009). As a member country of the UN and EU, the Netherlands is also a signatory of both the Paris Climate Agreement and the EU Green Deal. At the national level, the Netherlands is committed to reduce its GHG emissions up to 49% by 2030 and wants to achieve 95% reduction in its GHG emissions by 2050, both compared to the 1990 level of GHG emissions. Based on this the Netherlands drafted its own national climate agreement plan in 2019. According to this plan less dependence on fossil fuels for energy production and efficient use of energy in the built environment are two important strategies (Heerema, 2020; Spier, 2020). Considering the mitigation measures needed to combat climate change, apart from the national action plan in the Netherlands, the drinking water utilities and regional water authorities are aiming at becoming carbon neutral by optimizing their processes for drinking water production

and wastewater treatment and using energy resources efficiently (Reinder Brolsma, 2013; van der Hoek, 2011; van der Hoek, 2012a; Van der Hoek et al., 2018).

*Table 1.1: International and national agreements to combat climate change and reduce GHG emissions.*

| Year | Agreement | Targets |
|---|---|---|
| 2015 | Sustainable Development Goals (SDGs)-Worldwide | 17 SDGs to be achieved by 2030, climate action and sustainable cities are two of the targets |
| 2015 | Paris Climate Agreement-Worldwide | Limit the global temperature rise well below 2°C by 2030 |
| 2019 | European Green Deal-EU level | Achieve a more sustainable and energy efficient EU with zero net GHG emissions by the end of 2050 |
| 2019 | National Climate agreement plan of the Netherlands- National level | Compared to 1990 level of national GHG emissions:<br>49% GHG emission reduction by 2030<br>95% GHG emission reduction by 2050 |



## 1.2 Thermal energy recovery from the urban water cycle in the Netherlands

To reduce the GHG emissions, one of the mitigation measures is to harness more renewable energy resources to meet the energy needs (Rogelj et al., 2018). In the past decades renewable energy resources like hydropower, solar power, tidal energy, geothermal energy and wind power (Pachauri et al., 2014; Stocker et al., 2013) were widely harnessed and used but more recently urban water is also being explored and utilized for resource recovery (Jimenez Cisneros et al., 2014). Resource recovery from the urban water cycle is gaining much attention. The focus is much on materials from wastewater, such as nutrients, carbon, water itself, but also energy in the form of biogas (Li et al., 2015; van der Hoek et al., 2016). Resource recovery from drinking water has also been described and is applied in practice, e.g., the recovery of calcite from the pellet softening process in drinking water treatment (Schetters et al., 2014). A new approach is thermal energy recovery from the urban water cycle in the form of heat and cold. It has been shown that this has a high potential (Katja Kruit, 2018; van der Hoek et al., 2013)

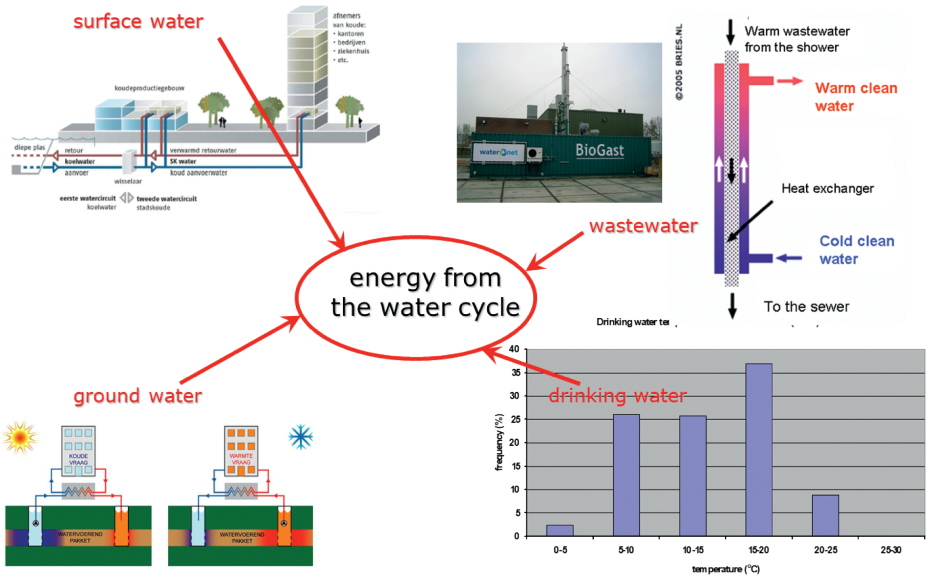


**Figure 1.1:** *Potential sources of thermal energy recovery from the urban water cycle (Van der Hoek et al., 2018).*

The potential sources of energy recovery from the urban water cycle are wastewater, surface water, groundwater and drinking water (Figure 1.1). In the Netherlands, the potential of thermal energy recovery from the water cycle has been estimated (Katja Kruit, 2018; van der Hoek, 2012a; van der Hoek et al., 2015). For surface water the potential is 150 PJ/year, for wastewater 56 PJ/year and for drinking water 4-6 PJ/year. Although resource recovery from the urban water cycle, including thermal energy, is gaining a lot of attention these days, at the same time it is stressed that more research is needed into environmental assessments of thermal energy recovery systems (Diaz-Elsayed et al., 2020).

### 1.2.1 Thermal energy recovery from drinking water

A specific source of thermal energy appeared to be drinking water in the drinking water distribution networks (Ahmad et al., 2020). While drinking water treatment and supply requires energy for production and distribution purposes (e.g. overall between 0.47 kWh/m$^3$ in the Netherlands) (Frijns, 2012), the drinking water distribution systems also contain thermal energy as a surplus of cold or heat. Depending on the drinking water temperature in the network, it can be used either for heating or cooling purposes. For example, in Amsterdam the temperature within the drinking water distribution network (DWDN) is between 4-10°C in winter and between 15-20°C in summer (van der Hoek, 2012b). These temperatures offer possibilities to recover cold during winter time and heat during summer time.

A specific application is the recovery of cold from drinking water for cooling purposes. By use of a heat exchanger in a drinking water main, or in a by-pass, drinking water exchanges its cold with a warm carrier medium (e.g. air, water, glycol, etc.) inside the heat exchanger and slightly heated water flows back into the DWDN (Blokker et al., 2013; van der Hoek, 2012b; van der Hoek et al., 2017). This cold temperature recovery from DWDNs, mostly available during winter time with

low drinking water temperatures, is scarcely available during times of high cooling demand (i.e., during summer with high drinking water temperatures). An option to overcome this hurdle is to recover and store the low temperature in aquifer thermal energy storage (ATES) systems for later use in summer. During winter the recovered thermal energy can also be utilized directly without intermediate storage as free available cooling (Figure 1.2).

According to a previous study, the theoretical potential of cold recovery from drinking water for the city of Amsterdam is around 2800 TJ/year while the energy required for space cooling for non-residential buildings in Amsterdam is estimated to be around 2161 TJ/year (Mol et al., 2011; Van der Hoek et al., 2018). In principle DWDSs harbour enough cooling capacity that could be recovered for cooling purpose.



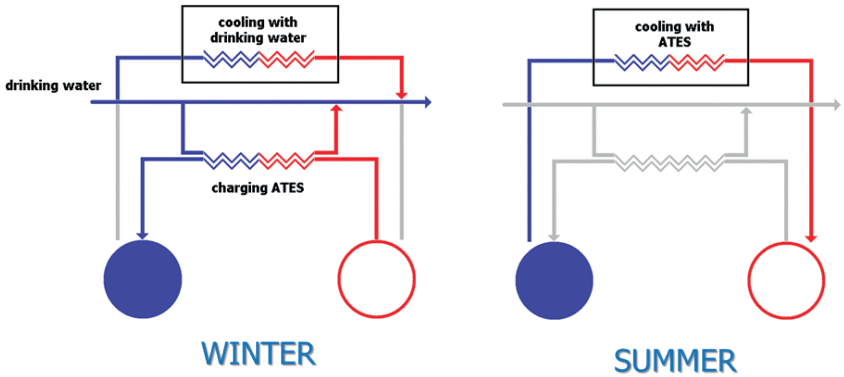


**Figure 1.2:** *Cold drinking water in wintertime (left) is directly utilized in winter periods for places with extensive cooling requirements or is used for charging an aquifer thermal energy storage system (ATES) to provide space cooling in upcoming summer periods (right) (Van der Hoek et al., 2018).*

In the European Union from the 90's till 2010 the use of central and room air conditioning units for space cooling has been increased by a factor 50 (Adnot, 2003.; Isaac and Van Vuuren, 2009). Providing this energy with traditional cooling methods (i.e. mechanical cooling or cooling towers) requires an intensive amount of electricity and water. Hence, there is a need to explore more sustainable cooling resources in order to reduce GHG emission and to achieve the goal of energy efficient buildings, under the EU Green Deal. This means that also for other European countries the use of drinking water for cooling purposes seems very interesting.

The idea to utilize DWDNs as cooling resource is quite new and is not yet explored. The reason lies in the fact that DWDNs are primarily used to deliver safe and healthy drinking water at the customers' tap and were not thought of as an energy resource. The required changes at the design and operational level within DWDNs, for thermal energy recovery, may pose microbial risks to drinking water quality, especially when cold is recovered which results in an increased drinking water temperature after the energy exchange process (van der Hoek, 2011). Also, the acceptable maximum temperature after cold recovery ($T_{max}$) is dependent on the allowed temperature for drinking water at the customer's tap in the Netherlands, which is 25°C (Staatscourant, 2011).

## 1.3 Drinking Water Distribution Systems

Drinking water supply requires raw water abstraction and treatment, followed by storage, transport and distribution of finished water. The water treatment processes are selected and adopted to purify water for drinking purposes based on the quality of the incoming water and the quality standards of the drinking water to comply with (Elías-Maxil et al., 2014; van der Hoek, 2012b). Further, the produced drinking water is distributed through extended drinking water transport and distribution systems (Prest et al., 2016a; van der Kooij and van der Wielen, 2014).

Each DWDS has its own distinctive micro-environment, where the biological stability of drinking water is maintained either by limiting nutrient concentrations (El-Chakhtoura et al., 2015; Prest et al., 2016b; Van der Kooij, 1992; Van der Kooij and Van der Wielen, 2013) or by maintaining a residual disinfectant during transport and distribution (McCoy and VanBriesen, 2012; Potgieter et al., 2018). Inside the DWDSs, loose deposits (Liu et al., 2014), suspended solids (Liu et al., 2013), water phase microbial communities (Prest et al., 2016a; Prest et al., 2016b) and biofilm microbial communities (the layer of microbes attached to the inside of the pipes) (Fish et al., 2016) are present. Biofilm and water phase contain the dominant part of the biomass (more than 80%) (Liu et al., 2017) within DWDSs.

The microbiological characteristics of the DWDNs have been studied widely and thoroughly both for chlorinated (Douterelo et al., 2013; Potgieter et al., 2018) and unchlorinated systems (Prest et al., 2016b; Vital et al., 2012). It is known that temperature is a crucial environmental factor for microbial growth and community dynamics (Kelly et al., 2014; Rogers et al., 1994). Especially, growth of biofilms (Diaz Villanueva et al., 2011), proliferation of opportunistic pathogens (which can cause diseases in people with compromised immune systems, like infants, elderly people and already sick people), like several *Pseudomonas spp*. and *Legionella spp*. (Van Der Wende et al., 1989; van der Wielen et al., 2013; Van der Wielen and Van der Kooij, 2013; Wingender and Flemming, 2011), occurrence of discolored water (Zhou et al., 2017) and sudden changes in microbial water quality parameters (like ATP and cell concentration) (Potgieter et al., 2018; Prest et al., 2016b) are linked with temperature changes.

It is also known that opportunistic pathogens (e.g. *Legionella pneumophila*, *Pseudomonas aeruginosa*, *Mycobacterium avium* complex and *Stenotrophomonas maltophilia*) could occur at temperatures above 25 °C (Tsao et al., 2019; van der Wielen et al., 2013) and biofilm growth could be accelerated at high temperatures (Boe-Hansen et al., 2002; Fish et al., 2016; Flemming and Wingender, 2010). Development of biofilms at different temperatures has not yet been studied inside DWDSs, but a study on river water has reported an acceleration of microbial colonization at higher temperatures (Diaz Villanueva et al., 2011).

Along with the growth and proliferation of opportunistic pathogens, the development and growth of the biofilms within DWDSs at high temperature should also be studied dynamically over time to trace changes during their formation, as biofilms are the micro-environments which are the

long-term residents (from days to decades) and are also thought to be the host for opportunistic pathogens within DWDSs (Flemming et al., 2016; Henne et al., 2012; Van Der Wende et al., 1989).

## 1.4 Research objectives and research questions

The impacts of sudden changes in temperature, within DWDNs, on overall microbial water quality and the development of biofilms have not been studied so far. It is assumed that cold recovery with subsequent sudden increase in the drinking water temperature might affect both the water and biofilm phases within DWDNs. For this reason, it is highly important to thoroughly investigate the effects of cold recovery on microbial water quality and biofilm characteristics in order to understand the impacts and risks of this proposed application in more detail before its full scale and wider application. Specially, the influence of increased temperature on proliferation of opportunistic pathogens, biofilm development over period of time and on microbial water quality parameters need attention.



Hence, this thesis was initiated with the objective to evaluate the potential effects of cold recovery on the microbial drinking water quality and to determine a temperature limit after cold recovery ($T_{max}$), that will allow for maximum cold recovery without compromising the drinking water quality. Based on the determined $T_{max}$ the amount of potential thermal (cold) energy and the subsequent carbon footprint savings will be evaluated.

The specific research questions were:

i) What are the changes in microbial drinking water quality within unchlorinated DWDSs due to a sudden increase in drinking water temperature after cold recovery?

ii) How does an instantaneous increase in drinking water temperature, as a result of cold recovery, affects the biofilm development within unchlorinated DWDSs?

iii) How does cold recovery affect the drinking water quality and biofilm development within chlorinated DWDSs?

iv) What is the maximum allowable temperature after cold recovery, that will not trigger the regrowth or proliferation of opportunistic pathogens within DWDSs, and what is the potential of energy recovery and the carbon footprint reductions by recovering cold from drinking water?

## 1.5 Research approach

To answer the above-mentioned research questions, pilot scale unchlorinated drinking water distribution systems were designed and operated at two different locations supplying microbiologically stable feed water, in Delft (AOC ≥ 2 µg C/L) and in Leiduin (AOC ≤ 2 µg C/L), the Netherlands. Two different temperatures after cold recovery, 25 °C and 30 °C, were studied. The reason for choosing these two temperatures lies in the fact that the former is the maximum limit for the drinking water temperature at the customers' tap in the Netherlands (Smeets et al., 2009; Staatscourant, 2011). In case no changes are observed at 25 °C, a temperature of 30 °C will significantly enhance the potential of cold recovery. Despite the fact that by Dutch law it is not allowed, the higher temperature was chosen as an extreme case for research purposes.

Based on this research and chosen temperature limits after cold recovery of 15 and 30 °C a desk research was conducted to determine the potential of energy recovery. Further, the drinking water temperature within DWDNs after cold recovery was modelled to determine the distance at which the water temperature becomes equivalent to the surrounding soil temperature before it reaches the customers' tap. In an additional study, also the effects of cold recovery in a chlorinated pilot scale distribution system was examined.

## 1.6 Thesis Outline

Following this introduction chapter, the research is described in five chapters. The last chapter 7 provides the overall outcomes of this thesis, including conclusions and future recommendations for applying cold recovery technology within DWDSs.

**Chapter 2** investigates how cold recovery after $T_{max}$ of 25 °C affects the drinking water quality parameters and growth of opportunistic pathogens in unchlorinated DWDSs.

**Chapter 3** describes the influence of $T_{max}$ of 25°C and 30°C on the microbiome of unchlorinated drinking water using drinking water with a very low AOC concentration (<2 μg C/l).

**Chapter 4** explores the effects of increased drinking water temperature after cold recovery (up to 25°C) on long term biofilm development.

**Chapter 5** studies the effects of cold recovery ($T_{max}$ 25 °C), on chlorine decay and microbial drinking water characteristics in chlorinated DWDSs.

**Chapter 6** explores the thermal energy recovery potential and GHG reduction potential of drinking water in a specific case based on a maximum temperature limit ($T_{max}$) after cold recovery of 15, 20, 25 and 30 °C, and the balancing of the drinking water temperature after cold recovery with the soil temperature.

**Chapter 7** describes the outcomes of this thesis in accordance with each of the four-research question mentioned in section 1.4. This chapter also provides the conclusions based on the outcomes of the thesis and gives an outlook for cold recovery applications in both unchlorinated and chlorinated drinking water distribution systems.

## References


Adnot, J. (2003) Energy Efficiency and Certification of Central Air Conditioners (EECCAC), Armines, Paris, France.

Ahmad, J.I., Liu, G., Van der Wielen, P.W.J.J., Medema, G. and Van der Hoek, J.P. (2020) Effects of cold recovery technology on the microbial drinking water quality in unchlorinated distribution systems. Environmental Research 183, 109175.

Blok, K., Afanador, A., van der Hoorn, I., Berg, T., Edelenbosch, O.Y. and van Vuuren, D.P. (2020) Assessment of Sectoral Greenhouse Gas Emission Reduction Potentials for 2030. Energies 13(4), 943.

Blokker, E.J.M., van Osch, A.M., Hogeveen, R. and Mudde, C. (2013) Thermal energy from drinking water and cost benefit analysis for an entire city. Journal of Water and Climate Change 4(1), 11-16.

Boe-Hansen, R., Albrechtsen, H.J., Arvin, E. and Jørgensen, C. (2002) Bulk water phase and biofilm growth in drinking water at low nutrient conditions. Water Research 36(18), 4477-4486.

Diaz Villanueva, V., Font, J., Schwartz, T. and Romani, A.M. (2011) Biofilm formation at warming temperature: acceleration of microbial colonization and microbial interactive effects. Biofouling 27(1), 59-71.

Diaz-Elsayed, N., Rezaei, N., Ndiaye, A. and Zhang, Q. (2020) Trends in the environmental and economic sustainability of wastewater-based resource recovery: A review. Journal of Cleaner Production 265, 121598.

Douterelo, I., Sharpe, R. and Boxall, J. (2013) Influence of hydraulic regimes on bacterial community structure and composition in an experimental drinking water distribution system. Water Research 47(2), 503-516.

El-Chakhtoura, J., Prest, E., Saikaly, P., Van Loosdrecht, M., Hammes, F. and Vrouwenvelder, H. (2015) Dynamics of bacterial communities before and after distribution in a full-scale drinking water network. Water Research 74, 180-190.

Elías-Maxil, J.A., van der Hoek, J.P., Hofman, J. and Rietveld, L. (2014) Energy in the urban water cycle: Actions to reduce the total expenditure of fossil fuels with emphasis on heat reclamation from urban water. Renewable and Sustainable Energy Reviews 30, 808-820.

Fish, K.E., Osborn, A.M. and Boxall, J. (2016) Characterising and understanding the impact of microbial biofilms and the extracellular polymeric substance (EPS) matrix in drinking water distribution systems. Environmental science: water research & technology 2(4), 614-630.

Flemming, H.-C. and Wingender, J. (2010) The biofilm matrix. Nature Reviews Microbiology 8(9), 623-633.

Flemming, H.-C., Wingender, J., Szewzyk, U., Steinberg, P., Rice, S.A. and Kjelleberg, S. (2016) Biofilms: an emergent form of bacterial life. Nature Reviews Microbiology 14, 563.

Frijns, J. (2012) Towards a common carbon footprint assessment methodology for the water sector. Water and Environment Journal 26(1), 63-69.

Heerema, K. (2020) Implementing International Climate Treaties into Dutch National Policy : a model-guided analysis on climate policy implementation in the Netherlands.

Henne, K., Kahlisch, L., Brettar, I. and Hofle, M.G. (2012) Analysis of structure and composition of bacterial core communities in mature drinking water biofilms and bulk water of a citywide network in Germany. Applied and environmental microbiology 78(10), 3530-3538.

Isaac, M. and Van Vuuren, D.P. (2009) Modeling global residential sector energy demand for heating and air conditioning in the context of climate change. Energy policy 37(2), 507-521.

Jimenez Cisneros, B.E., Oki, T., Arnell, N.W., Benito, G., Cogley, J.G., Doll, P., Jiang, T. and Mwakalila, S.S. (2014) Freshwater resources.

Karlsson-Vinkhuyzen, S., Kok, M.T.J., Visseren-Hamakers, I.J. and Termeer, C.J.A.M. (2017) Mainstreaming biodiversity in economic sectors: An analytical framework. Biological Conservation 210, 145-156.

Karlsson-Vinkhuyzen, S.I., Groff, M., Tamás, P.A., Dahl, A.L., Harder, M. and Hassall, G. (2018) Entry into force and then? The Paris agreement and state accountability. Climate Policy 18(5), 593-599.

Katja Kruit, B.S., Ronald Roosjen, Pascal Boderie (2018) Nationaal potentieel van aquathermie: Analyse en review van de mogelijkheden, p. 30, CE Delft, Delft.

Kelly, J.J., Minalt, N., Culotti, A., Pryor, M. and Packman, A. (2014) Temporal Variations in the Abundance and Composition of Biofilm Communities Colonizing Drinking Water Distribution Pipes. Public Library of Science 9(5), e98542.

Li, W.W., Yu, H.Q. and Rittmann, B.E. (2015) Chemistry: Reuse water pollutants. Nature 528(7580), 29-31.

Liu, G., Bakker, G.L., Li, S., Vreeburg, J.H.G., Verberk, J.Q.J.C., Medema, G.J., Liu, W.T. and Van Dijk, J.C. (2014) Pyrosequencing Reveals Bacterial Communities in Unchlorinated Drinking Water Distribution System: An Integral Study of Bulk Water, Suspended Solids, Loose Deposits, and Pipe Wall Biofilm. Environmental science & technology 48(10), 5467-5476.

Liu, G., Tao, Y., Zhang, Y., Lut, M., Knibbe, W.-J., Van der Wielen, P., Liu, W., Medema, G. and Van der Meer, W. (2017) Hotspots for selected metal elements and microbes accumulation and the corresponding water quality deterioration potential in an unchlorinated drinking water distribution system. Water Research 124, 435-445.

Liu, G., Verberk, J.Q.J.C. and Dijk, J.C. (2013) Bacteriology of drinking water distribution systems: an integral and multidimensional review. Applied Microbiology and Biotechnology 97(21), 9265-9276.

McCoy, S.T. and VanBriesen, J.M. (2012) Temporal variability of bacterial diversity in a chlorinated drinking water distribution system. Journal of Environmental Engineering 138(7), 786-795.

Mol, S., Kornman, J., Kerpershoek, A. and Van Der Helm, A. (2011) Opportunities for public water utilities in the market of energy from water. Water Science & Technology 63(12).

Pachauri, R.K., Allen, M., Barros, V., Broome, J., Cramer, W., Christ, R., Church, J., Clarke, L., Dahe, Q. and Dasgupta, P. (2014) Climate Change 2014: Synthesis Report. Contribution of Working Groups I, II and III to the Fifth Assessment Report of the Intergovernmental Panel on Climate Change.

Pachauri, R.K. and Reisinger, A. (2008) Climate change 2007. Synthesis report. Contribution of Working Groups I, II and III to the fourth assessment report, IPCC, Geneva (Switzerland); Intergovernmental Panel on Climate Change, Geneva (Switzerland).

Potgieter, S., Pinto, A., Sigudu, M., Du Preez, H., Ncube, E. and Venter, S. (2018) Long-term spatial and temporal microbial community dynamics in a large-scale drinking water distribution system with multiple disinfectant regimes. Water Research 139, 406-419.

Prest, E.I., Hammes, F., Van Loosdrecht, M.C.M. and Vrouwenvelder, J.S. (2016a) Biological Stability of Drinking Water: Controlling Factors, Methods, and Challenges. Frontiers in Microbiology 7, 45.

Prest, E.I., Weissbrodt, D.G., Hammes, F., van Loosdrecht, M.C.M. and Vrouwenvelder, J.S. (2016b) Long-Term Bacterial Dynamics in a Full-Scale Drinking Water Distribution System. Public Library of Science 11(10), e0164445.

Reinder Brolsma, B., P., Graaff, M. de, Bonte, M., Brand, R., Wit, J. de, Hofman, J. (2013) Combining water and energy supply, Deltares,.

Rogelj, J., Shindell, D., Jiang, K., Fifita, S., Forster, P., Ginzburg, V., Handa, C., Kheshgi, H., Kobayashi, S., Kriegler, E., Mundaca, L., Séférian, R., Vilarino, M.V., Calvin, K., de Oliveira de Portugal Pereira, J.C., Edelenbosch, O., Emmerling, J., Fuss, S., Gasser, T., Gillett, N., He, C., Hertwich, E., Höglund-Isaksson, L., Huppmann, D., Luderer, G., Markandya, A., Meinshausen, M., McCollum, D., Millar, R., Popp, A., Purohit, P., Riahi, K., Ribes, A., Saunders, H., Schädel, C., Smith, C., Smith, P., Trutnevyte, E., Xu, Y., Zhou, W. and Zickfeld, K. (2018) IPCC Special Report. Masson-Delmotte, V., Zhai, P., Pörtner, H.O., Roberts, D., Skea, J., Shukla, P.R., Pirani, A., Moufouma-Okia, W., Péan, C., Pidcock, R., Connors, S., Matthews, J.B.R., Chen, Y., Zhou, X., Gomis, M.I., Lonnoy, E., Maycock, T., Tignor, M. and Waterfield, T. (eds), pp. 93 - 174, Intergovernmental Panel on Climate Change (IPCC), Geneva.

Rogers, J., Dowsett, A.B., Dennis, P.J., Lee, J.V. and Keevil, C.W. (1994) Influence of temperature and plumbing material selection on biofilm formation and growth of Legionella pneumophila in a model potable water system containing complex microbial flora. Applied and environmental microbiology 60.

Schetters, M.J.A., van der Hoek, J.P., Kramer, O.J.I., Kors, L.J., Palmen, L.J., Hofs, B. and Koppers, H. (2014) Circular economy in drinking water treatment: reuse of ground pellets as seeding material in the pellet softening process. Water Science and Technology 71(4), 479-486.

Sikora, A. (2021) European Green Deal – legal and financial challenges of the climate change. ERA Forum 21(4), 681-697.

Smeets, P., Medema, G. and Van Dijk, J. (2009) The Dutch secret: how to provide safe drinking water without chlorine in the Netherlands. Drinking Water Engineering and Science 2(1), 1-14.

Solomon, S. (2007) Climate change 2007-the physical science basis: Working group I contribution to the fourth assessment report of the IPCC, Cambridge University Press.

Spier, J. (2020) 'The "Strongest" Climate Ruling Yet': The Dutch Supreme Court's Urgenda Judgment. Netherlands International Law Review 67(2), 319-391.

Staatscourant (2011) Staatscourant (State Journal in Dutch) 2011 Decree of 23 May 2011 concerning the regulations for the production and distribution of drinking water and the organisation of the public drinking water supply.The Netherlands

Stocker, T., Qin, D., Plattner, G., Tignor, M., Allen, S., Boschung, J., Nauels, A. and Xia, Y. (2013) IPCC, 2013: summary for policymakers in climate change 2013: the physical science basis, contribution of working group I to the fifth assessment report of the intergovernmental panel on climate change, Cambridge University Press, Cambridge, New York, USA.

Tsao, H.-F., Scheikl, U., Herbold, C., Indra, A., Walochnik, J. and Horn, M. (2019) The cooling tower water microbiota: Seasonal dynamics and co-occurrence of bacterial and protist phylotypes. Water Research 159, 464-479.

United Nations. (2019) The Sustainable Development Goals Report 2019, United Nations.

van der Hoek, J. (2011) Energy from the water cycle: a promising combination to operate climate neutral. Water Practice and Technology 6(2), wpt2011019.

van der Hoek, J.P. (2012a) Climate change mitigation by recovery of energy from the water cycle: a new challenge for water management. Water Science and Technology 65(1), 135-141.

van der Hoek, J.P. (2012b) Towards a climate neutral water cycle. Journal of Water and Climate Change 3(3), 163-170.

van der Hoek, J.P., Hartog, P. and Jacobs, E. (2013) Coping with climate change in Amsterdam – a watercycle perspective. Journal of Water and Climate Change 5(1), 61-69.

van der Hoek, J.P., Mol, S., Janse, T., Klaversma, E. and Kappelhof, J. (2015) Selection and prioritization of mitigation measures to realize climate neutral operation of a water cycle company. Journal of Water and Climate Change 7(1), 29-38.

van der Hoek, J.P., de Fooij, H. and Struker, A. (2016) Wastewater as a resource: Strategies to recover resources from Amsterdam's wastewater. Resources, Conservation and Recycling 113, 53-64.

van der Hoek, J.P., Mol, S., Ahmad, J.I., Liu , G. and Medema, G. (2017) Thermal energy recovery from drinking water. J. Krope, A.G.O., D. Goričanec, S. Božičnik, eds (ed), pp. 23-32, University of Maribor Press, Bled, Slovenia.

van der Hoek, J.P., Mol, S., Giorgi, S., Ahmad, J.I., Liu, G. and Medema, G. (2018) Energy recovery from the water cycle: Thermal energy from drinking water. Energy 162, 977-987.

van der Kooij, D. (1992) Assimilable organic carbon as an indicator of bacterial regrowth. Journal of American Water Works Association 84(2), 57-65.

van der Kooij, D. and Van der Wielen, P.W. (2013) Microbial growth in drinking-water supplies: problems, causes, control and research needs. Water Intelligence Online 12, 9781780400419.

van der Kooij, D. and van der Wielen, P.W.J.J. (2014) Microbial growth in drinking-water supplies: problems, causes, control and research needs. van der Kooij, D. and van der Wielen, P.W.J.J. (eds), pp. 1-20, IWA Publishing, London, UK.

van Der Wende, E., Characklis, W.G. and Smith, D.B. (1989) Biofilms and bacterial drinking water quality. Water Research 23(10), 1313-1322.

van der Wielen, P.W.J.J., Italiaander, R., Wullings, B.A., Heijnen, L. and van der Kooij, D. (2013) Microbial Growth in Drinking-Water Supplies. Problems, Causes, Control and Research Needs. van der Kooij, D. and van der Wielen, P.W.J.J. (eds), pp. 177-205, IWA Publishing, London, UK.

van der Wielen, P.W.J.J. and Van der Kooij, D. (2013) Nontuberculous mycobacteria, fungi, and opportunistic pathogens in unchlorinated drinking water in The Netherlands. Applied and environmental microbiology 79.

Vital, M., Dignum, M., Magic-Knezev, A., Ross, P., Rietveld, L. and Hammes, F. (2012) Flow cytometry and adenosine tri-phosphate analysis: Alternative possibilities to evaluate major bacteriological changes in drinking water treatment and distribution systems. Water Research 46(15), 4665-4676.

Wesselink, B. and Deng, Y. (2009) Sectoral Emission Reduction Potentials and Economic Costs for Climate Change (SERPEC-CC). Summary report, Ecofys, Utrecht (Netherlands); Ecofys, Utrecht (Netherlands).

Wingender, J. and Flemming, H.-C. (2011) Biofilms in drinking water and their role as reservoir for pathogens. International Journal of Hygiene and Environmental Health 214(6), 417-423.

Zhou, X., Zhang, K., Zhang, T., Li, C. and Mao, X. (2017) An ignored and potential source of taste and odor (T&O) issues-biofilms in drinking water distribution system (DWDS). Applied Microbiology and Biotechnology 101(9), 3537-3550.

PART 1

# Microbial drinking water quality from unchlorinated drinking water distribution systems

Chapter 2

# Effects of cold recovery technology on the microbial drinking water quality in unchlorinated distribution systems

CHAPTER 2


## Abstract

Drinking water distribution systems (DWDSs) are used to supply hygienically safe and biologically stable water for human consumption. The potential of thermal energy recovery from drinking water has been explored recently to provide cooling for buildings. Yet, the effects of increased water temperature induced by this "cold recovery" on the water quality in DWDSs are not known. The objective of this study was to investigate the impact of cold recovery, from DWDSs, on the microbiological quality of drinking water. For this purpose, three parallel pilot distribution systems were operated for 38 weeks: system 1 with an operational heat exchanger, mimicking the cold recovery system by maintaining the water temperature at 25 °C; system 2 operated with a non-operational heat exchanger and system 3 run without a heat exchanger. The results showed no significant effects on drinking water quality due to cold recovery among the three systems: cell numbers and ATP concentrations remained around $3.5 \times 10^5$ cells/ml and 4 ng ATP/l, operational taxonomic units (OTUs) were around 470–490 and similar Shannon indices were observed (7.7–8.9) respectively. In the system with the operational heat exchanger, resulting in an elevated drinking water temperature, a higher relative abundance of *Pseudomonas* spp. and *Chryseobacterium* spp. was observed in the drinking water microbial community, but only when the temperature difference (ΔT) between feed water and water after cold recovery was higher than 9 °C. Differently, in the 38 weeks old biofilm, significant changes were induced by increased temperature: higher ATP concentration (475 pg/cm$^2$ vs. 89 pg/cm$^2$), lower diversity (observed OTUs: 88 vs. 200 or more) and a different bacterial community composition (e.g. higher relative abundance of *Novosphingobium* spp. and slight increase in *Legionella* spp.). It is concluded that water temperature increased to 25°C in a pilot distribution system, mimicking cold recovery, does not affect the bacterial water quality in the drinking water phase, compared to the systems without heating. However, it affects the concentration and community composition of biofilm after 38 weeks. The observed changes after introducing cold recovery did not show clear impacts on water quality and biofilm. Regarding the biofilm, further investigation for a longer period is required to understand the dynamic responses of biofilm to the changed temperature.



**Keywords:** drinking water distribution system, microbial ecology, cold recovery, drinking water quality, biofilm, bacterial community, opportunistic pathogens

*This chapter has been published as: Ahmad, J.I., Liu, G., Van der Wielen, P.W.J.J., Medema, G. and Van der Hoek, J.P. (2020) Effects of cold recovery technology on the microbial drinking water quality in unchlorinated distribution systems. Environmental Research 183, 109175.*

## 1.1 Introduction

Drinking water supply requires raw water abstraction and treatment, followed by storage, transport and distribution of finished water. The water treatment processes are selected and adopted to purify water for drinking purposes based on the quality of the incoming water and the quality standards of the drinking water to comply with (Elías-Maxil et al., 2014;van der Hoek 2012). Further, the produced drinking water is distributed through extended drinking water transport and distribution systems (DWDSs) (Prest et al., 2016a;van der Kooij and van der Wielen 2014). Worldwide, the biological stability of drinking water is maintained either by limiting nutrient concentrations (Prest et al., 2016a) or by applying a disinfectant residual to minimize the regrowth of microorganisms (Berry et al., 2006).



Drinking water supply requires energy for production and distribution purposes (e.g. overall between 4-13 MJ/$m^3$ in the Netherlands) (Gerbens-Leenes 2016). Drinking water distribution systems also contain thermal energy as a surplus of cold or heat. For example, in the Netherlands, 1,160 million $m^3$ of drinking water is distributed annually by 120,000 km long DWDSs (Frijns et al., 2013;Hofman et al., 2011;Liu et al., 2017b). The temperature within these DWDSs remains in general below 10°C during winter which offers a potential for cold recovery, and above 15°C during summer which offers a potential for heat recovery.

In the Netherlands, the potential of thermal energy from surface water, wastewater and drinking water has been analyzed. Of a future total heat demand in the build environment of 350 PJ per year, 40% can be covered by thermal energy from surface water, 16% by thermal energy from wastewater and 2% by thermal energy from drinking water (Kruit K. 2018). For cooling purposes, thermal energy from surface water and drinking water may be attractive, although no extensive analysis has been made yet. In the case of Sanquin (full scale application of cold recovery, in Amsterdam, the Netherlands) for which location this study was based, thermal energy from drinking water was selected because supply (drinking water main) and demand (Sanquin) are located close to each other and surface water is not available nearby.

In Amsterdam (the Netherlands), the temperature within the DWDS is between 4–10°C in winter and between 15–20°C in summer. These temperatures offer possibilities to recover thermal energy by direct heat exchange: in case of cold recovery, drinking water exchanges its cold with a warm carrier medium (e.g. air, water, glycol, etc.) inside a heat exchanger and slightly heated water flows back into the DWDS (Blokker et al., 2013;van der Hoek 2012;van der Hoek et al., 2017). According to a previous study, the theoretical thermal energy (cold recovery) potential for the city of Amsterdam is around 2800 TJ/year and an estimated energy required for space cooling for non residential buildings in Amsterdam is around 2161 TJ/year (Mol et al., 2011;van der Hoek et al., 2018). In this case DWDSs offer enough cooling capacity that can either be stored in aquifer thermal energy storage (ATES) systems during the winters and that can be used in upcoming summers to provide space cooling, or utilized directly without intermediate storage during winters for facilities with extensive cooling requirements (e.g. blood banks, data centers, hospitals).

In principle, cold recovery from DWDSs is technically feasible, and environmentally and financially beneficial (van der Hoek et al., 2017). However, the temperature increase of drinking water due to cold recovery might influence the microbial activity and community of bacteria in bulk water and biofilm within DWDSs (Blokker et al., 2013;Elías-Maxil et al., 2014;van der Hoek 2012). It is known that temperature changes can influence biological water quality, such as the reported seasonal fluctuations in adenosine triphosphate (ATP), total cell count (TCC) and changes in microbial community dynamics of bulk water (Hammes et al., 2008;Kelly et al., 2014;Liu et al., 2013a;Pinto et al., 2014;van der Wielen and van der Kooij 2010). It has been documented that opportunistic pathogens (e.g. *Legionella pneumophila*, *Pseudomonas aeruginosa*, *Mycobacterium avium complex* and *Stenotrophomonas maltophilia*) could occur at temperatures above 25 °C (Tsao et al., 2019;van der Wielen et al., 2013) and biofilm growth could be accelerated at high temperatures (Boe-Hansen et al., 2002;Fish et al., 2016;Flemming and Wingender 2010). However, the impact of energy recovery from drinking water on water quality is not well understood. Therefore, it is critical to assess the potential impact of increased water temperature, due to cold recovery, on the microbial water quality within drinking water distribution systems.

The main objective of this study is to investigate the effects of temperature increase induced by cold recovery on 1) biomass within DWDSs, quantified as ATP and TCC; 2) microbial community composition and diversity, profiled by illumina sequencing and 3) occurrence of selected opportunistic pathogens within DWDSs. Additionally, biofilms were also examined at the end of the experiments to assess potential impacts induced by cold recovery on biofilm.

## 1.2 Materials and Methods

### 1.2.1 System description

#### 1.2.1.1 Pilot distribution systems

As illustrated in Figure 2.1, three pilot scale distribution systems (DSs) were designed and operated in parallel from May to December 2016. The DSs were situated in the laboratory of TU Delft. They were supplied continuously with unchlorinated drinking water (referred as Feed Water) from treatment plant of Evides, Rotterdam, the Netherlands. Each of the experimental DSs had an internal diameter of 25 mm and a length of 10 meter (residence time of water within DSs was 60 seconds), and was made of polyvinyl chloride-unplasticised (PVC-U) pipes. For this experiment the flow rate was set at 4.5 l/min (0.15 m/s), which is based on normal flow velocities within Dutch drinking water distribution systems. For water sampling, small taps of PVC-U were installed in each DSs. For biofilm sampling at the end of the study, from the pipe surface, 25 cm long PVC-U coupons were designed and inserted in all the three DSs: these are sections of pipes with valves on both ends. All the DSs were equipped with flow and temperature sensors, for continuously monitoring the flow and temperature of feed water and outgoing water. Dasy Lab software (version 13.0.1) was used for system monitoring and data logging.

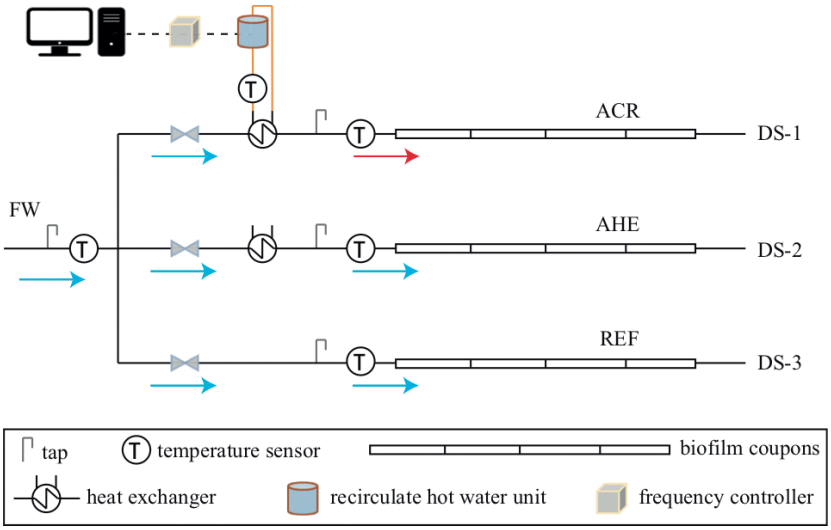


**Figure 2.1:** *Overview of the pilot facility consisting of three pilot distribution systems. DS-1: Cold recovery system; DS-2: System with non-operational Heat Exchanger (HE) and DS-3: Reference system. The overview shows the sampling locations (FW: Feed Water, ACR: After Cold Recovery, AHE: After the non-operational HE, REF: reference system), position of taps, coupons, HE (plate HE, where drinking water passes through the plates parallel to the plates with hot medium and absorb heat by heat transfer), recirculating hot water unit, temperature sensors and computer system connected with the experimental setup.*

#### 1.2.1.2 Design of operational Heat Exchanger system

Among the three DSs, DS-1 is the system that mimics cold recovery, which leads to an elevated drinking water temperature of 25°C after passing the heat exchanger (HE). For this purpose a plate HE (Minex, SWEP, Sweden) was used for the cold recovery to simulate the cold recovery situation at Sanquin project in Amsterdam, the Netherlands. Within the HE, on the plate surface heat is transferred between two fluids within a short time span (few seconds), cold (the drinking water under examination) and hot (recicrculating water). The HE consists of 6 plates, 3 plates for hot recirculating medium, 2 plates for cold drinking water and 1 blank plate. After having passed the HE and having absorbed the heat to gain the set point temperature of 25°C (which mimics the effect of cold recovery on the drinking water, which supplies cold with subsequent temperature increase), drinking water flows further through the main pipe and passes the whole length of DS-1. For recirculating heated water a hot tank (RVS boiler, AquaHeat, The Netherlands) along with a pump (Magna3, Grundfos, The Netherlands) and temperature sensor were connected with the hot channel of the HE. This setup was connected with a computer system through a frequency controller to further regulate the temperature on the HE surface, in order to maintain the threshold of 25°C ($T_{max}$) in drinking water leaving the HE after cold recovery. This set point, $T_{max}$, was maintained throughout the entire experimental period, irrespective of changes in the feed water temperature based on seasonal variations. The difference between the maximum temperature ($T_{max}$) after cold recovery and Feed Water (FW) is referred here as ΔT. During the current experimental period the ΔT was between 5-18°C (Figure S2.1 A).

#### 1.2.1.3 Reference and control systems

Similar to DS-1, DS-2 is the control system in which a non-operational heat exchanger was connected to the main pipe. In this control system, drinking water is passing the heat exchanger but no heating medium is flowing on the other side of the plates, thus water comes out of HE without temperature change. This system is operated in order to see if the HE itself has any effects because of the different HE plate material (stainless steel, with negligible biomass production potential of <15pg ATP/cm$^2$ (Tsvetanova and Hoekstra 2010)), the additional surface area in contact with water, and changes in hydrodynamics (Re <500). DS-3 is the reference system in which no HE is placed, mimicking a Dutch non-chlorinated drinking water distribution system without cold recovery. Throughout this study, it was used as a reference to compare with the cold recovery system.

## 1.2.2 Sampling

Water samples were taken every 7 days during the experimental period from Feed Water (FW), after operational heat exchanger, where temperature of drinking water increased to 25°C, mimicking cold recovery (ACR) (DS 1), after non-operational HE (AHE) (DS 2), and reference (REF) (DS3). After 38 weeks of experimental duration, biofilms were also sampled, in duplicate, from all three DSs (ACR, AHE and REF). For biofilm analysis, the valves on both sides of the pipe coupons were closed and the coupons were taken out of the systems and filled with DNA-free water (Thermo fisher scientific, Sweden). To remove the biofilm from the coupons, the pipe coupons were pretreated in 30 ml water by ultra-sonication, at a speed of 40 KHz, in a water bath (Ultrasonic 8800, Branson, USA) for two minutes. This sonication procedure was repeated for two additional times (Liu et al., 2014;Magic-Knezev and van der Kooij 2004). The obtained suspension of 90 ml was used for further analysis. All microbiological analysis were performed within 24 hours after sampling.

## 1.2.3 Quantification of Biomass

#### 1.2.3.1 Adenosine triphosphate and Total cell count

Bacterial cell numbers and active biomass were determined by measuring cell counts and the total adenosine triphosphate (ATP) concentration from both water samples (n=104) and biofilm samples (n=6). Cell counts were measured by a flow cytometer (C6-Flowcytometer, Accuri Cytometers, USA) using the same protocol that was previously developed and tested for drinking water samples (Prest et al., 2013). Total and membrane-intact cell counts were distinguished by adding two stains (SYBR Green 1 and propidium iodide) simultaneously as described by Prest et al. (2013). Active biomass was determined by measuring total ATP concentrations from both water and biofilm samples using a reagent kit for bacterial ATP and a luminometer (Celsis Advance Luminometer, Charles River, USA), as described previously (Liu et al., 2017a;Magic-Knezev and van der Kooij 2004).

### 1.2.4 Microbial community composition and diversity

#### 1.2.4.1 DNA extraction and amplicon sequencing of 16S rRNA genes

DNA was extracted from 104 water samples (2 litres of water was filtered for each sample) and 6 biofilm samples, using a DNeasy PowerBiofilm kit (Qiagen, USA). Due to low amount of DNA (<2ug/ml), 5 of the water samples were excluded for 16S rRNA gene sequencing analysis and the duplicate biofilm samples were pooled together for achieving enough DNA to further process the samples for 16S rRNA gene sequencing. For 16S rRNA gene sequencing, the V3-V4 region of the 16S rRNA gene was amplified using primers 341F: 5'-CCTACGGGNGGCWGCAG-3' and 785R: 5'-GACTACHVGGGTATCTAATCC-3' (Thijs et al., 2017). Paired-end sequence reads were generated using the Illumina MiSeq platform. FASTQ sequence files were generated using the Illumina Casava pipeline version 1.8.3. The initial quality assessment was based on data passing the Illumina Chastity filtering. Subsequently, reads containing the PhiX control signal were removed using an in-house filtering protocol at BaseClear laboratory, Leiden, the Netherlands. In addition, reads containing (partial) adapters were clipped (up to a minimum read length of 50bp). The second quality assessment was based on the remaining reads using the FASTQC quality control tool version 0.10.0. The final quality scores per sample were used further downstream to analyse Bioinformatics. All sequencing files were deposited in the sequence read archive (SRA) under accession number PRJNA475793.



#### 1.2.4.2 Data processing and statistical analysis

The obtained sequence libraries (which consisted of 4,945,856 sequences) after quality control from FASTQC were imported into the Quantitative Insights into Microbial Ecology (QIIME2) (version 2018.11) pipeline (Caporaso et al., 2010). The sequences were further screened, at the maximum length of 298 bp and minimum of 253 bp, denosied paired ends were merged and chimeras were removed using the inbuilt Divisive Amplicon Denoising Algorithm 2 (DADA2) (Callahan et al., 2016). The remaining representative sequences were clustered to operational taxonomic units (OTUs) at an identity of 97%. The sequences were normalized at sequence depth of 5,532. For taxonomic assignment, feature-classifier plugin in QIIME2 was used against the SILVA database (132 release) for generating taxa bar plots and heat maps. Both, alpha (Shannon, Pielou's richness, observed OTUs) and beta (weighted UniFrac) diversity indices were calculated using phylogenetically based rooted tree (generated by aligning sequences using MAFFT plugin for phylogenetic reconstruction in FastTree), using QIIME2 diversity plugin. Further, Kruskal-Wallis (pairwise) test was performed on alpha diversity indices to determine the similarity/dissimilarity distances within the groups when data was divided based on locations and months (for water samples). The differences among different groups were determined by using quantitative beta diversity distance metrices (weighted UniFrac) and their statistical significance was calculated by performing permutational analysis of variance (PERMANOVA), with 999 permutations and using pairwise approach, to determine the effects of different groupings based on sampling location. Principal coordinate (PCO) plots were generated using weighted UniFrac distance in emperor plot plugin.

### 1.2.5 Identification of targeted microorganisms

#### 1.2.5.1 *Legionella* spp.

Samples from both the water phase (only during months of June-August, for possible occurrence of *Legionella* within feed water) and the biofilm phase were tested for cultivable *Legionella* spp. The colony forming units (cfu) of *Legionella* spp. were determined using buffered charcoal yeast extract agar according to NEN standard 6265 (van der Wielen and van der Kooij 2013). The positive and confirmed colonies of *Legionella* spp. were tested for presence of *Legionella pneumophila* or non-*pneumophila* species, with MALDITOF (Matrix Assisted Laser Desorption/Ionization Time of Flight Mass spectrometry) according to the protocol used at Het Waterlabortarium (HWL), Haarlem, the Netherlands.

#### 1.2.5.2 Quantitative Polymerase Chain Reaction (qPCR)

The number of gene copies of the selected bacterial species (*Legionella anisa*, *Mycobacterium kansasii*, *Pseudomonas aeruginosa*, *Stenotrophomonas maltophilia Chit A)* and protozoan species (*Vermamoeba vermiformis*) were determined using quantitative PCR (qPCR). For all the 5 targeted species both water and biofilm samples were analyzed. The qPCRs used to quantify these species have been described previously (van der Wielen and van der Kooij 2013). For each organism, targeted genes, primers, probes, and type of PCR, its protocols and efficiency are given in Table S2.1. The qPCR results were only reported for samples that had an amplification efficiency higher than 20%.

## 1.3 Results

### 1.3.1 Microbial quantification

Cell counts and ATP concentrations in drinking water are shown in Figure 2.2. Both ATP and cell counts showed comparable values among the distribution systems (DSs) (2–8 ng/l ATP, 2.0–6.5×$10^5$ cells/ml), indicating that the introduction of HE and increase in temperature has a minor influence on the concentration of planktonic bacteria and their activity in water. A clear seasonal trend was noticed in FW, showing higher cell numbers and ATP concentrations during summer (June to August) when the temperature of the incoming water is higher than 15°C, than during the winter (Oct–Dec) when temperatures of the incoming water is lower than 15°C. The ACR, AHE and REF systems did not influence this observed seasonal pattern in the water. Furthermore, the seasonal trend was also observed for the ATP concentrations measured in the water leaving the treatment plant (Figure S2.1B).

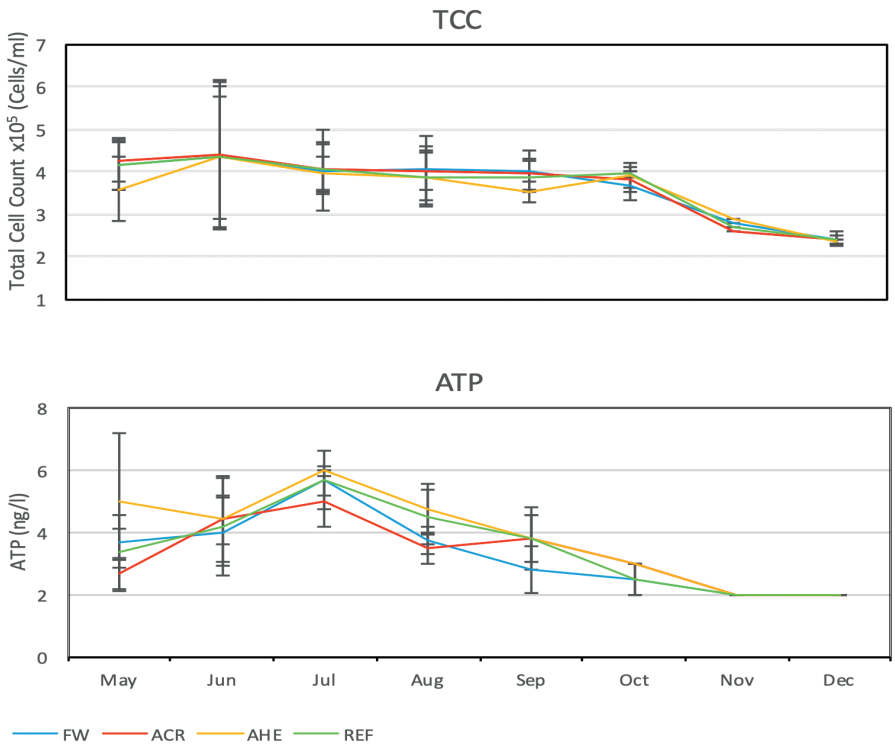


**Figure 2.2:** *Cell counts and ATP concentrations in water samples taken from the feed water and the three pilot drinking water distribution systems (FW: Feed Water; ACR: After Cold Recovery; AHE: After non-operational Heat Exchanger and REF: Reference).*

In contrast to the water samples, 3.6-5.3 times more biofilm was formed after introducing cold recovery (ACR: 7.5×10$^6$ cells/cm$^2$; 475 ATP pg/cm$^2$) compared to biofilm formed without cold recovery after non-operational HE (AHE: 1.4×10$^6$ cells/cm$^2$; 89 ATP pg/cm$^2$) or the reference system (REF: 1.9×10$^6$ cells/cm$^2$; 130 ATP pg/cm$^2$) (Figure 2.3).

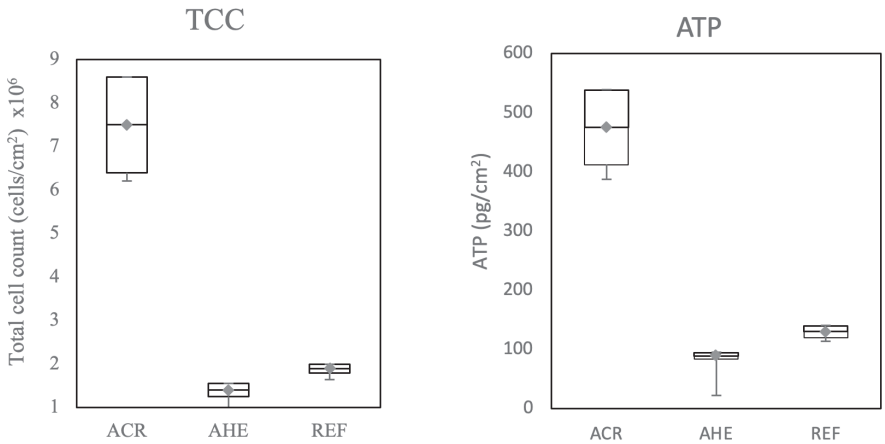


**Figure 2.3:** *Cell counts and ATP concentrations of biofilms sampled from the three pilot distribution systems with and without cold recovery (ACR: After Cold Recovery; AHE: After non-operational Heat Exchanger and REF: Reference).*

Moreover, the membrane-intact cell count in the biofilm from the ACR system ($10^6$ membrane-intact cells/cm$^2$) was 10 times higher than in the biofilm from the other two systems ($10^5$ membrane-intact cells/cm$^2$), whereas membrane-intact cell numbers were comparable for planktonic bacteria among all systems (Figure S2.2).

### 1.3.2 Microbial community comparison

#### 1.3.2.1 Alpha diversity

In total, 1,565,519 sequences were generated after QIIME2 quality filtering process and these sequences have been assigned to 47,644 operational taxonomic units (OTUs). In bulk water, comparable numbers of OTUs were observed for FW (472±128), ACR (476±126), AHE (485±136) and REF (481±133). Although seasonal differences were observed and the number of observed OTUs, Shannon index and Pielous's evenness differed between different months, no differences were observed between different locations (Figure S2.3). The months were grouped together based on the temperature of the feed water: the first group was from June to October (17–21°C) and the second group consisted of May and December (14–16°C). The differences in temperature between these two groups were statistically significant (Kruskal-Wallis , $p<0.05$) (data not shown).

Fewer OTUs were observed in the biofilms (88–295 OTUs) compared to the number of observed OTUs in bulk water. For the biofilms formed in the systems without cold recovery, comparable numbers of OTUs were detected (295 and 288 OTUs for AHE and REF). Both are higher than the number of OTUs observed in the biofilm formed in the system with cold recovery (ACR, 88 OTUs). The results of the Shannon index (ACR: 4.2; AHE: 6.9; REF: 7.2) and Pielou's evenness (ACR: 0.64; AHE: 0.84; REF: 0.87) showed significant differences in alpha diversity between the systems with (ACR) and without (AHE and REF) cold recovery (Kruskal-Wallis, $p <0.05$).

#### 1.3.2.2 Beta diversity

Results of bacterial community similarity analysis revealed different clusters for planktonic bacteria and biofilm (Figure 2.4A), and these differences were also statistically significant ($p<0.05$). Minor differences in bacterial community were found among water samples from all systems, while significant differences were observed among bacterial communities in the biofilm samples: the biofilm ACR clustered separately from the biofilms in AHE and REF systems, which clustered closely together. Comparing the water samples taken every month, the bacterial community composition of the samples were clustered based on seasonal variations corresponding to the microbial dynamics of the incoming drinking water (Figure 2.4B). Water samples from each month clusterd separately and these differences were significant ($p<0.05$), as can also be seen by the percentage of variance explained by the two coordinates in Figure 2.4B (21.3 and 14.0%, respectively). Furthermore, the differences between sampling locations were not significant ($p>0.05$).

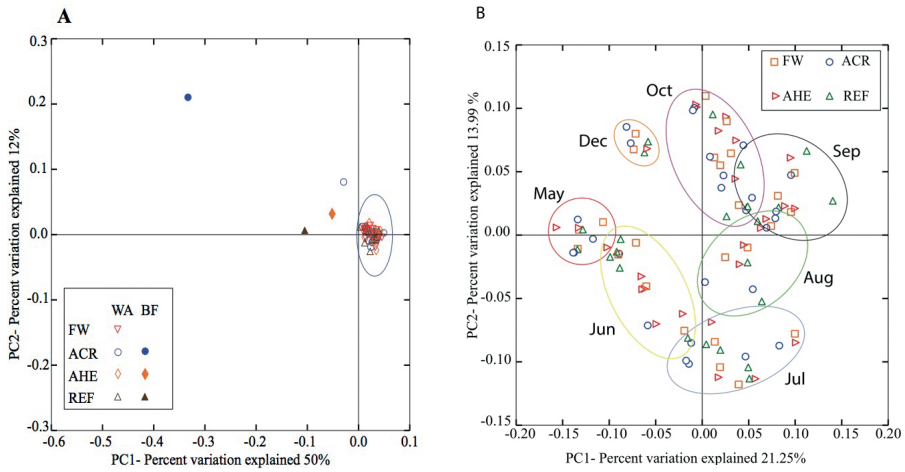


**Figure 2.4:** *Principle coordinate (PCO) plots based on weighted unifrac distance matrix, A) for both water (WA) and biofilm (BF) samples, and B) for only water samples. Samples from feed water and from the three pilot distribution systems: ACR, After Cold Recovery; AHE, After non-operational Heat Exchanger; REF, Reference and FW: Feed Water for only water phase.*

### 1.3.3 Microbial community composition

For both planktonic bacteria and biofilm, the bacterial community was dominated by Proteobacteria at phylum level, with a relative abundance of 41–44% for water and 55-95% for biofilm, followed by the phyla of GN02 (8–9%), Planctomycetes (8%), Bacteroidetes (6–7%), OD1 (6–8%), and Cyanobacteria (1–2%) in water (Figure 2.5A), and the phyla of Cyanobacteria (0.2–0.8%), OD1 (0.2–3%), Nitrospirae (0–3%), Chlamydiae (0–7%), Bacteroidetes (0.2–9%) and Planctomycetes (1–16%) in the biofilm (Figure 2.5B).

No significant changes in microbial community composition were observed among the bulk water samples from different locations ($p>0.05$) but microbial composition differed significantly between months ($p<0.05$), which was similar to the results of the beta diversity analysis. At the class level, relative abundances of Alpha and Gammaproteobacteria were changing over the time period, where we observed >11% Gammaproteobacteria from June-October and <11% in the months of May and December. Comparable to this was the observation that >20% Alphaproteobacteria was found from June-August and < 20% during months of May and from Sep-December (Figure S2.4A). In addition, the orders of Betaproteobacteriales, Pseudomonadales, Rhizobiales and Flavobacteriales were changing over the period of time as well. Higher relative abundance of Pseudomonadales and Flavobacteriales was observed after cold recovery compared to feed water and the other two locations (REF and AHE) (Figure S2.4B). At the genus level, a higher relative abundance of *Pseudomonas* spp. (2.5%) and *Chryseobacterium* spp. (2.3%) was observed in the bulk water (Figure 2.5C) of the ACR system than in the other two systems (*Pseudomonas* spp in AHE: 0.5% and REF: 0.5%; *Chryseobacterium* spp 0.1% in both REF and AHE).

In the biofilm phase, the relative abundance of Proteobacteria was clearly higher in the ACR system (95.0%) than in the AHE (81.4%) and REF (57.5%) system. Also, at class level the relative abundances of Alpha and Gammaproteobacteria were higher in biofilm ACR (55% and 27% respectively) compared to both biofilms without cold recovery situations, REF (37% and 22% respectively) and AHE (30% and 14% respectively). The orders of Pseudomonadales, Legionalles and Sphingomonadales were also higher in abundance within ACR biofilm compared to other two locations without cold recovery (Figure S2.5). Further, at genus level a higher relative abundance of *Novosphingobium* spp. (23.9%) and *Legionella* spp. (1.9%) was observed after introducing cold recovery (ACR system) compared to the AHE (0.2% *Novosphingobium* spp. and 0.03% *Legionella* spp.) and REF (0.02% *Novosphingobium* spp. and 0.01% *Legionella* spp.) systems (Figure 2.5D).

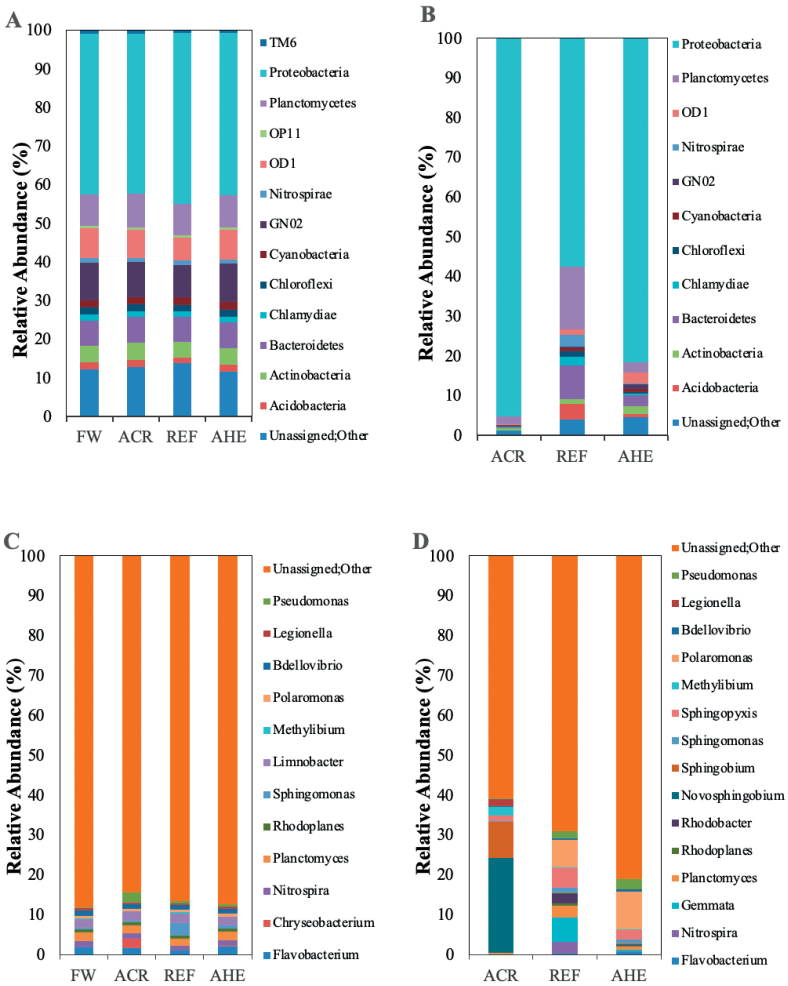


**Figure 2.5:** *Taxonomic composition for the identification of microbial community groups; at Phylum level, A) for water and B) for biofilm, and at Genus level C) for water and D) for biofilm samples from the three pilot distribution systems (ACR: After Cold Recovery; AHE: After non-operational Heat Exchanger; REF: Reference and FW: Feed Water for only water phase).*

### 1.3.4 Opportunisitic pathogens

In bulk water, 10–40% of the samples were positive for *Legionella* spp. (>100 cfu/l, Figure 2.6 A) across all systems, with no significant changes caused by applying cold recovery. In the biofilm phase, cultivable *Legionella* was detected in the REF system (3 cfu/cm$^2$) (Table 2.1), but it was not detected from the ACR and AHE systems. The MALDITOF results revealed that the detected *Legionella* spp. colonies were not *L. pneumophila*.

q-PCR results showed that *L. anisa* was detected in all water samples with comparable numbers ($2.6\times10^3$–$1.5\times10^4$ gene copies/l) between the systems (Figure 2.6 B). In the biofilm, *L. anisa* was only detected in the biofilm formed in the system with cold recovery (ACR: 7 gene copies/cm$^2$) (Table 2.1). *V. vermiformis,* a host protozoan for *Legionella*, was also detected in all water samples at numbers between $3.5\times10^2$–$1.4\times10^3$ gene copies/l (Figure 2.6 C). In the biofilm, *V. vermiformis* was detected in the system with cold recovery (ACR: $1.6\times10^3$ copies/cm$^2$), but not in the systems without cold recovery (AHE, REF; Table 2.1).

Similarly, in all water samples *S. maltophilia* was detected with comparable concentrations, although they were slightly higher after applying cold recovery (ACR: $1.5\times10^3$; AHE: $1.14\times10^3$ ; REF: $2\times10^2$ gene copies/l; Figure 2.6 D). In the biofilm, *S. maltophilia* was below the detection limit in all samples (Table 2.1). *Pseudomonas aeruginosa* and *Mycobacterium kansasii* were not detectable in all water and biofilm samples.

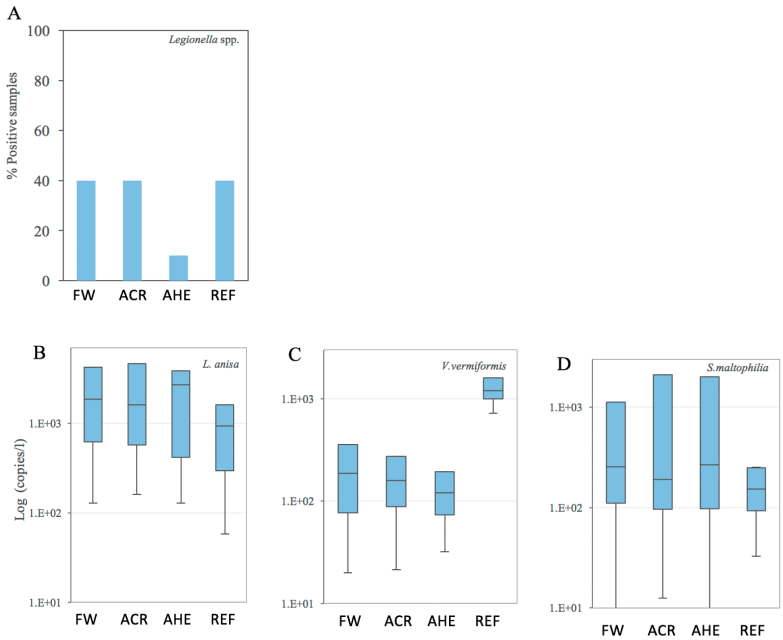


**Figure 2.6:** *A) Percent positive samples of Legionella spp. in drinking water, B) Cell copies of Legionella anisa, C) its host protozoa Vermamoeba vermiformis and D) Stenotrophomonas maltophilia measured by qPCR from water samples. The sampling locations for water are FW: Feed Water; ACR: After Cold Recovery; AHE: After non-operational Heat Exchanger; REF: Reference.*

*Table 2.1: Colony forming units (cfu) of Legionella spp. and cell copies determined with qPCR, of targeted microbes in biofilm samples within pilot DWDSs, from all sampling locations (ACR: After Cold Recovery; AHE: After non-operational Heat Exchanger; REF: Reference; UD: under detection limit).*

| | ACR | AHE | REF |
|---|---|---|---|
| *Legionella* spp. (cfu/cm$^2$) | 0 | 0 | 3 |
| *Legionella anisa* (copies/cm$^2$) | 7 | UD | UD |
| *Vermamoeba vermiformis* (copies/cm$^2$) | 1.6x10$^3$ | UD | UD |
| *Stenotrophomonas maltophilia* (copies/cm$^2$) | UD | UD | 3x10$^1$ |

## 1.4 Discussion

### 1.4.1 Effect of cold recovery on planktonic bacteria in drinking water

Generally, our data set revealed that introducing cold recovery technology in a pilot drinking water distribution system has minor influences on the presence, concentration (e.g. ATP and TCC), and type (community composition and diversity) of microbes and presence of selected opportunistic pathogens in drinking water, where it was observed that temperature is an important selection pressure for microbes (Proctor et al., 2018) and temperature increase in water systems can lead to an increase in bacterial quantity and a decrease in diversity of microbes (Inkinen et al., 2016;Proctor et al., 2017). One example is the observed correlation between cell counts and seasonal temperature fluctuations (Fish et al., 2015;Henne et al., 2013;Lautenschlager et al., 2010;Liu et al., 2013b;Prest et al., 2016b). In our study, we also found seasonally triggered differences in drinking water microbiology, although the overall microbial active biomass (ATP) and cell numbers remain stable over the study period. However, changes were observed in microbial community composition, with certain microbial groups remaining higher in summer and relatively lower in abundance during times when temperature was lower than 14–15 °C. But, seasonal fluctuations change water temperatures for a long period, while in a cold recovery system, the water resided in the system, inside the HE, for a very short time, in this study only 60 seconds.

Interestingly, at the genus level, it was observed that the relative abundance of *Pseudomonas* spp. (from 0.5 % to 2.5%) and *Chryseobacterium* spp. (from 0.1% to 2.3%) increased, but only when the temperature differences between feed water and water after cold recovery were higher than 9°C, which was the case during spring and winter periods ($\Delta T \geq 9$ °C). This is reasonable, because *Pseudomonas* spp. prefers to grow in warm tap water under oligotrophic conditions (Proctor et al., 2017). For the cold recovery system, the regrowth of *Pseudomonas* spp. might be triggered by the exposure to higher temperature on the surface of HE during winter season ($\Delta T \geq 9$ °C) . The optimal temperature for *Chryseobacterium* spp. growth is between 25-28 °C (Gallego et al., 2006). Our findings suggest that there are no significant effects of cold recovery on drinking water quality at the set temperature of 25°C. Future research is needed to understand the potential impact of larger temperature differences/higher drinking water temperatues in cold recovery systems. On the basis of the seasonal change of the feed water mcrobiome in this study, it is desirable to continue investigating them when cold recovery technology is applied. For example, to define the threshold for drinking water temperature ($T_{max}$) in distribution systems and the maximum temperature differences ($\Delta T$).

### 1.4.2 Effect of cold recovery on biofilm bacteria

Compared to planktonic bacteria in drinking water, biofilms were more responsive to the increased temperature caused by cold recovery, which is plausible given the longer exposure time of the biofilm compared to that of bulk water (38 weeks vs. 60 seconds). Although there is no previous study regarding the effects of temperature changes on biofilm developed inside drinking water distribution systems, the significant impact of temperature on the physical structure, quantity and community of biofilm has been widely observed across other different aquatic systems, such as river sediment biofilm (Villanueva et al., 2011), sea water biofilm (Smale et al., 2017), biofilm/biofouling in membrane systems for water purification (Farhat et al., 2016) and biofilm in hot water premise plumbing systems (Proctor et al., 2017). The significant increase of biofilm concentration, at 38 weeks, after introducing cold recovery (5 times more ATP) is consistent with previous studies, which reported higher biofilm concentrations resulting from temperature increase, and concluded that bacterial growth kinetics were governed by temperature in the biofilm phase (van der Kooij and van der Wielen 2014;Villanueva et al., 2011;Vital et al., 2010).



Similar to the quantitative results, significant changes in the bacterial community composition and diversity were observed, confirming the previously reported importance of temperature in structuring bacterial communities (Smale et al., 2017). This study found the system with cold recovery formed biofilm was less diverse in bacterial community than the other systems without cold recovery. The higher relative abundance of *Methylibium* spp.*, Polaromonas* spp., *Leptothrix* spp., *Nitrospira* spp., *Pseudomona* spp. and *Sphingomonas* spp. in the system without cold recovery corresponds to the early stage of biofilm development (Martiny et al., 2003;van der Kooij et al., 2018), while the less diversity, more *Novosphingobium* spp. and *Legionella* spp., less *Nitrospira* spp. and *Betaproteobacteriales* in the biofilm from the system with cold recovery agreed with later stage of biofilm development that approaching a stabilized microbial community (Martiny et al., 2003). This may indicate that the biofilms in the system with and without cold recovery might at different stage of biofilm development due to the differences in temperature.

This shows that constantly stable and higher temperature inside the cold recovery system over the period of 38 weeks has selected for less diverse and more stable biofilm community composition compared to fluctuating temperatures inside the systems without cold recovery. However, in the present study the biofilm was sampled at the age of 38 weeks and the duplicate biofilm samples from all the three DSs showed good reproducibility in terms of microbial activity, as well as the results of biofilm samples from DSs without increase in temperature (REF and AHE) were highly similar. It is recommended to have long term studies following biofilm development dynamics to have a good understanding on the effects of increased temperature induced by cold recovery. The present study demonstrateed that the experimental setup is suitable and reliable for future long term studies.

## 1.5 Practical implication and recommendations

The present study simulated the introduction of cold recovery into a drinking water distribution system that will increase the water temperature locally to 25 °C. According to the biomass

concentrations and community compositions, no significant deterioration of microbial water quality was observed; though changes were found in the biofilms, there is no evidence of mass transfer between biofilm and bulk water causing any changes in microbial water quality irrespective of increased biofilm concentrations. The influence of the formed biofilm on the microbiological water quality needs to be studied on the long-term during the cold recovery process.

Regarding the presence of selected opportunistic pathogens in our study, under the conditions applied (ΔT between 5–18 °C and a maximum temperature after cold recovery of 25 °C) and the feed water used, cold recovery does not pose a health risk. However, in the biofilm phase after cold recovery we did observe a higher concentration of *Legionella anisa* and its host protozoa, which indicates the potential growth of these temperature sensitive microbes in the biofilm phase. This needs further investigation in the biofilm phase (for example by inoculating the system with potential opportunistic pathogens) to see their behavior under different temperature settings (both ΔT and maximum temperature after cold recovery).

For future research, besides the above recommendations of establishing temperature thresholds of $T_{max}$ and ΔT and conducting long term dynamic studies on biofilm development and water quality, it is recommended to investigate the contribution of nutrient levels on the effects of temperature increase and the response of an already established and old biofilm that has been developed over decades in distribution systems, to the sudden introduction of higher water temperature. A reason for this is that in a previous study it was found that the exposure to higher temperatures resulted in greater biofilm detachment (Fink et al., 2015). Therefore, it is important to study potential risks associated with such water temperature changes and subsequent biofilm detachment, which is the same as so called "transition effects" (Liu et al., 2017b).

The operational application of this concept in Amsterdam, the Netherlands, at a specific location (providing thermal energy for cooling to Sanquin, a company that produces products from blood plasma which requires a huge cooling capacity) is running with a temperature threshold of 15 °C as the maximum allowable drinking water temperature ($T_{max}$) after cold recovery (van der Hoek et al., 2018). Based on further research on drinking water quality under various temperature profiles during cold recovery, it may be possible to push the upper temperature threshold higher (e.g. from the current 15 °C to the 25 °C in the Dutch water regulation) which will significantly enlarge the potential of energy can be recovered. This will not only increase the potential of recoverable energy by increasing the ΔT, but will also significantly extend the period over the year this concept can be operated.

## 1.6 Conclusion

From the perspectives of the bacterial quantity, community composition and the studied opportunistic pathogens, it is evident that our study showed minor effects of cold recovery on the bulk water. For the community composition of planktonic bacteria, cold recovery increased slightly the relative abundances of *Pseudomonas* spp. (0.4 % to 2.4%) and *Chryseobacterium* spp. (0.1% to 2.1%). Regarding the selected microorganisms, increasing the temperature to 25 °C did

not show any influence, except the slight increase of *S. maltophilia* gene copies ($2\times10^2$ to $1.5\times10^3$ gene copies/l). Some differences were observed between the biofilm formed in the pilot distribution system with and without cold recovery (e.g. higher biomass and lower diversity of the community). A long term study (at least 2 years) on the potential influences of cold recovery on the dynamics of biofilm formation and detachments is highly recommended to have a solid understanding regarding the biofilm related processes after introducing cold recovery.

## References

Berry, D., Xi, C. and Raskin, L. (2006) Microbial ecology of drinking water distribution systems. Current Opinion in Biotechnology 17(3), 297-302.

Blokker, E.J.M., van Osch, A.M., Hogeveen, R. and Mudde, C. (2013) Thermal energy from drinking water and cost benefit analysis for an entire city. Journal of Water and Climate Change 4(1), 11-16.

Boe-Hansen, R., Albrechtsen, H.J., Arvin, E. and Jørgensen, C. (2002) Bulk water phase and biofilm growth in drinking water at low nutrient conditions. Water Research 36(18), 4477-4486.

Callahan, B.J., McMurdie, P.J., Rosen, M.J., Han, A.W., Johnson, A.J.A. and Holmes, S.P. (2016) DADA2: High-resolution sample inference from Illumina amplicon data. Nature Methods 13, 581.

Caporaso, J.G., Kuczynski, J., Stombaugh, J., Bittinger, K., Bushman, F.D., Costello, E.K., Fierer, N., Pēa, A.G., Goodrich, J.K., Gordon, J.I., Huttley, G.A., Kelley, S.T., Knights, D., Koenig, J.E., Ley, R.E., Lozupone, C.A., McDonald, D., Muegge, B.D., Pirrung, M., Reeder, J., Sevinsky, J.R., Turnbaugh, P.J., Walters, W.A., Widmann, J., Yatsunenko, T., Zaneveld, J. and Knight, R. (2010) QIIME allows analysis of high-throughput community sequencing data. Nature Methods 7(5), 335-336.

Elías-Maxil, J.A., van der Hoek, J.P., Hofman, J. and Rietveld, L. (2014) Energy in the urban water cycle: Actions to reduce the total expenditure of fossil fuels with emphasis on heat reclamation from urban water. Renewable and Sustainable Energy Reviews 30, 808-820.

Farhat, N., Vrouwenvelder, J.S., Van Loosdrecht, M., Bucs, S.S. and Staal, M. (2016) Effect of water temperature on biofouling development in reverse osmosis membrane systems. Water research 103, 149-159.

Fink, R., Oder, M., Rangus, D., Raspor, P. and Bohinc, K. (2015) Microbial adhesion capacity. Influence of shear and temperature stress. International Journal of Environmental Health Research 25(6), 656-669.

Fish, K.E., Collins, R., Green, N.H., Sharpe, R.L., Douterelo, I., Osborn, A.M. and Boxall, J.B. (2015) Characterisation of the Physical Composition and Microbial Community Structure of Biofilms within a Model Full-Scale Drinking Water Distribution System. PLoS ONE 10(2), e0115824.

Fish, K.E., Osborn, A.M. and Boxall, J. (2016) Characterising and understanding the impact of microbial biofilms and the extracellular polymeric substance (EPS) matrix in drinking water distribution systems. Environmental Science: Water Research & Technology 2(4), 614-630.

Flemming, H.-C. and Wingender, J. (2010) The biofilm matrix. Nature Reviews Microbiology 8(9), 623-633.

Frijns, J., Hofman, J. and Nederlof, M. (2013) The potential of (waste)water as energy carrier. Energy Conversion and Management 65, 357-363.

Gallego, V., Garcia, M.T. and Ventosa, A. (2006) Chryseobacterium hispanicum sp. nov., isolated from the drinking water distribution system of Sevilla, Spain. Int J Syst Evol Microbiol 56(Pt 7), 1589-1592.

Gerbens-Leenes, P.W. (2016) Energy for freshwater supply, use and disposal in the Netherlands: a case study of Dutch households. International Journal of Water Resources Development 32(3), 398-411.

Hammes, F., Berney, M., Wang, Y., Vital, M., Köster, O. and Egli, T. (2008) Flow-cytometric total bacterial cell counts as a descriptive microbiological parameter for drinking water treatment processes. Water Research 42(1–2), 269-277.

Henne, K., Kahlisch, L., Höfle, M.G. and Brettar, I. (2013) Seasonal dynamics of bacterial community structure and composition in cold and hot drinking water derived from surface water reservoirs. Water Research 47(15), 5614-5630.

Hofman, J., Hofman-Caris, R., Nederlof, M., Frijns, J. and van Loosdrecht, M. (2011) Water and energy as inseparable twins for sustainable solutions. Water Science and Technology 63(1), 88-92.

Inkinen, J., Jayaprakash, B., Santo Domingo, J.W., Keinänen-Toivola, M.M., Ryu, H. and Pitkänen, T. (2016) Diversity of ribosomal 16S DNA- and RNA-based bacterial community in an office building drinking water system. Journal of Applied Microbiology 120(6), 1723-1738.

Kelly, J.J., Minalt, N., Culotti, A., Pryor, M. and Packman, A. (2014) Temporal Variations in the Abundance and Composition of Biofilm Communities Colonizing Drinking Water Distribution Pipes. PLoS ONE 9(5), e98542.

Kruit K., S.B., Roosjen R., Boderie P. (2018) National potential of aquathermal energy – Analysis and review of possibilities, Delft, The Netherlands.

Lautenschlager, K., Boon, N., Wang, Y., Egli, T. and Hammes, F. (2010) Overnight stagnation of drinking water in household taps induces microbial growth and changes in community composition. Water research 44(17), 4868-4877.

Liu, G., Bakker, G.L., Li, S., Vreeburg, J.H.G., Verberk, J.Q.J.C., Medema, G.J., Liu, W.T. and Van Dijk, J.C. (2014) Pyrosequencing Reveals Bacterial Communities in Unchlorinated Drinking Water Distribution System: An Integral Study of Bulk Water, Suspended Solids, Loose Deposits, and Pipe Wall Biofilm. Environmental Science & Technology 48(10), 5467-5476.

Liu, G., Ling, F., Magic-Knezev, A., Liu, W., Verberk, J.Q.J.C. and Van Dijk, J.C. (2013a) Quantification and identification of particle associated bacteria in unchlorined drinking water from three treatment plants by cultivation-independent methods. Water Research 47(10), 3523-3533.

Liu, G., Tao, Y., Zhang, Y., Lut, M., Knibbe, W.-J., van der Wielen, P., Liu, W., Medema, G. and van der Meer, W. (2017a) Hotspots for selected metal elements and microbes accumulation and the corresponding water quality deterioration potential in an unchlorinated drinking water distribution system. Water Research 124(Supplement C), 435-445.

Liu, G., Van der Mark, E.J., Verberk, J.Q.J.C. and Van Dijk, J.C. (2013b) Flow Cytometry Total Cell Counts: A Field Study Assessing Microbiological Water Quality and Growth in Unchlorinated Drinking Water Distribution Systems. BioMed Research International 2013, 595872.

Liu, G., Zhang, Y., Knibbe, W.-J., Feng, C., Liu, W., Medema, G. and van der Meer, W. (2017b) Potential impacts of changing supply-water quality on drinking water distribution: A review. Water research 116, 135-148.

Magic-Knezev, A. and van der Kooij, D. (2004) Optimisation and significance of ATP analysis for measuring active biomass in granular activated carbon filters used in water treatment. Water Research 38(18), 3971-3979.

Martiny, A.C., Jørgensen, T.M., Albrechtsen, H.-J., Arvin, E. and Molin, S. (2003) Long-term succession of structure and diversity of a biofilm formed in a model drinking water distribution system. Applied and environmental microbiology 69(11), 6899-6907.

Mol, S., Kornman, J., Kerpershoek, A. and Van Der Helm, A. (2011) Opportunities for public water utilities in the market of energy from water. Water Science & Technology 63(12).

Pinto, A.J., Schroeder, J., Lunn, M., Sloan, W. and Raskin, L. (2014) Spatial-Temporal Survey and Occupancy-Abundance Modeling To Predict Bacterial Community Dynamics in the Drinking Water Microbiome. mBio 5(3), e01135-01114.

Prest, E.I., Hammes, F., Kötzsch, S., van Loosdrecht, M.C.M. and Vrouwenvelder, J.S. (2013) Monitoring microbiological changes in drinking water systems using a fast and reproducible flow cytometric method. Water Research 47(19), 7131-7142.

Prest, E.I., Hammes, F., van Loosdrecht, M.C.M. and Vrouwenvelder, J.S. (2016a) Biological Stability of Drinking Water: Controlling Factors, Methods, and Challenges. Frontiers in Microbiology 7, 45.

Prest, E.I., Weissbrodt, D.G., Hammes, F., van Loosdrecht, M.C.M. and Vrouwenvelder, J.S. (2016b) Long-Term Bacterial Dynamics in a Full-Scale Drinking Water Distribution System. PLoS ONE 11(10), e0164445.

Proctor, C.R., Dai, D., Edwards, M.A. and Pruden, A. (2017) Interactive effects of temperature, organic carbon, and pipe material on microbiota composition and Legionella pneumophila in hot water plumbing systems. Microbiome 5(1), 130.

Proctor, C.R., Reimann, M., Vriens, B. and Hammes, F. (2018) Biofilms in shower hoses. Water Research 131, 274-286.

Smale, D.A., Taylor, J.D., Coombs, S.H., Moore, G. and Cunliffe, M. (2017) Community responses to seawater warming are conserved across diverse biological groupings and taxonomic resolutions. Proceedings of the Royal Society B: Biological Sciences 284(1862), 20170534.

Thijs, S., Op De Beeck, M., Beckers, B., Truyens, S., Stevens, V., Van Hamme, J.D., Weyens, N. and Vangronsveld, J. (2017) Comparative Evaluation of Four Bacteria-Specific Primer Pairs for 16S rRNA Gene Surveys. Frontiers in Microbiology 8, 494.

Tsao, H.-F., Scheikl, U., Herbold, C., Indra, A., Walochnik, J. and Horn, M. (2019) The cooling tower water microbiota: Seasonal dynamics and co-occurrence of bacterial and protist phylotypes. Water Research 159, 464-479.

Tsvetanova, Z.G. and Hoekstra, E.J. (2010) The effect of the surface-to-volume contact ratio on the biomass production potential of the pipe products in contact with drinking water, pp. 105-112.

van der Hoek, J.P. (2012) Towards a climate neutral water cycle. Journal of Water and Climate Change 3(3), 163-170.

van der Hoek, J.P., Mol, S., Ahmad, J.I., Liu , G. and Medema, G. (2017) Thermal energy recovery from drinking water. J. Krope, A.G.O., D. Goričanec, S. Božičnik, eds (ed), pp. 23-32, University of Maribor Press, Bled, Slovenia.

van der Hoek, J.P., Mol, S., Giorgi, S., Ahmad, J.I., Liu, G. and Medema, G. (2018) Energy recovery from the water cycle: Thermal energy from drinking water. Energy 162, 977-987.

van der Kooij, D. and van der Wielen, P.W.J.J. (2014) Microbial growth in drinking-water supplies: problems, causes, control and research needs. van der Kooij, D. and van der Wielen, P.W.J.J. (eds), pp. 1-20, IWA Publishing, London, UK.

van der Kooij, D., Veenendaal, H.R., Italiaander, R., van der Mark, E.J. and Dignum, M. (2018) Primary Colonizing Betaproteobacteriales Play a Key Role in the Growth of Legionella pneumophila in Biofilms on Surfaces Exposed to Drinking Water Treated by Slow Sand Filtration. Applied and environmental microbiology 84(24), e01732-01718.

van der Wielen, P.W.J.J., Italiaander, R., Wullings, B.A., Heijnen, L. and van der Kooij, D. (2013) Microbial Growth in Drinking-Water Supplies. Problems, Causes, Control and Research Needs. van der Kooij, D. and van der Wielen, P.W.J.J. (eds), pp. 177-205, IWA Publishing, London, UK.

van der Wielen, P.W.J.J. and van der Kooij, D. (2010) Effect of water composition, distance and season on the adenosine triphosphate concentration in unchlorinated drinking water in the Netherlands. Water Research 44(17), 4860-4867.

van der Wielen, P.W.J.J. and van der Kooij, D. (2013) Nontuberculous mycobacteria, fungi, and opportunistic pathogens in unchlorinated drinking water in the Netherlands. Applied and environmental microbiology 79(3), 825-834.

Villanueva, V.D., Font, J., Schwartz, T. and Romaní, A.M. (2011) Biofilm formation at warming temperature: acceleration of microbial colonization and microbial interactive effects. Biofouling 27(1), 59-71.

Vital, M., Stucki, D., Egli, T. and Hammes, F. (2010) Evaluating the growth potential of pathogenic bacteria in water. Applied and environmental microbiology 76(19), 6477-6484.

# Supplementary Information chapter 2

**Table S2.1:** Primers, probes and PCR protocol for selected opportunistic pathogens targeted in current study.

| | Targeted organism | Targeted Genes | Primers | Probe and detection limit | PCR efficiency(%) | PCR protocol |
|---|---|---|---|---|---|---|
| 1 | *Legionella anisa* | macrophage infectivity potentiator (Mip) surface protein | Lanisa F<br>sequentie<br>5'-CAATGTCTACTGTAATGGCAGCT-3′<br>LanisaR<br>sequentie 5′-AACCGCTTGGCAGTACCGT-3′ | LanisaP<br>sequentie 5′-Cy5-<br>AGACGGAATGTCTGGTGCCCAATTGA-3′<br>5 gene copies per reaction well averaged | 84.0 | 5 minute 95°C<br>20seconds95°C<br>48seconds60°C |
| 2 | *Mycobacterium kansasii* | 16S-23S ITS | MK1713F<br>sequentie:<br>5'-CGAAAAGCATCCCAACAAGTGG-3'<br>MK1875R<br>Sequentie: 5'-GTGGGACAACTCTCGAACAG -3' | MK1742P<br>Sequentie:<br>5'-TCTGTAGTGGACGAAAGCCGGG-FAM-3<br>5 gene copies per reaction well averaged | 100.2 | 5 minute 95°C<br>20seconds95°C<br>48seconds60°C |
| 3 | *Pseudomonas aeruginosa* | toxA positive regulatory gene (regA) | PaerFb<br>Sequentie: 5'-ATCGAGTACCTGAACCGGC-3'<br>PaerRb<br>Sequentie: 5'- TGGTGCAGTTCCTCATTGTC-3' | PAER PrA<br>Sequentie: 5'- FAM-<br>CCAGATGCTTTGCCTCAAC-BHQ1-3'<br>5 gene copies per reaction well averaged | 94.8 | 2 minute 95°C<br>20seconds95°C<br>1minute 60°C |
| 4 | *Stenotrophomonas maltophilia* | Chitinase A | ChitA-F<br>Sequentie: 5'- TACCACCCGTACCTGGACTT -3'<br>ChitA-R<br>Sequentie: 5'-ATCGCATCGTTGCTGTTGTA -3' | Not applicable<br>25 gene copies per reaction well averaged | 88.6 | 5 minute 95°C<br>30seconds95°C<br>30seconds58°C<br>1 minute72°C<br>10 minute 72°C<br>10 seconds 95°C<br>+smelt curve (65-95 °C,0.5 °C increment, 5 seconds |
| 5 | *Vermamoeba vermiformis* | 18S rRNA | Hv1227F<br>Sequentie 5′-TTACGAGGTCAGGACACTGT-3′<br>Hv1728R<br>Sequentie 5′-GACCATCCGGAGTTCTCG-3′ | Not applicable<br>one cell per analyzed volume (in the case of biofilm, the $cm^2$) | 84.5 | 30 seconds 95°C<br>20seconds95°C<br>30seconds56°C<br>40seconds72°C<br>2minutes72°C<br>1minute95°C<br>1minute65°C<br>30 seconds 25 °C-65 °C,<br>0.5 °C increment |

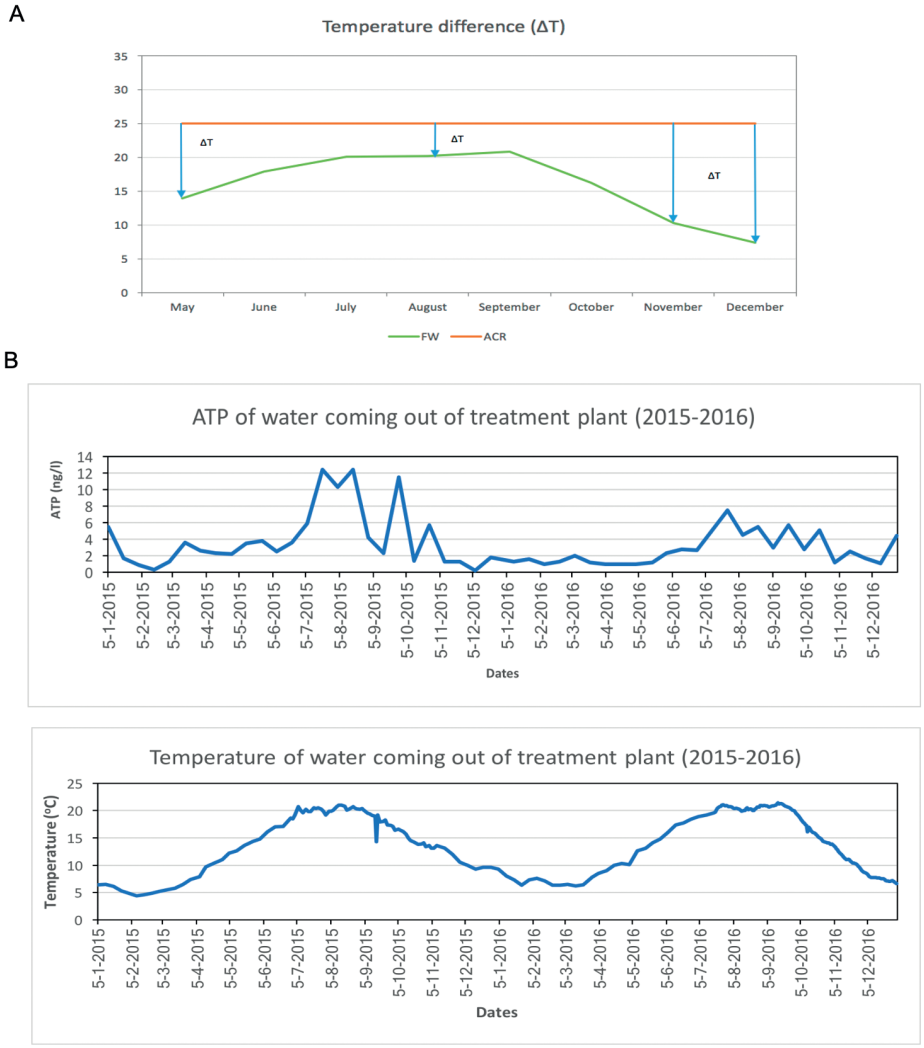


**Figure S2.1:** A) temperature difference between feed water (FW) and After cold recovery (ACR), B) Microbial activity and temperature of water from treatment plant for 2 years.

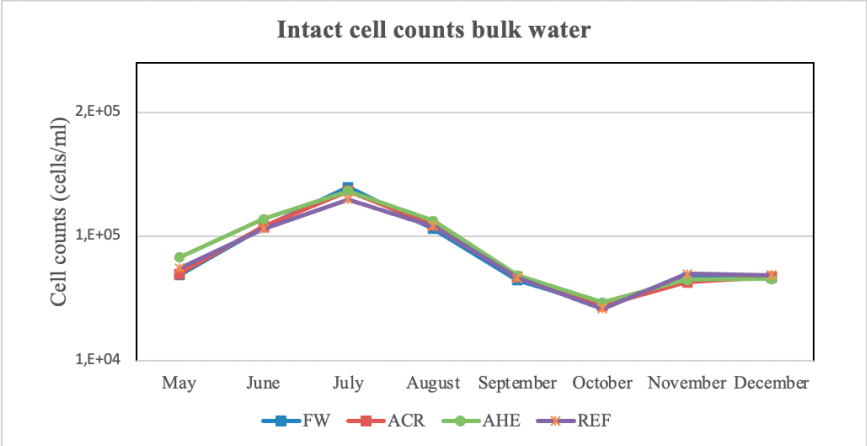


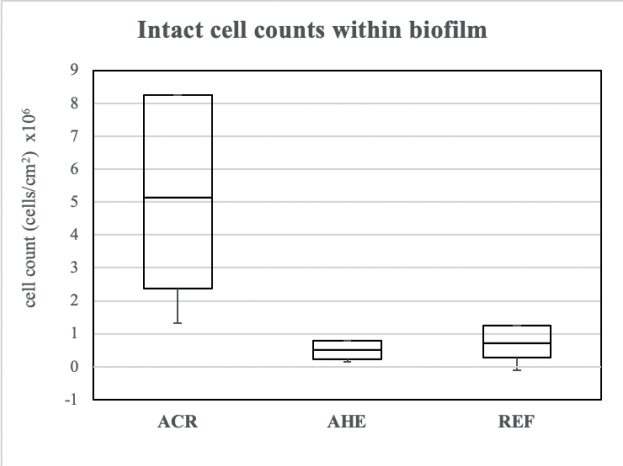


**Figure S2.2:** Intact cell counts for both bulk water and biofilm samples at different locations from three Drinking water distribution systems (FW: Feed Water, ACR: After Cold Recovery; AHE: After non-operational Heat Exchanger and REF: Reference).


**Figure S2.3:** Average monthly operational taxonomic units (Observed taxa), Shannon diversity and Evenness, from all 4 sampling locations in water phase, during the study period.

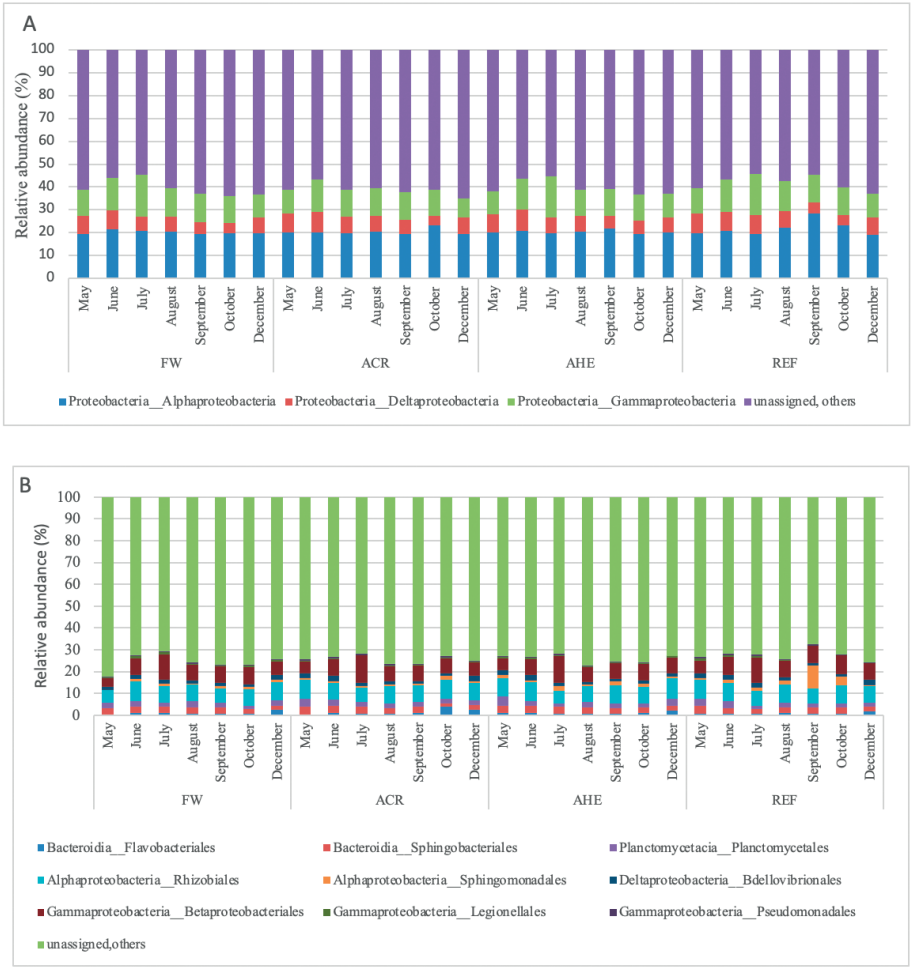


**Figure S2.4:** Relative abundances at Class (A) and Order (B) level, within drinking water samples, from all 4 locations.

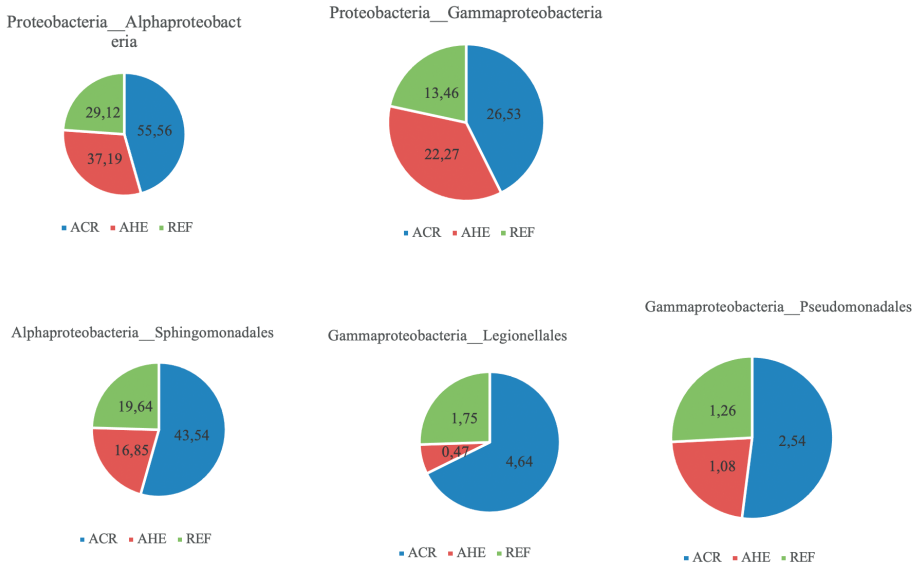


**Figure S2.5:** Relative abundances at Class and Order level, within biofilm samples, from 3 studied locations.

PART 2

# Biofilm development within unchlorinated drinking water distribution systems

Chapter 3

# Changes in biofilm composition and microbial water quality in drinking water distribution systems by temperature increase induced through thermal energy recovery

—

CHAPTER 3


## Abstract

Drinking water distribution systems (DWDSs) have been thoroughly studied, but the concept of thermal energy recovery from DWDSs is very new and has been conceptualized in the past few years. Cold recovery results in a temperature increase of the drinking water. Its effects on drinking water quality and biofilm development are unclear. Hence, we studied both bulk water and biofilm phases for 232 days in two parallel pilot scale distribution systems with two temperature settings after cold recovery, 25 °C and 30 °C, and compared these with a reference pilot system without cold recovery. In all three pilot distributions systems (DSs) our results showed an initial increase in biomass (ATP) in the biofilm phase, along with occurrence of primary colonizers (*Betaproteobacteriales*) and subsequently a decrease in biomass and an increasing relative abundance of other microbial groups (amoeba resisting groups; *Xanthobacteraceae*, *Legionellales*), including those responsible for EPS formation in biofilms (*Sphingomonadaceae*). The timeline for biofilm microbial development was different for the three pilot DSs: the higher the temperature, the faster the development took place. With respect to the water phase within the three pilot DSs, major microbial contributions came from the feed water (17–100%) and unkown sources (2–80%). Random contributions of biofilm (0–70%) were seen between day 7–77. During this time period six-fold higher ATP concentration (7–11ng/l) and two-fold higher numbers of high nucleic acid cells (5.20–5.80×$10^4$ cells/ml) were also observed in the effluent water from all three pilot DSs, compared to the feed water. At the end of the experimental period the microbial composition of effluent water from three pilot DSs revealed no differences, except the presence of a biofilm related microbial group (*Sphingomonadaceae*), within all three DSs compared to the feed water. In the biofilm phase higher temperatures initiated the growth of primary colonizing bacteria but this did not lead to differences in microbial diversity and composition at the end of the experimental period. Hence, we propose that the microbiological water quality of DWDSs with cold recovery should be monitored more frequently during the first 2–3 months of operation.



**Keywords:** Cold recovery, drinking water distribution system, temperature increase, microbial water quality, primary colonizers, microbial source tracking, biofilm

*This chapter has been published as: Ahmad, J.I.; Dignum, M.; Liu, G.; Medema, G.; van der Hoek, J.P.* (2021) *Changes in biofilm composition and microbial water quality in drinking water distribution systems by temperature increase induced through thermal energy recovery. Environmental Research 2021, 194, 110648.*

## 1.1 Introduction

Thermal energy recovery from drinking water distribution systems (DWDSs) is a novel and innovative concept. In the Netherlands the temperature within DWDSs stays between 4 and 10 °C in winter and between 15 and 20 °C in summer (Ahmad et al., 2020; Van der Hoek et al., 2018). This means that drinking water contains thermal energy, in the form of cold or heat, which provides opportunities to recover this energy for cooling or heating purposes. According to a previous study, the theoretical potential of cold recovery from drinking water for the city of Amsterdam is around 2800 TJ/year while the energy required for space cooling for non-residential buildings in Amsterdam is estimated to be around 2161 TJ/year (Mol et al., 2011; Van der Hoek et al., 2018). So, in principle DWDSs harbour enough cooling capacity that could be recovered in the winter and stored underground, through an aquifer thermal energy storage, to provide space cooling in summers, or utilized directly in winters for facilities with extensive cooling requirements (e.g. blood banks, data centers, hospitals).



However, the cold transfer to the user, with subsequent heat transfer to the DWDSs, will cause the drinking water temperature to increase. How this increase will affect the microbiology in unchlorinated DWDSs has not been explored yet. These distribution systems have their distinctive micro-environments, where the biological stability of drinking water is maintained by limiting nutrient concentrations (El-Chakhtoura et al., 2015; Prest et al., 2016a; Van der Kooij, 1992; Van der Kooij and Van der Wielen, 2013). The microbial environment of DWDSs consists of loose deposits (Liu et al., 2014), suspended solids (Liu et al., 2013), water phase (Prest et al., 2016a; Prest et al., 2016b) and biofilm phase (Fish et al., 2016). Among these, biofilm and water phase contain the dominant part of the biomass (more than 80%) (Liu et al., 2017) in unchlorinated DWDSs. They contribute significantly in shaping the microbiome of drinking water during distribution (Hull et al., 2019; Ling et al., 2018). An increase in temperature after applying cold recovery might affect these habitats (water and biofilm), as temperature is a crucial environmental factor for microbial growth and community dynamics (Kelly et al., 2014; Rogers et al., 1994). Especially, growth of biofilms (Diaz Villanueva et al., 2011), proliferation of opportunistic pathogens (OPs) (Van Der Wende et al., 1989; Wingender and Flemming, 2011) like *Pseudomonas* and *Legionella* (Van der Kooij and Van der Wielen, 2013), occurrence of discolored water (Zhou et al., 2017) and sudden changes in microbial water quality parameters (like ATP and cell concentration) (Potgieter et al., 2018; Prest et al., 2016a) are linked with temperature changes. For this reason, it is highly important to investigate the effects of cold recovery on microbial water quality and biofilm characteristics to understand the impacts of full scale application in more detail.

Hence, the current study was initiated with the goal to determine the potential changes in microbiology, both in terms of drinking water quality and microbiome, in DWDSs due to cold recovery. The study was carried out using pilot scale distribution systems. We studied two temperatures after cold recovery, 25 °C and 30 °C. The reason for choosing these two temperatures lies in the fact that the former is the maximum limit for the drinking water temperature within DWDSs in the Netherlands (Smeets et al., 2009; Staatscourant, 2011). In case no changes are observed at

25 °C, a temperature of 30 °C will significantly enhance the potential for cold recovery. However, this higher temperature may result in changes in microbiology. So, despite the fact that by Dutch law it is not allowed, the higher temperature was chosen as an extreme case for research purpose.

We hypothesized that the microbiology of DWDSs will be different after an increase in temperature of the water due to cold recovery application. For this purpose we studied both water and biofilm phases within pilot scale, unchlorinated drinking water distribution systems. Time series data of ATP concentrations, total cell concentrations, heterotrophic plate counts, *Aeromonas* spp., *Legionella* spp. and next generation gene sequencing (NGS) were generated (over a period of 232 days) to determine changes in microbial community composition of both water and biofilm. Microbial source tracker was used in combination with the NGS data to determine the relative contribution of feed water and biofilm microbiology on drinking water microbiology coming out of the pilot scale distribution systems. This analysis of the interactions of biofilm and water phase at higher temperatures (after applying cold recovery) will help water companies to take into account the potential consequences of applying cold recovery on shaping the microbial water quality within DWDSs.

## 1.2 Materials and Methods

### 1.2.1 Location and design of pilot scale distribution systems

Three pilot scale distribution systems (DSs) were designed and operated for almost 232 days from April till November, 2018 (Figure 3.1). The pilot scale DSs were situated at the drinking water treatment facility "Leiduin" of water utility Waternet near Amsterdam, and fed continuously with unchlorinated drinking water (Feed water (FW) from this plant . Details of the treatment of the source water can be found in (Baghoth et al., 2011).

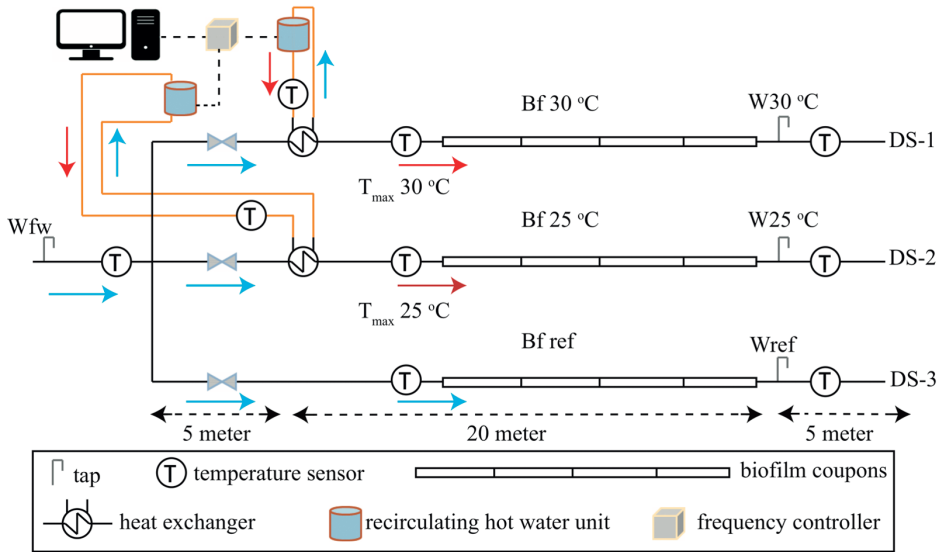


**Figure 3.1:** *Three, 30-meter-long (each), pilot scale distribution systems (DSs) supplied with unchlorinated feed water, continuously for 24/7 for 232 days, to study the potential impacts of recovering cold. All the sampling sites for both water (W) and biofilm (Bf) samples were labelled. ($W_{fw}$ = feed water, $W_{ref}$ = water from reference system, $W_{25\,^{o}C}$ = water after cold recovery ($T_{max}$ = 25 °C), $W_{30\,^{o}C}$ = water after cold recovery ($T_{max}$ = 30 °C), $Bf_{ref}$ = biofilm from reference system, $Bf_{25\,^{o}C}$ = biofilm formed after cold recovery ($T_{max}$ = 25 °C), $Bf_{30\,^{o}C}$ = biofilm formed after cold recovery ($T_{max}$ = 30 °C).*

Among the three pilot scale DSs, DS-1 and DS-2 are the systems in which the temperature of the feed water was increased by using a heat exchanger (HE) to an elevated drinking water temperature of 30 °C and 25 °C respectively (HE description in supplementary information). After having passed the HE and having absorbed the heat to gain the maximum ($T_{max}$) set point temperatures of 30 and 25 °C, the heated drinking water flowed through the pipes and passed the whole length of the DSs. The set points were maintained throughout the entire experimental period, irrespective of changes in the feed water temperature due to seasonal variations. DS-3 is the reference system, where no heat exchanger was used and the temperature of the drinking water followed the seasonal variation of the source and treatment plant. This represents the Dutch non-chlorinated drinking water distribution systems. Throughout this study, it was used as a reference to DS-1 and DS-2.

Each pilot scale DSs had an internal diameter of 25 mm and a length of 30 meter, and was made of polyvinyl chloride-unplasticised (PVC-U) pipes. For this experiment the flow rate was maintained at 4.5 l/min (flow velocity 0.15 m/s), which is based on typical flow velocities within Dutch drinking water distribution systems. All the DSs were equipped with flow and temperature sensors, for continuously monitoring the flow and temperature of the water. Dasy Lab software (version 13.0.1) was used for system monitoring and data logging. The difference between the temperature of the feed water and the temperature after cold recovery was termed as ΔT.

### 1.2.2 Sampling points and sampling frequency

For water sampling, small taps of PVC-U were installed within each pilot scale DSs (Figure 3.1). During the study period, the water samples were taken every two weeks from each of the DSs at four sampling points: $W_{fw}$ (feed water: treated/finished drinking water coming from the treatment plant), $W_{25\,^{\circ}C}$, $W_{30\,^{\circ}C}$ (after passing the heat exchangers) and $W_{ref}$ (from the reference system). In total 64 (16 weeks × 4 points) water samples were taken and analysed. For biofilm sampling from the pipe surface, 30 cm long PVC-U coupons were designed and inserted in all three pilot DSs. These pipe sections have valves on both ends for easy removal. Duplicate biofilm samples were collected at different days of the study, starting from day 7 till day 232 ($D_7$, $D_{14}$, $D_{28}$, $D_{49}$, $D_{84}$, $D_{140}$, $D_{232}$). In total 42 biofilm samples were collected from the three pilot scale DSs (from DS-1 referred in this study as $Bf_{30\,^{\circ}C}$, from DS-2 referred as $Bf_{25\,^{\circ}C}$ and from DS-3 referred as $Bf_{ref}$). From each system, biofilm sampling was started from the distal end of the system in order to avoid disturbances within the systems related to the sampling procedure. For both water and biofilm samples, all microbiological analysis were performed within 24 hours of sampling.

### 1.2.3 Biofilm samples preparation

For biofilm analysis, the valves on both sides of the pipe coupons were closed and the coupons were taken out of the systems and filled with 30 ml of DNA-free water. To remove the biofilm from the coupons, the pipe coupons were pretreated by ultra-sonication, at a frequency of 40 KHz, in a water bath (Ultrasonic 8800, Branson, USA) for two minutes. This sonication procedure was repeated twice (Liu et al., 2014; Magic-Knezev and van der Kooij, 2004). The obtained suspension of 90 ml was used for further analysis, and results for each measured parameter were normalized based on the surface area of the pipe coupon (236 $cm^2$) and the obtained suspension volume.

### 1.2.4 Analyses

#### *1.2.4.1* Dissolved organic carbon (DOC), Heterotrophic plate count (HPC), *Aeromonas* and *Legionella* spp.

From both water and biofilm samples cultivable bacteria (HPC), *Aeromonas* spp. and *Legionella* spp. were analysed according to the Dutch standard procedures for these parameters (NEN-6222, NEN-6263 and NEN-6265 respectively), as described in (Van der Kooij et al., 2018). Dissolved organic carbon (DOC) was measured only from water samples according to the Dutch procedure (NEN-1484)(Zlatanović et al., 2017).

#### *1.2.4.2* Adenosine triphosphate and total cell count

Bacterial cell numbers and active biomass were determined by measuring cell counts and the total adenosine triphosphate (ATP) concentration from both biofilm (n = 42) and water (n = 64) samples. Cell counts were measured by a flow cytometer (C6-Flowcytometer, Accuri Cytometers, USA) using the same protocol that was previously developed and tested for drinking water samples (Prest et al., 2013). Total and membrane-intact cell counts were distinguished by adding two stains simultaneously as described by Prest et al. (2013). Active biomass was determined by measuring total ATP concentrations from both biofilm and water samples using a reagent kit for bacterial ATP

and a luminometer (Celsis Advance Luminometer, Charles River, USA), as described previously (Magic-Knezev and van der Kooij, 2004).

### 1.2.5 DNA extraction and 16S rRNA gene sequencing

To examine the microbiome of the pilot scale DSs, DNA was extracted using a DNeasy PowerBiofilm kit (Qiagen, USA) from both water samples (n = 64) and biofilm samples (n = 42). Each sample (for water, a volume of 2 litres and for biofilm, 30 ml suspension from each sample) was filtered through a 47 mm polycarbonate filter (0.22 µm pore size, Sartorius, Germany). Subsequently the filters were stored at -20 °C and further used for DNA extraction according to the mentioned protocol. For 16S rRNA gene sequencing, the V3-V4 region of the 16S rRNA gene was amplified using primers 341F: 5'-CCTACGGGNGGCWGCAG-3' and 785R: 5'-GACTACHVGGGTATCTAATCC-3' (Thijs et al., 2017). Paired-end sequence reads were generated using the Illumina MiSeq platform. FASTQ sequence files were generated using the Illumina Casava pipeline version 1.8.3. The initial quality assessment was based on data passing the Illumina Chastity filtering. Subsequently, reads containing the PhiX control signal were removed using an in-house filtering protocol at BaseClear laboratory, Leiden, the Netherlands. In addition, reads containing (partial) adapters were clipped (up to a minimum read length of 50 bp). The second quality assessment was based on the remaining reads using the FASTQC quality control tool version 0.10.0, where low quality sequence ends were removed (Quality score = 30) and remaining sequences were used further downstream to analyse Bioinformatics. All sequencing files were deposited in the sequence read archive of the NCBI (National Center for Biotechnology Information) under theaccession number PRJNA613992.



### 1.2.6 Sequence data processing and statistical analysis

The obtained sequence libraries after quality control from FASTQC were imported into the Quantitative Insights into Microbial Ecology (QIIME2) (version 2019.7) pipeline (Bolyen et al., 2019). The sequences were further screened (at the maximum length of 298 bp), denoised, paired ends were merged and chimeras were removed using the inbuilt, Divisive Amplicon Denoising Algorithm 2 (DADA2) (Callahan et al., 2016). The remaining representative sequences were clustered to operational taxonomic units (OTUs) at an identity of 97%. For taxonomic assignment, feature-classifier plugin in QIIME2 (2019.7) was used against the SILVA database (132 release) for determining the microbial community composition at different taxonomic levels. Further, core microbial community was defined based on OTUs which were present among at least 80% of the samples (in the water phase) and in both duplicates in the biofilm samples, with a relative abundance higher than 1%. The taxa bar plots were generated based on core OTUs at different taxonomic levels of Class, Family and Order.

Both alpha (Shannon, observed OTUs, pielou's eveness) and beta (Jaccard distance matrix and weighted Unifrac) diversity indices were calculated using phylogenetically based rooted tree (generated by aligning sequences using MAFFT plugin for phylogenetic reconstruction in FastTree) and with a sampling depth of 2000 sequences using QIIME2 diversity plugin. Principal coordinate analysis (PCoA) plots were generated using Jaccard and weighted distance matrix in emperor plot plugin.

Single factor ANOVA and pearson correlation were performed in Microsoft Excel for mac (version 15.40), to determine the significance of differences between quantitative microbial parameters (ATP, TCC, HPC, DOC) and correlation of these parameters with feed water temperature and ΔT, for both DS-1 and DS-2.

### 1.2.7 Source tracker for microbial source tracking of bulk water from DSs

After assigning the taxonomic classification, the obtained OTU table was used as input for microbial source tracking of effluent water from the three pilot DSs ($W_{25\,^{o}C}$, $W_{30\,^{o}C}$, $W_{ref}$). The source tracker method was previously described by (Knights et al., 2011). The method identifies the extent of contributions of each source to a designated sink by comparing their community fingerprinting. The obtained results show the percentage contribution of each source to the sink. In this study feed water and biofilms from each respective DS were defined as sources and effluent water from each pilot DS on a particular sampling day was defined as sink (Table 3.1). The analysis was performed using default settings with a rarefaction depth of 1000, burn-in 100, restart 10, alpha (0.001), and beta (0.01) Dirichlet hyper parameter. The analysis was performed with QIIME software and percentages were calculated as previously described and also applied for drinking water communities by (Liu et al., 2018).

## 1.3 Results

### 1.3.1 Microbial activity in the biofilm phase

The three pilot distribution systems showed similar patterns of biofilm development both in terms of ATP and cell concentration (Figure 3.2a and 3.2b). Growth reached an initial maximum biomass within the first 28 days, then decreased to a minimum on day 140 and finally increased till day 232, at the end of sampling.

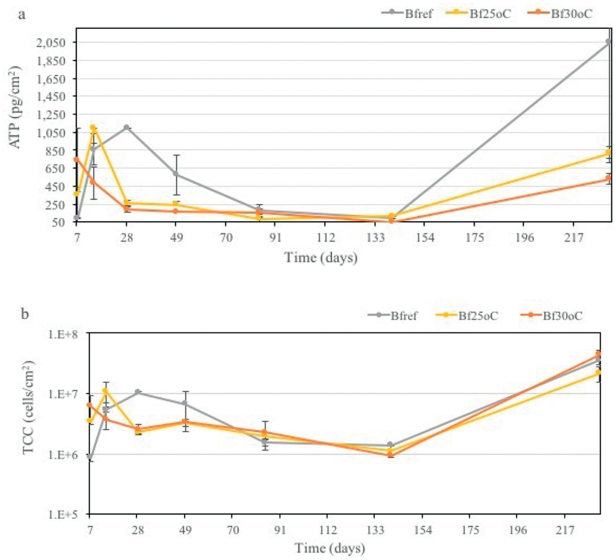


**Figure 3.2:** *Biomass formation measured in terms of ATP (a) and cell concentration (b), from biofilms formed over the period of 232 days, within three pilot distribution systems ($Bf_{ref}$ = biofilm from reference system, $Bf_{25\,^{o}C}$ = biofilm formed after cold recovery ($T_{max}$ = 25 °C), $Bf_{30\,^{o}C}$ = biofilm formed after cold recovery ($T_{max}$ = 30 °C)).*

On day 7, the ATP in $Bf_{ref}$ was 95 ± 3 pg/cm$^2$, and continued to grow till day 28. It reached a maximum biomass concentration of 1100 pg/cm$^2$ and then decreased to a minimum on day 140 (100 pg/cm$^2$), and subsequently reached a maximum of 2050 ± 1000 pg/cm$^2$ on day 232. The latter measurement showed a large difference between the duplicates. For $Bf_{25\ ^{\circ}C}$, the same maximum level in ATP was observed earlier on day 14, which then decreased to a minimum of 115 pg/cm$^2$ on day 140, and increased again to 815 ± 77 pg/cm$^2$ on day 232. The maximum ATP in $Bf_{30\ ^{\circ}C}$ was observed on day 7 (740 ± 300 pg/cm$^2$) and decreased from day 7 through day 140 (53 ± 7 pg/cm$^2$) and reached an increased final concentration on day 232 (530 ± 56 pg/cm$^2$).

Similar to the growth patterns of ATP, an initial maximum cell concentration was observed in the $Bf_{ref}$ on day 28 (1×10$^7$ cells/cm$^2$), then a minimum was observed on day 140 (1×10$^6$ cells/cm$^2$) and an increased final cell concentration (3×10$^7$ cells/cm$^2$) was observed on day 232. In $Bf_{25\ ^{\circ}C}$ a maximum cell concentration was measured on day 14 (1×10$^7$ cells/cm$^2$), a minimum on day 140 (1×10$^6$ cells/cm$^2$) and a final concentration of 2×10$^7$ cells/cm$^2$ on the last day of sampling. $Bf_{30\ ^{\circ}C}$ showed an initial maximum cell concentration of 6×10$^6$ cells/cm$^2$ on day 7, which then decreased to a minimum on day 140 (9×10$^5$ cells/cm$^2$) and finally an increase was observed on day 232 (4×10$^7$ cells/cm$^2$) (Figure 3.2b). Interestingly, from day 28 through day 232 the $Bf_{25\ ^{\circ}C}$ and $Bf_{30\ ^{\circ}C}$ showed comparable cell concentrations (Figure 3.2b), intact cell counts (1×10$^6$–6×10$^6$ cells/cm$^2$) and HPC counts (3×10$^4$–2×10$^4$ cells/cm$^2$) (data not shown here). Later on, from day 84 till day 232 a comparable microbial cell concentration was found within all three biofilms.

*Legionella* spp. and *Aeromonas* spp. were not found in the biofilms using plate counts, neither in the situation with cold recovery, nor in the situation without cold recovery. They were absent in the feed water and no growth was observed in the biofilms.

### 1.3.2 Microbial activity in bulk water phase

During the experimental period, the temperature of the $W_{fw}$ ranged from 8.9 to 21.2 °C and ΔT for $W_{30\ ^{\circ}C}$ and $W_{25\ ^{\circ}C}$ was between 9 and 21 °C and 4 and 19 °C respectively (Table S3.2). Irrespective of the seasonal variations in water temperature, the feed drinking water used for this experiment was biologically stable with Assimilable Organic Carbon (AOC) concentrations below 10 ± 2 µg-C/l (data from Waternet). DOC ranged between 1.2 and 2.0 mg C/l (Figure S3.1). The ATP (Figure 3.3a) and total cell concentration (Figure S3.2a) of $W_{fw}$ varied between 2 and 3 ng/l and 1.00–1.80 ×10$^5$ cells/ml, respectively, the observed HPC were between 2 and 20 cfu/ml (Figure S3.2c).

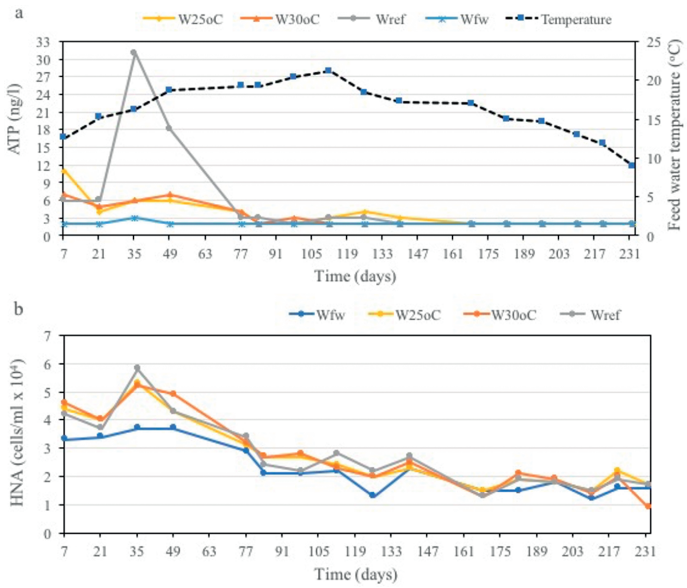


**Figure 3.3:** Microbiological water quality measured by ATP (a) and high nucleic acid cells (b), from feed water ($W_{fw}$ = feed water) and all three sampling sites from pilot distribution systems ($W_{ref}$ = water from reference system, $W_{25\,°C}$ = water after cold recovery ($T_{max}$ = 25 °C), $W_{30\,°C}$ = water after cold recovery ($T_{max}$ = 30 °C)).

From day 7 to day 77, ATP levels in the effluent drinking water from all three DSs were higher than in the feed water (Figure 3.3a). This was most pronounced in $W_{ref}$, where a maximum ATP concentration was observed on day 35 (31 ng/l), followed by a decrease till day 77 (3 ng/l). Later on, a more or less stable ATP concentration (2–3 ng/l) was observed between day 84 and the final sampling day 232. The maximum ATP concentration in the $W_{25\,°C}$ (11 ng/l) and $W_{30\,°C}$ (7 ng/l) was measured on day 7, a decrease on day 77 (4 ng/l) and a final ATP concentration of 2 ng/l on day 232.

Overall, from all four sampling sites of water, the total cell concentration (Figure S3.2a) remained higher from day 7 to day 77 (1.70–1.90 $\times 10^5$ cells/ml) and later on a stable and lower cell concentration was observed till day 232 ($7.60 \times 10^4$–$1.10 \times 10^5$ cells/ml). Similar to the results of ATP, high nucleic acid (HNA) cells increased considerably within $W_{30\,°C}$, $W_{25\,°C}$ and $W_{ref}$ compared to $W_{fw}$ between day 7 and 49 (Figure 3.3b). From all three DSs maximum HNA cells ($5.20–5.80 \times 10^4$ cells/ml) were observed on day 35, then decreased to $2.40–2.70 \times 10^4$ cells/ml on day 84 and reached a final concentration of $9 \times 10^3$–$1.70 \times 10^4$ cells/ml on day 232. Regarding low nucleic acid (LNA) cells, no differences between sampling sites were observed but overall a decreasing trend in total LNA cells was noticed in all water samples (Figure S3.2b), along with a decrease in $W_{fw}$ temperature (Pearson's r = 0.5). The heterotrophic plate counts (Figure S3.2c) showed an increase in the colony forming units within the three systems compared to the $W_{fw}$ and significant ($p < 0.05$) differences in HPC were observed between all four water sampling sites ($W_{fw}$, $W_{30\,°C}$, $W_{25\,°C}$ and $W_{ref}$).

*Legionella* spp. and *Aeromonas* spp. were not detected from the $W_{fw}$ and no regrowth was observed after applying cold recovery ($W_{25\,°C}$, $W_{30\,°C}$) or within $W_{ref}$ (results not shown).

### 1.3.3 Microbial diversity and biofilm composition

The biofilm was characterized by a steady increase in species diversity (shannon diversity index) and evenness (pielous' e). With respect to observed taxonomic units (OTUs), very few numbers of OTUs were observed from biofilm samples on day 7 (Figure 3.4a), with higher numbers observed in $Bf_{ref}$ (34 ± 3) compared to $Bf_{25\,^{\circ}C}$ (18 ± 4) and $Bf_{30\,^{\circ}C}$ (20 ± 4). In the $Bf_{ref}$ a decrease in OTUs was noticed from day 7 to day 14 (25 ± 7), and later an increase from day 28 to day 232, by reaching the maximum number of 266 ± 30 OTUs. In the $Bf_{25\,^{\circ}C}$ and $Bf_{30\,^{\circ}C}$ OTUs were increasing between day 7 and day 232 and reached a maximum of 289 ± 4 and 245 ± 30 OTUs, respectively. Overall $Bf_{30\,^{\circ}C}$ showed lower numbers of OTUs compared to $Bf_{25\,^{\circ}C}$ and $Bf_{ref}$. In terms of species diversity (Figure 3.4b) and evenness (Figure 3.4c), $Bf_{ref}$ was steadily increasing from day 7 (diversity: 1.2 ± 0.7, evenness: 0.2 ± 0.1) and reached its maximum on day 232 (diversity: 7.3 ± 0.2, evenness: 0.9 ± 0.01). $Bf_{25\,^{\circ}C}$ and $Bf_{30\,^{\circ}C}$ were more diverse (1.6–1.8) and even (0.4) at day 7 compared to $Bf_{ref}$, then steadily increased and reached a maximum on day 49 (diversity: 5.3–5.6, evenness: 0.7–0.8). Then a decrease was observed between day 49 and day 84, and an increased final diversity (7.2–7.4) and evenness (0.9) was measured on day 232.

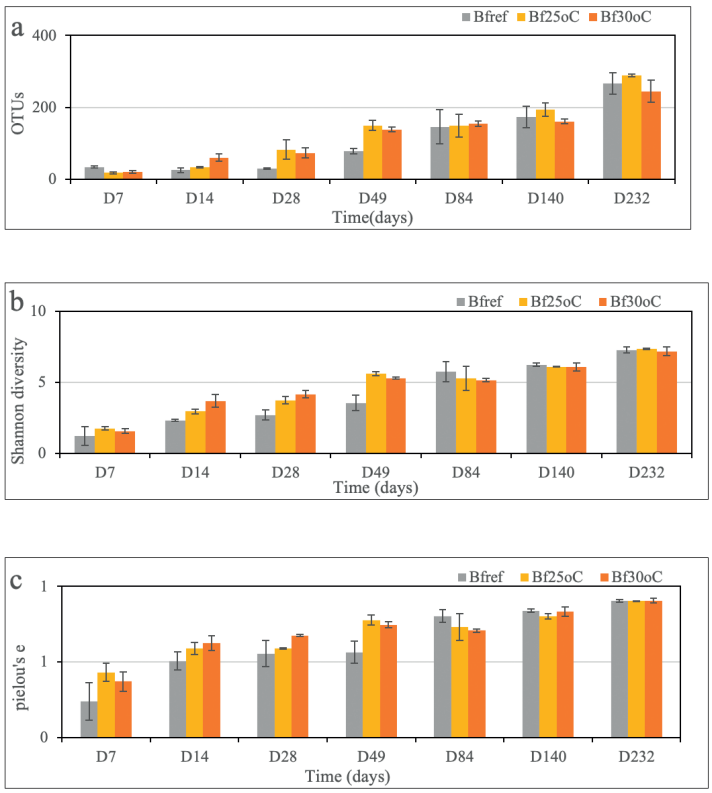


**Figure 3.4:** *Microbial community diversity, richness and evenness measured by a) number of observed taxonomic units (OTUs), b) Shannon diversity index and c) as pielou's e from all biofilms formed within three pilot distribution systems ($Bf_{ref}$ = biofilm from reference system, $Bf_{25\,^{\circ}C}$ = biofilm formed after cold recovery ($T_{max}$ = 25 °C), $Bf_{30\,^{\circ}C}$ = biofilm formed after cold recovery ($T_{max}$ = 30 °C)).*

In total, four core Phyla were observed (Table S3.3a) comprising 95–100% of the microbial communities among all biofilms, on different days. As shown in Figure S3.3, *Proteobacteria* was the most dominant phylum constituting almost 90-100% of the microbial community between day 7 and day 28 in $Bf_{25\,^{\circ}C}$ and $Bf_{30\,^{\circ}C}$, and till day 49 in $Bf_{ref}$. The four dominantly observed classes were *Gammaproteobacteria* (30–95%), *Alphaproteobacteria* (1–50%), *Planctomycetacia* (1–6%) and *Deltaproteobacteria* (1–5%), simultaneously over the period of time. From day 7 till day 232, the relative abundance of *Gammaproteobacteria* was decreasing and three other classes (*Alphaproteobacteria, Planctomycetacia*, *Deltaproteobacteria*) were increasing in abundance respectively (Figure S3.3).

At the Order level, *Betaproteobacteriales* (Figure 3.5a), was most abundant in $Bf_{25\,^{\circ}C}$ (88%) and $Bf_{30\,^{\circ}C}$ (87%) on day 7 and in $Bf_{ref}$ (82%) on day 14. During day 7–49, at Family level (Figure 3.5b), the community composition data showed *Burkholderiaceae* (member of order *Betaproteobacteriales*) and *Sphingomonadaceae* as the most dominant microbial groups among all three biofilms ($Bf_{ref}$, $Bf_{25\,^{\circ}C}$ and $Bf_{30\,^{\circ}C}$). Where the highest relative abundance of *Burkholderiaceae* was observed on day 7 within all biofilms ($Bf_{ref}$: 78%, $Bf_{25\,^{\circ}C}$: 87%, $Bf_{30\,^{\circ}C}$: 86%), its relative abundance decreased over time. *Sphingomonadaceae* was observed in $Bf_{25\,^{\circ}C}$ (6%) and $Bf_{30\,^{\circ}C}$ (8%) starting from day 7 and in $Bf_{ref}$ (13%) on day 14. The relative abundances of *Burkholderiaceae* and *Sphingomonadaceae* were gradually decreasing when biofilms became more diverse with the presence of other microbial groups, such as *Xanthobacteraceae,* which was observed in $Bf_{25\,^{\circ}C}$ and $Bf_{30\,^{\circ}C}$ on day 28 and in $Bf_{ref}$ on day 49 with the relative abundances of 3% and 1%, respectively. Simultaneously, occurrence of *Legionellales* in $Bf_{30\,^{\circ}C}$, $Bf_{25\,^{\circ}C}$ and in $Bf_{ref}$ (1%) on day 28, 49 and 84 respectively was noticed. Among other groups the higher relative abundance of *Pseudomonadaceae* was observed on day 7 in $Bf_{ref}$ (17%) and $Bf_{25\,^{\circ}C}$ (5%), and on day 140 in $Bf_{30\,^{\circ}C}$ (15%). Overall, six core taxa (Table S3.3b) were observed in biofilm samples belonging to these dominant microbial groups.


**Figure 3.5:** *Microbiome of biofilms shown as relative abundances (%) of core microbial groups, at both Order (a) and Family (b) level of taxonomic classification, from three sampling locations, developed within pilot distribution systems ($Bf_{ref}$ = biofilm from reference system, $Bf_{25\ ^{o}C}$ = biofilm formed after cold recovery ($T_{max}$ = 25 °C), $Bf_{30\ ^{o}C}$ = biofilm formed after cold recovery ($T_{max}$ = 30 °C)).*

### 1.3.4 Microbial diversity and composition of bulk water

Based on gene sequencing analysis of drinking water samples from the feed water and effluent water coming out of the three DSs ($W_{25\ ^{o}C}$, $W_{30\ ^{o}C}$ and $W_{ref}$), the OTUs, shannon diversity and community evenness were fluctuating considerably over the course of this study and largely followed a varying pattern of the feed water (Figure 3.6a). From day 7 through day 182 more fluctuations were observed in numbers of OTUs, with an average number of OTUs ranging from 141 to 200 and with a very high standard deviation of 107-179. In contrast, comparatively stable numbers of OTUs were observed from day 196 through day 232, ranging between 58 ± 25 and 87 ± 82. Similar results were observed for the other alpha diversity metrices like shannon diversity index (Figure 3.6b) and pileou's evenness (Figure 3.6c). These metrices showed a more diverse (Shannon index: 5.1 ± 2.5) and noticeably even (pielou's e: 0.7 ± 0.2) microbial community from day 7 to day 182, and a relatively less diverse (Shannon index: 3.5 ± 1) and less even (pielou's e: 0.5 ± 0.1) but comparatively more stable/consistent community from day 196 to day 232.

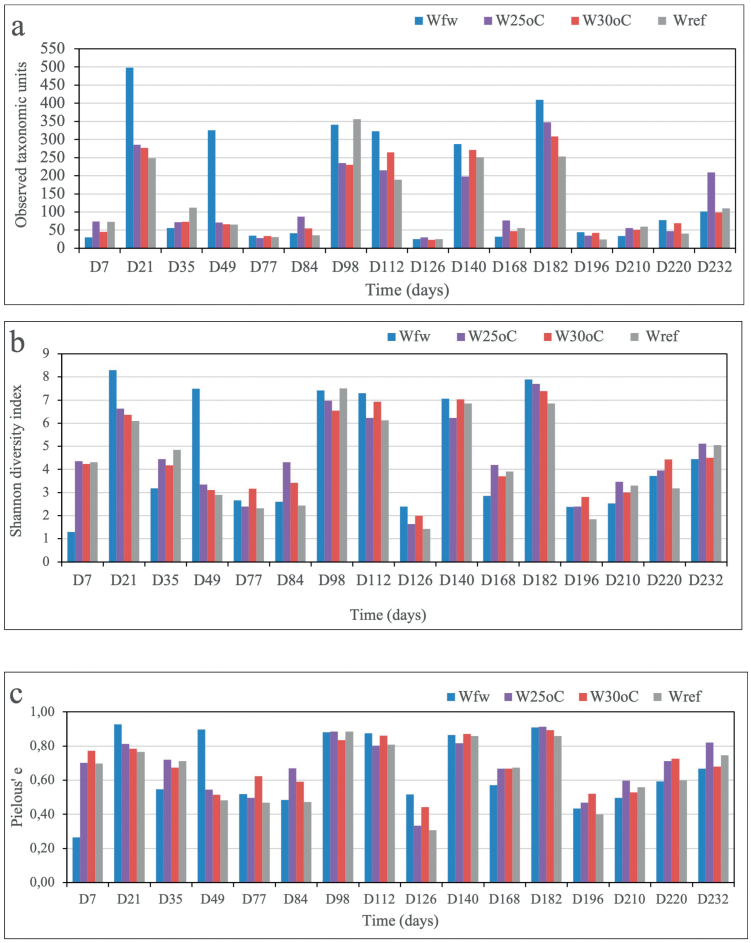


**Figure 3.6:** *Alpha diversity of water samples measured by a) observed taxonomic units, b) Shannon diversity and c) pielous' e, in order to determine the community richness, diversity and evenness from all four sampling locations ($W_{fw}$ = feed water, $W_{ref}$ = water from reference system, $W_{25\,^{\circ}C}$ = water after cold recovery ($T_{max}$ = 25 °C), $W_{30\,^{\circ}C}$ = water after cold recovery ($T_{max}$ = 30 °C)).*

Furthermore, the community composition data revealed similar patterns as the community diversity indices. In total, three core phyla were detected from $W_{fw}$ and $W_{ref}$, five from $W_{25\,^{\circ}C}$, and four from $W_{30\,^{\circ}C}$ (Table S3.4a). Five major classes were observed (Figure S3.4), comprising 20–100% of the total microbial communities in all water samples. The most dominant were *Gammaproteobacteria*, *Parcubacteria* and *Alphaproteobacteria* in $W_{fw}$ and $W_{ref}$. In $W_{25\,^{\circ}C}$ and $W_{30\,^{\circ}C}$ two additional classes were also observed, namely *Subgroup 6* (Phylum *Acidobacteria*) and *Actinobacteria*.

At Family level of taxonomic classification, four major microbial groups were observed in all water samples (Figure 3.7), with *Burkholderiaceae* (10–80%) and *Pseudomonadaceae* (10–70%) as the most dominant groups, followed by *Methylophilaceae* (4–40%). *Sphingomonadaceae* was only observed in samples from $W_{25\,^{\circ}C}$ (1–9%), $W_{30\,^{\circ}C}$ (1–8%) and $W_{ref}$ (1–3%), starting from day 7

through day 232. *Pseudomonadaceae* (5–69%) was observed at all sampling points and its relative abundance was higher in $W_{25\,^{\circ}C}$, $W_{30\,^{\circ}C}$ and $W_{ref}$ compared to $W_{fw}$, between day 7 and day 77. Later on, no pattern was observed for its occurrence. Also, periodically a higher relative abundance of *Burkholderiaceae* was measured in $W_{fw}$ between day 7 and 182, but $W_{25\,^{\circ}C}$, $W_{30\,^{\circ}C}$ and $W_{ref}$ showed comparatively less variation in its abundance during this time period.

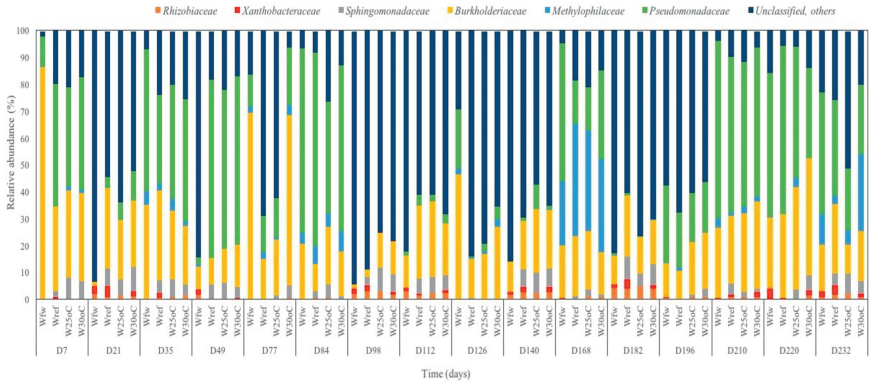


**Figure 3.7:** *Microbiome of drinking water, represented by relative abundances (%) of core microbial groups, at family level of taxonomic classification. From all four studied sampling sites ($W_{fw}$ = feed water, $W_{ref}$ = water from reference system, $W_{25\,^{\circ}C}$ = water after cold recovery ($T_{max}$ = 25 °C), $W_{30\,^{\circ}C}$ = water after cold recovery ($T_{max}$ = 30 °C)).*

Overall, very few (<10) core taxa (relative abundance >1% and present in 80% of the samples from each sampling location) were observed from water samples. All of those were belonging to the above mentioned microbial groups, from all water sampling locations (Table S3.4b). Comparatively, more taxa were detected from the water phase after applying cold recovery ($W_{25\,^{\circ}C}$, $W_{30\,^{\circ}C}$) than from the reference and feed water ($W_{ref}$ and $W_{fw}$).

### 1.3.5 Source tracking of bulk water communities within three DSs

For the microbial communities of bulk water coming out of the three DSs ($W_{ref}$, $W_{25\,^{\circ}C}$, $W_{30\,^{\circ}C}$), feed water ($W_{fw}$) and biofilm ($Bf_{ref}$, $Bf_{25\,^{\circ}C}$, $Bf_{30\,^{\circ}C}$) bacterial communities were treated as potential sources. Within all three DSs, $W_{fw}$ was the main contributor towards the microbial bulk water communities, alongwith contributions from unknown sources. Within all three pilot DSs, the contributions of biofilm communities to the bulk water microbial community showed a random pattern but it was corresponding with the initial higher ATP and HNA cell concentrations of bulk water. At the start the biofilms made an initial maximum contribution, then the contribution decreased and finally increased, except for the 30 °C system where the decrease and increase were observed twice (Figure 3.8).

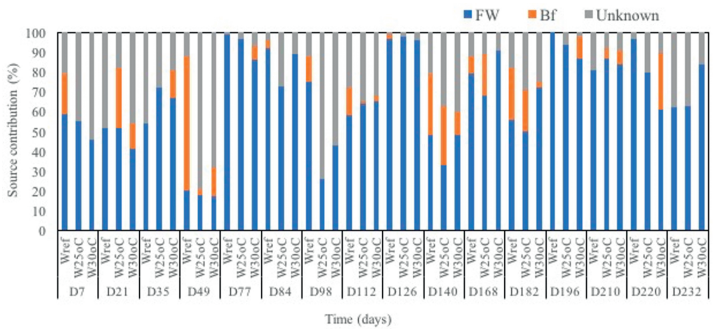


**Figure 3.8:** *The results of source tracker method, showing percent contributions of microbial communities from different sources (feed water =FW, biofilm from relevant pilot DS=Bf, Unkown sources) into sinks ($W_{ref}$ = water from reference system, $W_{25\,^{\circ}C}$ = water after cold recovery ($T_{max}$ = 25 °C), $W_{30\,^{\circ}C}$ = water after cold recovery ($T_{max}$ = 30 °C)) on each water sampling day.*

The results obtained from the source tracker for the $W_{ref}$ showed the $W_{fw}$ as the main contributor (52–100%) from day 7 till day 232 and the contributions of $W_{fw}$ were varying over time based on the contribution from unkown sources (3-38%) and from $Bf_{ref}$. The latter has an input of 20% on day 7 and a maximum contribution on day 49 (68%). The contribution of $Bf_{ref}$ decreased between day 77 and day 84 (0–4%) and was increasing again from day 98 (12%) to day 182 with a contribution of 26%. Later on, from day 196 till day 232 $W_{fw}$ was observed to contribute 62–100%.

In the $W_{25\,^{\circ}C}$, feed water also made the major contributions (26–98%) and the contributions from unknown sources ranged from 2 to 79% over the study period. $Bf_{25\,^{\circ}C}$ made the highest contribution on day 21 (30%) and a decrease or no contribution was observed from day 35 till day 126. Then an increase was seen from day 140 to 182 (21–30%) and a final contribution of 5% on day 210.

In the $W_{30\,^{\circ}C}$ from day 7 to day 232, feed water contributions ranged from 17 to 96% and the unknown sources were contributing 2–57%. The $Bf_{30\,^{\circ}C}$ had a maximum contribution from day 21 to day 77 (7–15%), then a decrease or no contributions from day 84 to day 126 and again an increase was observed on day 140 (12%). Later on, a decrease or no contribution was seen on day 168, then an increase was observed on day 182, and a final contribution of 29% on day 220.

## 1.4 Discussion

### 1.4.1 Influence of cold recovery on the early growth and development of biofilms

The microbiological characteristics of the DWDSs have been studied widely and thoroughly both for chlorinated (Douterelo et al., 2013; Potgieter et al., 2018) and unchlorinated systems (Prest et al., 2016b; Vital et al., 2012). The current study focused on the microbial impacts of application of a new technology, cold recovery, within unchlorinated systems. Especially development and growth of the biofilms were studied dynamically over time to trace changes during their formation, as biofilms are the micro-environments which are thought to be long-term residents (from days to decades) within DWDSs (Flemming et al., 2016; Henne et al., 2012; Van Der Wende et al., 1989). Bacterial biofilm development on pipe surfaces are characterized by a series of developmental stages, which

includes: 1) initial preconditioning of surface (recruitment of organic substances from bulk water; as soon as (minutes/hours) the surface is exposed to flowing water, on which bacteria will attach), 2) attachment of primary colonizers, 3) growth of attached bacteria, 4) protozoans grazing and 5) finally detachment of bacterial cells from biofilm into the flowing bulk water (Mathieu et al., 2019).

Development of biofilms at different temperatures has not yet been studied inside DWDSs, but a study on river water has reported an acceleration of microbial colonization at higher temperatures (Diaz Villanueva et al., 2011). Similarly, we observed here temperature as a controlling factor for the initial growth of biofilms within unchlorinated pilot DSs, not only by accelerating the primary colonization (higher relative abundance of *Betaproteobacteriales* starting from day 7) of microbes within biofilms, grown at 30 °C (Figure 3.5), but also by enhancing the early biomass formation in the biofilms, developed at 30 °C after cold recovery, which grew faster at the beginning (day 7), in terms of ATP and TCC (Figure 3.2). At the higher temperature, the peaks in biofilm development (ATP and TCC) during the first 50 days occurred earlier. The biofilm at 30 °C became more diverse and complex in microbial community composition earlier (day 14) compared to the biofilms which were grown at lower ($Bf_{25\ ^{\circ}C}$ on day 28) and fluctuating ($Bf_{ref}$ on day 49) temperatures (Figure 3.5).



The biofilms that developed in all three pilot DSs, although following an independent timeline for their development, showed an increase in biomass, along with occurrence of primary colonizers (*Betaproteobacteriales*) and consequently a decrease in biomass and an increasing relative abundance of other microbial groups (amoeba resisting groups; *Xanthobacteraceae*, *Legionellales*), including those responsible for EPS formation in biofilms (*Sphingomonadaceae*) which protects them from outer stresses (Balkwill et al., 2006; Fish et al., 2016). This biomass decrease was possibly related to protozoan grazing within the first 50 days (Van der Kooij et al., 2018), which was observed on day 28 in $Bf_{25\ ^{\circ}C}$ and $Bf_{30\ ^{\circ}C}$, and on day 49 in $Bf_{ref}$ (Figure 3.2 a and b). Later in time, biofilms reached a more even/mature state of growth (Henne et al., 2012), in terms of microbial diversity and abundance, which has been observed here around day 49 for biofilms grown after cold recovery (25 °C, 30 °C) and day 84 for reference biofilms (Figure 3.4).

The microbial similarities among biofilms after day 84 showed that feed water quality and composition determines the microbial diversity and composition of more stable/mature biofilms (Ling et al., 2015; Neu et al., 2019). The environmental conditions (Rogers et al., 1994) (temperature in this case) only play a significant role during early primary colonization and growth of microbes, where differences in microbial composition and biomass were observed among the three pilot DSs.

### 1.4.2 Influence of biofilm development on pipe surface on bulk water characteristics

In the first few months of operation (7–77 days), the amount of biomass, as measured by ATP and specifically the number of high nucleic acid (HNA) cells in the bulk water from all three DSs was higher than that in the feed water (Figure 3.3b). This was most pronounced in the system without cold recovery ($W_{ref}$). HNA cells are associated with active biomass (Lebaron et al., 2001) and primary colonizers (Proctor et al., 2018). Indeed, higher relative abundance of these groups (primary colonizers-Figure 3.7) was observed in the bulk water in the pilot DSs, from day 7 to day 77. The

increased presence of these groups in the bulk water is possibly linked to the fast growth of biomass and proliferation of primary colonizers (*Betaproteobacteriales*, *Pseudomonadales*, *Sphingomonadales*) (Van der Kooij et al., 2018) within biofilms on the pipe surfaces.

Furthermore, the presence of a biofilm associated bacterial group (*Sphingomonadales*), only in effluent water ($W_{ref}$, $W_{25\,°C}$, $W_{30\,°C}$) of the DSs and not in the feed water, shows the detachment of these cells from biofilm into the bulk water. This is confirmed by the results of the microbial source tracking (Figure 3.8), where microbial communities of biofilms ($Bf_{ref}$, $Bf_{25\,°C}$, $Bf_{30\,°C}$) along with feed water communities showed a relevant contribution to the effluent water from all three DSs. The increased contribution from biofilms coincided with the initial maximum biomass growth within the biofilms. In the system without cold recovery ($W_{ref}$) these were observed later (on day 49, between day 98 and day 112 and from day 140 to day 182) than in the 25 °C and 30 °C systems (on day 21, day 49 and from day 140 to day 182 (25 °C) and from day 196 to day 220 (30 °C)). The biofilm in the reference system was relatively dense for a longer period, during which increased ATP and HNA were observed in the bulk water ($W_{ref}$). Thus it can be inferred that it took a longer period to form more stable biofilms in terms of detachment.

The microbial composition of the bulk water was largely determined by the composition of the feed water as revealed by the source tracking, which showed remarkable fluctuations in numbers of OTUs and in diversity. The higher numbers of OTUs within the feed water on different days of study (day 21, 49, 98, 112, 140 and 182, Figure 3.6a) did not affect ATP concentrations and cell numbers for all three systems, and similar abundance and diversity were observed in effluent water of the DSs after cold recovery and the reference system. Overall, similar microbial groups were present in the feed water (Figure S3.5) but with different relative abundances on different days of the study (Figure 3.7). It is noted that the upstream treatment processes (biologically activated carbon filtration and slow sand filtration) contain biofilms that are allowed to mature over long periods of time. The fluctuating microbial composition of water after treatment with slow sand filtration was previously described (Bai et al., 2013; Oh et al., 2018), and is linked to scraping the schmutzdecke layer while periodically changing the sand filters, resulting in varying microbial composition, evenness and diversity of effluent water from the treatment plant (Chan et al., 2018; Haig et al., 2015).

Overall, cold recovery with subsequent increase in temperature to 25 and 30 °C showed no negative effects on microbial drinking water quality parameters (ATP, TCC) as compared to the reference. The observed changes in bulk water characteristics relative to the feed water were mostly linked with formation and growth of biofilms on pipe surface, during initial growth and decline periods (day 7–77). However, there were some differences in water after the cold recovery systems compared to the feed water and the reference water, for example the presence of specific OTUs (*Methyloversatilis*, *Sphingobium*, *Sphingomonas*) . The occurrence of *Methyloversatilis* is possibly related to its utilization of low molecular weight carboxylic acids released from pipe surfaces under warm water conditions (Smalley et al., 2015; Van der Kooij et al., 2018). However, this bacterium's nutritional conditions and growth kinetics are not studied here and require further research. Further, the *Sphingobium* and *Sphingomonas* are relevant to biofilm formation and colonization of bacteria on

pipe surface (Costerton et al., 1995; Flemming et al., 2016), which caused their regrowth in the water phase within the pilot DSs.

## 1.5 Practical implications for water utilities

Our study showed how cold recovery, or increase in temperature, influenced the microbiology within DWDSs, such as faster primary colonization by *Betaproteobacteriales*. These may serve as prey for amoeba (Van der Kooij et al., 2018), which is followed by the simultaneous occurrence of amoeba resistant microbial groups (*Xanthobacteraceae*, *Legionellales*) in the biofilms. In contrast to observations from biofilms, *Legionellales* were not found in bulk water samples, but their persistent presence in the biofilms (within the DSs operated at 25 and 30 °C till day 232) might lead to a regrowth problem in the bulk water under favourable circumstances of higher temperature after cold recovery. Also the presence of *Pseudomonas* (in the feed water, as well as in the pilot DSs) as a core OTU among all water samples and their regrowth in biofilms needs to be closely monitored while applying cold recovery.



Hence, based on our findings new drinking water distribution systems need to be monitored more frequently within the first 2–3 months of applying cold recovery for possible effects on water quality parameters, like ATP, TCC (especially HNA cells) as well as for opportunistic pathogens like some species of *Legionella* and *Pseudomonas*. This is similar to the transition effects of changing quality of the feed water (Chen et al., 2020), where it was also suggested to monitor the system for a period of six months during which the system is restabilized in terms of microbiological water quality. The application of cold recovery in existing DWDSs which are already in operation since many years or decades may similarly require a comparable transition period to achieve stable and uniform microbiological characteristics in terms of water quality, biofilm development and habitat formation inside the pipes.

## 1.6 Conclusion

- Cold recovery from drinking water results in a subsequent increase of the drinking water temperature. The higher the water temperature after cold recovery, the faster the primary colonization stage of biofilm development.
- Higher temperatures did not lead to higher biomass density or differences in diversity in the biofilm.
- The primary colonization stage of biofilm development on new pipes led to increased biomass activity (ATP) and, specifically, increased numbers of HNA cells within the water phase, which was most pronounced in the reference system without cold recovery.
- DWDSs need to be monitored more frequently for microbiological water quality, after start of the application of cold recovery in terms of microbial composition and diversity during the first 2–3 months of operation.

# References

Ahmad, J.I., Liu, G., Van der Wielen, P.W.J.J., Medema, G. and Van der Hoek, J.P. (2020) Effects of cold recovery technology on the microbial drinking water quality in unchlorinated distribution systems. Environmental Research 183, 109175.

Baghoth, S.A., Sharma, S.K. and Amy, G.L. (2011) Tracking natural organic matter (NOM) in a drinking water treatment plant using fluorescence excitation–emission matrices and PARAFAC. Water Research 45(2), 797-809.

Bai, Y., Liu, R., Liang, J. and Qu, J. (2013) Integrated Metagenomic and Physiochemical Analyses to Evaluate the Potential Role of Microbes in the Sand Filter of a Drinking Water Treatment System. Public Library of Science 8(4), e61011.

Balkwill, D.l., Fredrickson, J.K. and Romine, M.F. (2006) The Prokaryotes. Martin Dworkin (Editor-in-Chief), S.F., Eugene Rosenberg, and Karl-Heinz Schleifer, E.S.E. (eds), Springer International Publishing, Singapore.

Bolyen, E., Rideout, J.R., Dillon, M.R., Bokulich, N.A., Abnet, C.C., Al-Ghalith, G.A., Alexander, H., Alm, E.J., Arumugam, M., Asnicar, F., Bai, Y., Bisanz, J.E., Bittinger, K., Brejnrod, A., Brislawn, C.J., Brown, C.T., Callahan, B.J., Caraballo-Rodríguez, A.M., Chase, J., Cope, E.K., Da Silva, R., Diener, C., Dorrestein, P.C., Douglas, G.M., Durall, D.M., Duvallet, C., Edwardson, C.F., Ernst, M., Estaki, M., Fouquier, J., Gauglitz, J.M., Gibbons, S.M., Gibson, D.L., Gonzalez, A., Gorlick, K., Guo, J., Hillmann, B., Holmes, S., Holste, H., Huttenhower, C., Huttley, G.A., Janssen, S., Jarmusch, A.K., Jiang, L., Kaehler, B.D., Kang, K.B., Keefe, C.R., Keim, P., Kelley, S.T., Knights, D., Koester, I., Kosciolek, T., Kreps, J., Langille, M.G.I., Lee, J., Ley, R., Liu, Y.-X., Loftfield, E., Lozupone, C., Maher, M., Marotz, C., Martin, B.D., McDonald, D., McIver, L.J., Melnik, A.V., Metcalf, J.L., Morgan, S.C., Morton, J.T., Naimey, A.T., Navas-Molina, J.A., Nothias, L.F., Orchanian, S.B., Pearson, T., Peoples, S.L., Petras, D., Preuss, M.L., Pruesse, E., Rasmussen, L.B., Rivers, A., Robeson, M.S., Rosenthal, P., Segata, N., Shaffer, M., Shiffer, A., Sinha, R., Song, S.J., Spear, J.R., Swafford, A.D., Thompson, L.R., Torres, P.J., Trinh, P., Tripathi, A., Turnbaugh, P.J., Ul-Hasan, S., van der Hooft, J.J.J., Vargas, F., Vázquez-Baeza, Y., Vogtmann, E., von Hippel, M., Walters, W., Wan, Y., Wang, M., Warren, J., Weber, K.C., Williamson, C.H.D., Willis, A.D., Xu, Z.Z., Zaneveld, J.R., Zhang, Y., Zhu, Q., Knight, R. and Caporaso, J.G. (2019) Reproducible, interactive, scalable and extensible microbiome data science using QIIME 2. Nature Biotechnology 37(8), 852-857.

Callahan, B.J., McMurdie, P.J., Rosen, M.J., Han, A.W., Johnson, A.J.A. and Holmes, S.P. (2016) DADA2: High-resolution sample inference from Illumina amplicon data. Nature Methods 13, 581.

Chan, S., Pullerits, K., Riechelmann, J., Persson, K.M., Rådström, P. and Paul, C.J. (2018) Monitoring biofilm function in new and matured full-scale slow sand filters using flow cytometric histogram image comparison (CHIC). Water Research 138, 27-36.

Chen, L., Ling, F., Bakker, G., Liu, W.-T., Medema, G., Van der Meer, W. and Liu, G. (2020) Assessing the transition effects in a drinking water distribution system caused by changing supply water quality: an indirect approach by characterizing suspended solids. Water Research 168, 115-159.

Costerton, J.W., Lewandowski, Z., Caldwell, D.E., Korber, D.R. and Lappin-Scott, H.M. (1995) Microbial biofilms. Annual Reviews in Microbiology 49(1), 711-745.

Diaz Villanueva, V., Font, J., Schwartz, T. and Romani, A.M. (2011) Biofilm formation at warming temperature: acceleration of microbial colonization and microbial interactive effects. Biofouling 27(1), 59-71.

Douterelo, I., Sharpe, R. and Boxall, J. (2013) Influence of hydraulic regimes on bacterial community structure and composition in an experimental drinking water distribution system. Water Research 47(2), 503-516.

El-Chakhtoura, J., Prest, E., Saikaly, P., Van Loosdrecht, M., Hammes, F. and Vrouwenvelder, H. (2015) Dynamics of bacterial communities before and after distribution in a full-scale drinking water network. Water Research 74, 180-190.

Fish, K.E., Osborn, A.M. and Boxall, J. (2016) Characterising and understanding the impact of microbial biofilms and the extracellular polymeric substance (EPS) matrix in drinking water distribution systems. Environmental science: water research & technology 2(4), 614-630.

Flemming, H.-C., Wingender, J., Szewzyk, U., Steinberg, P., Rice, S.A. and Kjelleberg, S. (2016) Biofilms: an emergent form of bacterial life. Nature Reviews Microbiology 14, 563.

Haig, S.-J., Quince, C., Davies, R.L., Dorea, C.C. and Collins, G. (2015) The Relationship between Microbial Community Evenness and Function in Slow Sand Filters. mBio 6(5), e00729-00715.

Henne, K., Kahlisch, L., Brettar, I. and Hofle, M.G. (2012) Analysis of structure and composition of bacterial core communities in mature drinking water biofilms and bulk water of a citywide network in Germany. Applied and environmental microbiology 78(10), 3530-3538.

Hull, N.M., Ling, F., Pinto, A.J., Albertsen, M., Jang, H.G., Hong, P.-Y., Konstantinidis, K.T., LeChevallier, M., Colwell, R.R. and Liu, W.-T. (2019) Drinking Water Microbiome Project: Is it Time? Trends in Microbiology 27(8), 670-677.

Kelly, J.J., Minalt, N., Culotti, A., Pryor, M. and Packman, A. (2014) Temporal Variations in the Abundance and Composition of Biofilm Communities Colonizing Drinking Water Distribution Pipes. Public Library of Science 9(5), e98542.

Knights, D., Kuczynski, J., Charlson, E.S., Zaneveld, J., Mozer, M.C., Collman, R.G., Bushman, F.D., Knight, R. and Kelley, S.T. (2011) Bayesian community-wide culture-independent microbial source tracking. Nature Methods 8(9), 761-763.

Lebaron, P., Servais, P., Agogué, H., Courties, C. and Joux, F. (2001) Does the high nucleic acid content of individual bacterial cells allow us to discriminate between active cells and inactive cells in aquatic systems? Applied and environmental microbiology 67(4), 1775-1782.

Ling, F., Hwang, C., LeChevallier, M.W., Andersen, G.L. and Liu, W.-T. (2015) Core-satellite populations and seasonality of water meter biofilms in a metropolitan drinking water distribution system. The ISME Journal 10, 582.

Ling, F., Whitaker, R., LeChevallier, M.W. and Liu, W.-T. (2018) Drinking water microbiome assembly induced by water stagnation. The ISME Journal 12(6), 1520-1531.

Liu, G., Bakker, G.L., Li, S., Vreeburg, J.H.G., Verberk, J.Q.J.C., Medema, G.J., Liu, W.T. and Van Dijk, J.C. (2014) Pyrosequencing Reveals Bacterial Communities in Unchlorinated Drinking Water Distribution System: An Integral Study of Bulk Water, Suspended Solids, Loose Deposits, and Pipe Wall Biofilm. Environmental science & technology 48(10), 5467-5476.

Liu, G., Tao, Y., Zhang, Y., Lut, M., Knibbe, W.-J., van der Wielen, P., Liu, W., Medema, G. and van der Meer, W. (2017) Hotspots for selected metal elements and microbes accumulation and the corresponding water quality deterioration potential in an unchlorinated drinking water distribution system. Water Research 124, 435-445.

Liu, G., Verberk, J.Q.J.C. and Van Dijk, J.C. (2013) Bacteriology of drinking water distribution systems: an integral and multidimensional review. Applied Microbiology and Biotechnology 97(21), 9265-9276.

Liu, G., Zhang, Y., Van der Mark, E., Magic-Knezev, A., Pinto, A., Van den Bogert, B., Liu, W., Van der Meer, W. and Medema, G. (2018) Assessing the origin of bacteria in tap water and distribution system in an unchlorinated drinking water system by SourceTracker using microbial community fingerprints. Water Research 138, 86-96.

Magic-Knezev, A. and van der Kooij, D. (2004) Optimisation and significance of ATP analysis for measuring active biomass in granular activated carbon filters used in water treatment. Water Research 38(18), 3971-3979.

Mathieu, L., Paris, T. and Block, J.-C. (2019) The Structure and Function of Aquatic Microbial Communities. Hurst, C.J. (ed), pp. 261-311, Springer International Publishing, Cham.

Mol, S., Kornman, J., Kerpershoek, A. and Van Der Helm, A. (2011) Opportunities for public water utilities in the market of energy from water. Water Science & Technology 63(12).

Neu, L., Proctor, C.R., Walser, J.-C. and Hammes, F. (2019) Small-Scale Heterogeneity in Drinking Water Biofilms. Frontiers in Microbiology 10(2446).

Oh, S., Hammes, F. and Liu, W.-T. (2018) Metagenomic characterization of biofilter microbial communities in a full-scale drinking water treatment plant. Water Research 128, 278-285.

Potgieter, S., Pinto, A., Sigudu, M., Du Preez, H., Ncube, E. and Venter, S. (2018) Long-term spatial and temporal microbial community dynamics in a large-scale drinking water distribution system with multiple disinfectant regimes. Water Research 139, 406-419.

Prest, E.I., Hammes, F., Kötzsch, S., Van Loosdrecht, M.C.M. and Vrouwenvelder, J.S. (2013) Monitoring microbiological changes in drinking water systems using a fast and reproducible flow cytometric method. Water Research 47(19), 7131-7142.

Prest, E.I., Hammes, F., van Loosdrecht, M.C.M. and Vrouwenvelder, J.S. (2016a) Biological Stability of Drinking Water: Controlling Factors, Methods, and Challenges. Frontiers in Microbiology 7, 45.

Prest, E.I., Weissbrodt, D.G., Hammes, F., Van Loosdrecht, M.C.M. and Vrouwenvelder, J.S. (2016b) Long-Term Bacterial Dynamics in a Full-Scale Drinking Water Distribution System. Public Library of Science 11(10), e0164445.

Proctor, C.R., Besmer, M.D., Langenegger, T., Beck, K., Walser, J.-C., Ackermann, M., Bürgmann, H. and Hammes, F. (2018) Phylogenetic clustering of small low nucleic acid-content bacteria across diverse freshwater ecosystems. The ISME Journal 12(5), 1344-1359.

Rogers, J., Dowsett, A.B., Dennis, P.J., Lee, J.V. and Keevil, C.W. (1994) Influence of temperature and plumbing material selection on biofilm formation and growth of Legionella pneumophila in a model potable water system containing complex microbial flora. Applied and environmental microbiology 60.

Smalley, N.E., Taipale, S., De Marco, P., Doronina, N.V., Kyrpides, N., Shapiro, N., Woyke, T. and Kalyuzhnaya, M.G. (2015) Functional and genomic diversity of methylotrophic Rhodocyclaceae: description of Methyloversatilis discipulorum sp. nov. Int J Syst Evol Microbiol 65(7), 2227-2233.

Smeets, P., Medema, G. and Van Dijk, J. (2009) The Dutch secret: how to provide safe drinking water without chlorine in the Netherlands. Drinking Water Engineering and Science 2(1), 1-14.

Staatscourant (2011) Staatscourant (State Journal in Dutch) 2011 Decree of 23 May 2011 concerning the regulations for the production and distribution of drinking water and the organisation of the public drinking water supply, The Netherlands.

Thijs, S., Op De Beeck, M., Beckers, B., Truyens, S., Stevens, V., Van Hamme, J.D., Weyens, N. and Vangronsveld, J. (2017) Comparative Evaluation of Four Bacteria-Specific Primer Pairs for 16S rRNA Gene Surveys. Frontiers in Microbiology 8, 494.

Van der Hoek, J.P., Mol, S., Giorgi, S., Ahmad, J.I., Liu, G. and Medema, G. (2018) Energy recovery from the water cycle: Thermal energy from drinking water. Energy 162, 977-987.

Van der Kooij, D. (1992) Assimilable organic carbon as an indicator of bacterial regrowth. Journal of American Water Works Association 84(2), 57-65.

Van der Kooij, D. and Van der Wielen, P.W. (2013) Microbial growth in drinking-water supplies: problems, causes, control and research needs. Water Intelligence Online 12, 9781780400419.

Van der Kooij, D., Veenendaal, H.R., Italiaander, R., Van der Mark, E.J. and Dignum, M. (2018) Primary Colonizing Betaproteobacteriales Play a Key Role in the Growth of Legionella pneumophila in Biofilms on Surfaces Exposed to Drinking Water Treated by Slow Sand Filtration. Applied and environmental microbiology 84(24), e01732-01718.

Van Der Wende, E., Characklis, W.G. and Smith, D.B. (1989) Biofilms and bacterial drinking water quality. Water Research 23(10), 1313-1322.

Vital, M., Dignum, M., Magic-Knezev, A., Ross, P., Rietveld, L. and Hammes, F. (2012) Flow cytometry and adenosine tri-phosphate analysis: Alternative possibilities to evaluate major bacteriological changes in drinking water treatment and distribution systems. Water Research 46(15), 4665-4676.

Wingender, J. and Flemming, H.-C. (2011) Biofilms in drinking water and their role as reservoir for pathogens. International Journal of Hygiene and Environmental Health 214(6), 417-423.

Zhou, X., Zhang, K., Zhang, T., Li, C. and Mao, X. (2017) An ignored and potential source of taste and odor (T&O) issues-biofilms in drinking water distribution system (DWDS). Applied Microbiology and Biotechnology 101(9), 3537-3550.

Zlatanović, L., Van der Hoek, J.P. and Vreeburg, J.H.G. (2017) An experimental study on the influence of water stagnation and temperature change on water quality in a full-scale domestic drinking water system. Water Research 123, 761-772.

# Supplementary Information chapter 3

## Heat Exchanger description:

For increasing the temperature of water and mimicking cold recovery, two plate heat exchangers (HE's) (Minex, SWEP, Sweden) were used for each of the cold recovery system. Within the HE, on the plate surface heat is transferred between two fluids within a short time span (few seconds), cold (the feed drinking water) and hot (recirculating water). The HE consists of 6 plates, 3 plates for hot recirculating medium, 2 plates for cold drinking water and 1 blank plate. For recirculating heated water a hot tank (RVS boiler, AquaHeat, The Netherlands) and temperature sensor were connected with the hot channel of the HE. This setup was connected with a computer system through a frequency controller to further regulate the temperature on the HE surfaces, in order to maintain the threshold of 25 $^{0}$C and 30 $^{0}$C respectively, in effluent drinking water leaving the HEs.

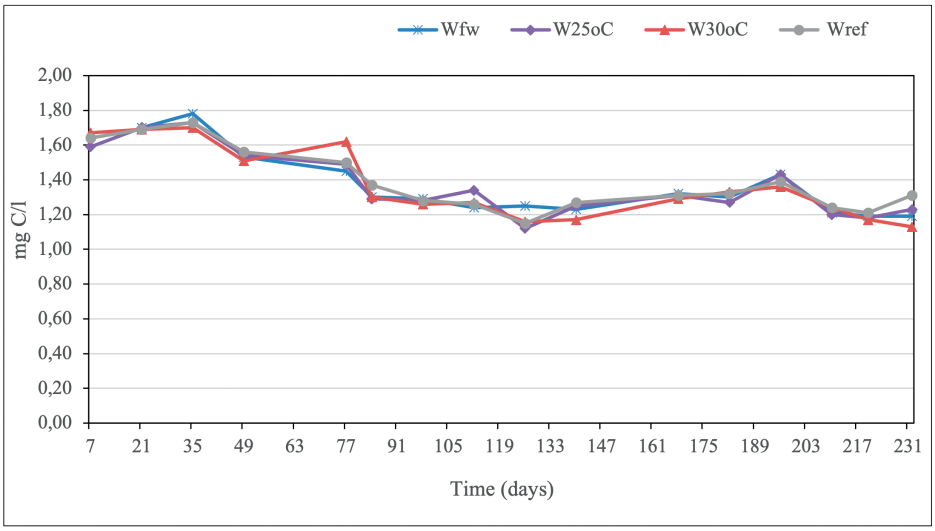


**Figure S3.1:** Dissolved organic carbon measured from all drinking water samples (($W_{fw}$ = feed water, $W_{ref}$ = water from reference system, $W_{25\,^{\circ}C}$ = water after cold recovery ($T_{max}$ = 25 °C), $W_{30\,^{\circ}C}$ = water after cold recovery ($T_{max}$ = 30 °C)).

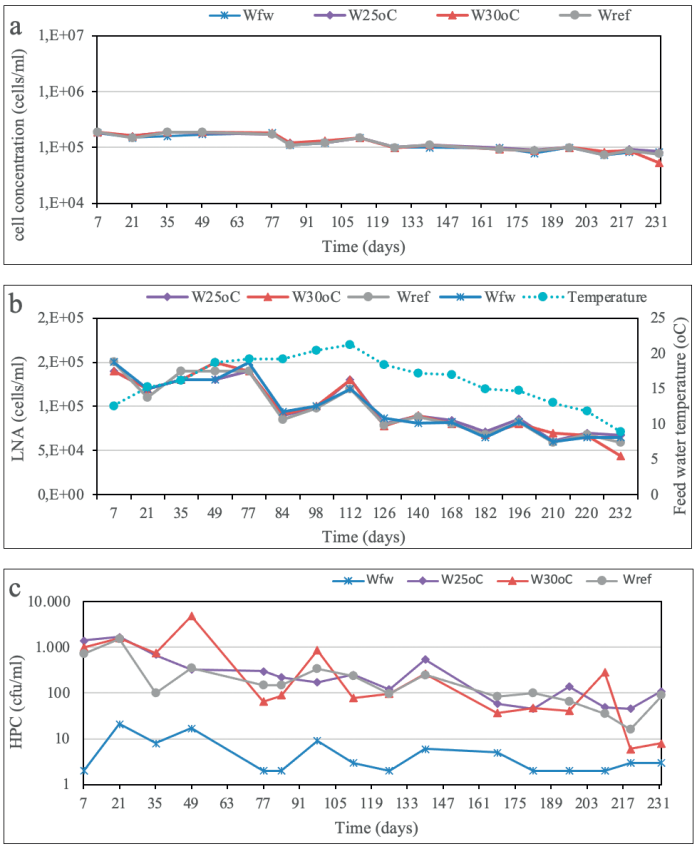


**Figure S3.2:** Biomass from drinking water samples measured as a) Total cell concentration, b) Low nucleic acid (LNA) cells and c) Heterotrophic plate counts (HPC), from all studied sampling sites ($W_{fw}$ = feed water, $W_{ref}$ = water from reference system, $W_{25\ °C}$ = water after cold recovery ($T_{max}$ = 25 °C), $W_{30\ °C}$ = water after cold recovery ($T_{max}$ = 30 °C)).

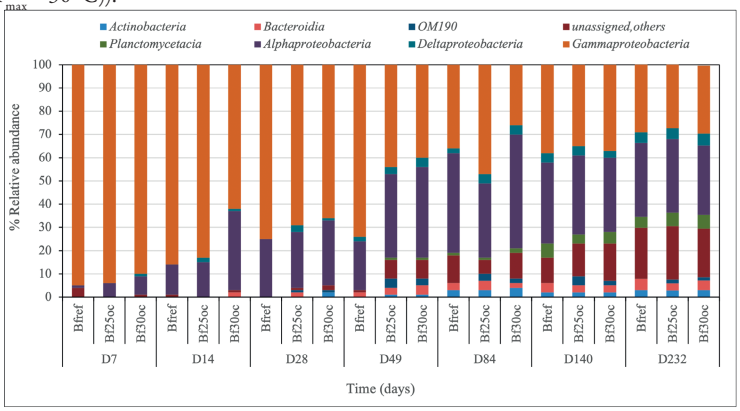


**Figure S3.3:** Percent Relative abundance (%) of core microbial groups at Class level of taxonomic composition, from all biofilm samples ($Bf_{ref}$ = biofilm from reference system, $Bf_{25\ °C}$ = biofilm formed after cold recovery ($T_{max}$ = 25 °C), $Bf_{30\ °C}$ = biofilm formed after cold recovery ($T_{max}$ = 30 °C)).


**Figure S3.4:** Relative abundances of core microbial groups at class level of taxonomic composition, from all water samples ($W_{fw}$ = feed water, $W_{ref}$ = water from reference system, $W_{25\ ^{\circ}C}$ = water after cold recovery ($T_{max}$ = 25 °C), $W_{30\ ^{\circ}C}$ = water after cold recovery ($T_{max}$ = 30 °C)).

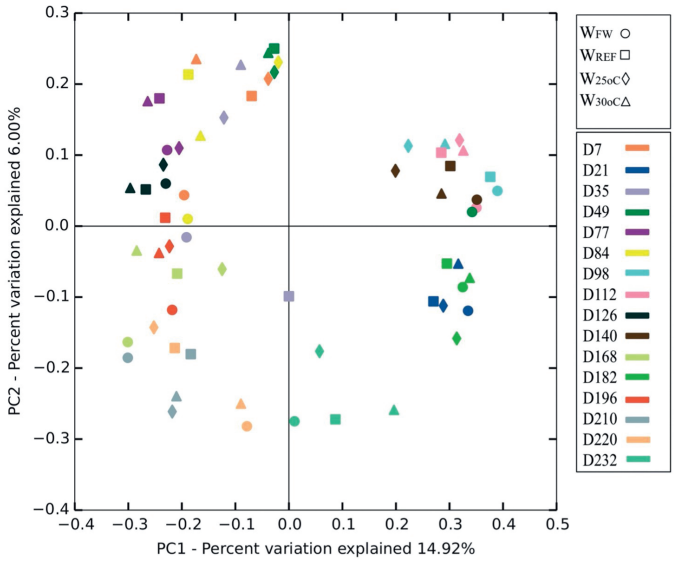


**Figure S3.5:** Principle coordinate analysis (PCoA) of water samples shown here are based on measures from Jaccard distance matrix (representing presence or absence of OTUs). This figure includes samples of feed water ($W_{FW}$) and effluent water from all three distribution systems, DS-1 30 °C ($W_{30\ °C}$), DS-2 25 °C ($W_{25\ °C}$), and DS-3 REF ($W_{REF}$), from day 7 through day 232 of experiment (as shown in colour scheme).

**Table S3.1:** The microbial community sources used by source tracker method for determining their contributions (%) in effluent water (sink) from each system on designated sampling day.

| Sink Days | Sources | |
|---|---|---|
| | Feed water samples (days) | Biofilm samples (days) |
| 7 | 7 | 7 |
| 21 | 21 | 7+14 |
| 35 | 35 | 7+14+28 |
| 49 | 49 | 7+14+28+49 |
| 77 | 77 | 7+14+28+49 |
| 84 | 84 | 7+14+28+49+84 |
| 98 | 98 | 7+14+28+49+84 |
| 112 | 112 | 7+14+28+49+84 |
| 126 | 126 | 7+14+28+49+84 |
| 140 | 140 | 7+14+28+49+84+140 |
| 168 | 168 | 7+14+28+49+84+140 |
| 182 | 182 | 7+14+28+49+84+140 |
| 196 | 196 | 7+14+28+49+84+140 |
| 210 | 210 | 7+14+28+49+84+140 |
| 220 | 220 | 7+14+28+49+84+140 |
| 232 | 232 | 7+14+28+49+84+140+232 |

**Table S3.2:** Temperature details for the drinking water throughout the study period. Here its representing the temperature of the feed water ($W_{fw}$) and reference water ($W_{ref}$) samples and the differences ($\Delta T$) between the temperature after cold recovery systems of both pilot cold recovery distribution systems (DS-1 and DS-2).

| | Temperature (°C) | | |
|---|---|---|---|
| **Days** | **Temperature $W_{fw}$ and $W_{ref}$** | **$\Delta T$ $W_{25\ ^{o}C}$** | **$\Delta T$ $W_{30\ ^{o}C}$** |
| $D_{7}$ | 12.6 | 12 | 17 |
| $D_{21}$ | 15.2 | 10 | 15 |
| $D_{35}$ | 16.2 | 9 | 14 |
| $D_{49}$ | 18.7 | 6 | 11 |
| $D_{77}$ | 19.2 | 6 | 11 |
| $D_{84}$ | 19.2 | 6 | 11 |
| $D_{98}$ | 20.4 | 5 | 10 |
| $D_{112}$ | 21.2 | 4 | 9 |
| $D_{126}$ | 18.4 | 7 | 12 |
| $D_{140}$ | 17.2 | 8 | 13 |
| $D_{168}$ | 17 | 8 | 13 |
| $D_{182}$ | 15 | 10 | 15 |
| $D_{196}$ | 14.7 | 10 | 15 |
| $D_{210}$ | 13 | 12 | 17 |
| $D_{220}$ | 11.8 | 13 | 18 |
| $D_{231}$ | 8.9 | 16 | 21 |

**Table S3.3:** a) Major core phyla and b) core taxa (at genus level), observed from all biofilm samples ($Bf_{ref}$ = biofilm from reference system, $Bf_{25\ ^{o}C}$ = biofilm formed after cold recovery ($T_{max}$ = 25 °C), $Bf_{30\ ^{o}C}$ = biofilm formed after cold recovery ($T_{max}$ = 30 °C)).

| **a** | **$Bf_{ref}$** | **$Bf_{25\ ^{o}C}$** | **$Bf_{30\ ^{o}C}$** |
|---|---|---|---|
| **Core Phyla observed** | Planctomycetes | Bacteroidetes | Actinobacteria |
| | Proteobacteria | Planctomycetes | Bacteroidetes |
| | | Proteobacteria | Planctomycetes |
| | | | Proteobacteria |

| **b** | **Phylum** | **Class** | **Order** | **Family** | **Genus** |
|---|---|---|---|---|---|
| **$Bf_{ref}$** | Proteobacteria | Alphaproteobacteria | Sphingomonadales | Sphingomonadaceae | Sphingobium |
| | Proteobacteria | Alphaproteobacteria | Sphingomonadales | Sphingomonadaceae | Sphingomonas |
| | Proteobacteria | Alphaproteobacteria | Sphingomonadales | Sphingomonadaceae | Sphingopyxis |
| | Proteobacteria | Gammaproteobacteria | Betaproteobacteriales | Rhodocyclaceae | Methyloversatilis |
| | Proteobacteria | Gammaproteobacteria | Pseudomonadales | Pseudomonadaceae | Pseudomonas |

**Table S3.3:** Continued

| b | Phylum | Class | Order | Family | Genus |
|---|---|---|---|---|---|
| $Bf_{25\ °C}$ | Proteobacteria | Alphaproteobacteria | Sphingomonadales | Sphingomonadaceae | Novosphingobium |
| | Proteobacteria | Alphaproteobacteria | Sphingomonadales | Sphingomonadaceae | Sphingobium |
| | Proteobacteria | Alphaproteobacteria | Sphingomonadales | Sphingomonadaceae | Sphingomonas |
| | Proteobacteria | Alphaproteobacteria | Sphingomonadales | Sphingomonadaceae | Sphingopyxis |
| | Proteobacteria | Gammaproteobacteria | Betaproteobacteriales | Rhodocyclaceae | Methyloversatilis |
| | Proteobacteria | Gammaproteobacteria | Pseudomonadales | Pseudomonadaceae | Pseudomonas |
| $Bf_{30\ °C}$ | Proteobacteria | Alphaproteobacteria | Sphingomonadales | Sphingomonadaceae | Novosphingobium |
| | Proteobacteria | Alphaproteobacteria | Sphingomonadales | Sphingomonadaceae | Sphingobium |
| | Proteobacteria | Alphaproteobacteria | Sphingomonadales | Sphingomonadaceae | Sphingomonas |
| | Proteobacteria | Alphaproteobacteria | Sphingomonadales | Sphingomonadaceae | Sphingopyxis |
| | Proteobacteria | Gammaproteobacteria | Pseudomonadales | Pseudomonadaceae | Pseudomonas |

**Table S3.4:** a) Major core phyla and b) core taxa (at genus level), observed from all water samples ($W_{fw}$ = feed water, $W_{ref}$ = water from reference system, $W_{25\ °C}$ = water after cold recovery ($T_{max}$ = 25 °C), $W_{30\ °C}$ = water after cold recovery ($T_{max}$ = 30 °C)).

| a | $W_{fw}$ | $W_{25\ °C}$ | $W_{30\ °C}$ | $W_{ref}$ |
|---|---|---|---|---|
| **Observed Phyla** | Acidobacteria | Acidobacteria | Acidobacteria | Acidobacteria |
| | Patescibacteria | Actinobacteria | Actinobacteria | Patescibacteria |
| | Proteobacteria | Patescibacteria | Patescibacteria | Proteobacteria |
| | | Planctomycetes | Proteobacteria | |
| | | Proteobacteria | | |

| b | Phylum | Class | Order | Family | Genus |
|---|---|---|---|---|---|
| | Patescibacteria | Parcubacteria | Candidatus Kaiserbacteria | Parcubacteria group bacterium CG1_02_50_68 | Parcubacteria group bacterium CG1_02_50_68 |
| | Proteobacteria | Gammaproteobacteria | Betaproteobacteriales | Burkholderiaceae | Duganella |
| $W_{fw}$ | Proteobacteria | Gammaproteobacteria | Betaproteobacteriales | Burkholderiaceae | Polaromonas |
| | Proteobacteria | Gammaproteobacteria | Betaproteobacteriales | Burkholderiaceae | Undibacterium |
| | Proteobacteria | Gammaproteobacteria | Betaproteobacteriales | Burkholderiaceae | not available |
| | Proteobacteria | Gammaproteobacteria | Pseudomonadales | Pseudomonadaceae | Pseudomonas |

**Table S3.4:** Continued

| b | Phylum | Class | Order | Family | Genus |
|---|---|---|---|---|---|
| | Patescibacteria | Parcubacteria | Candidatus Kaiserbacteria | Parcubacteria group bacterium CG1_02_50_68 | Parcubacteria group bacterium CG1_02_50_68 |
| | Proteobacteria | Alphaproteobacteria | Sphingomonadales | Sphingomonadaceae | Sphingopyxis |
| $W_{ref}$ | Proteobacteria | Gammaproteobacteria | Betaproteobacteriales | Burkholderiaceae | Aquabacterium |
| | Proteobacteria | Gammaproteobacteria | Betaproteobacteriales | Burkholderiaceae | Polaromonas |
| | Proteobacteria | Gammaproteobacteria | Betaproteobacteriales | Burkholderiaceae | not available |
| | Proteobacteria | Gammaproteobacteria | Pseudomonadales | Pseudomonadaceae | Pseudomonas |
| | Actinobacteria | Actinobacteria | Corynebacteriales | Nocardiaceae | Nocardia |
| | Epsilonbacteraeota | Campylobacteria | Campylobacterales | Thiovulaceae | Sulfuricurvum |
| | Patescibacteria | Parcubacteria | Candidatus Kaiserbacteria | Parcubacteria group bacterium CG1_02_50_68 | Parcubacteria group bacterium CG1_02_50_68 |
| $W_{30^{o}C}$ | Proteobacteria | Alphaproteobacteria | Rhizobiales | Rhizobiaceae | Allorhizobium-Neorhizobium-Pararhizobium-Rhizobium |
| | Proteobacteria | Alphaproteobacteria | Sphingomonadales | Sphingomonadaceae | Sphingobium |
| | Proteobacteria | Alphaproteobacteria | Sphingomonadales | Sphingomonadaceae | Sphingopyxis |
| | Proteobacteria | Gammaproteobacteria | Betaproteobacteriales | Burkholderiaceae | not available |
| | Proteobacteria | Gammaproteobacteria | Betaproteobacteriales | Rhodocyclaceae | Methyloversatilis |
| | Proteobacteria | Gammaproteobacteria | Pseudomonadales | Pseudomonadaceae | Pseudomonas |
| | Patescibacteria | Parcubacteria | Candidatus Kaiserbacteria | Parcubacteria group bacterium CG1_02_50_68 | Parcubacteria group bacterium CG1_02_50_68 |
| | Proteobacteria | Alphaproteobacteria | Rhizobiales | Rhizobiaceae | Allorhizobium-Neorhizobium-Pararhizobium-Rhizobium |
| $W_{25^{o}C}$ | Proteobacteria | Alphaproteobacteria | Sphingomonadales | Sphingomonadaceae | Sphingobium |
| | Proteobacteria | Alphaproteobacteria | Sphingomonadales | Sphingomonadaceae | Sphingomonas |
| | Proteobacteria | Alphaproteobacteria | Sphingomonadales | Sphingomonadaceae | Sphingopyxis |
| | Proteobacteria | Gammaproteobacteria | Betaproteobacteriales | Burkholderiaceae | not available |
| | Proteobacteria | Gammaproteobacteria | Betaproteobacteriales | Methylophilaceae | not available |
| | Proteobacteria | Gammaproteobacteria | Betaproteobacteriales | Rhodocyclaceae | Methyloversatilis |
| | Proteobacteria | Gammaproteobacteria | Pseudomonadales | Pseudomonadaceae | Pseudomonas |

Chapter 4

# Temporal development of biofilms within non-chlorinated drinking water distribution systems at high temperature after thermal energy (cold) recovery

CHAPTER 4


## Abstract

The surplus of thermal energy in the form of cold within drinking water distribution systems (DWDSs) can be used as a potential energy resource for space cooling. The temperature of the drinking water increases after cold recovery, and how this increase in water temperature affects the biofilm development within DWDSs is not yet clear. The current research studied biofilm development within three pilot distribution systems. The high temperature (HT) system, with an operational heat exchanger, operated at a constantly stable and high temperature of 25 °C for a period of 99 weeks. Comparisons were made with a reference system (REF, without heat exchanger) and a control system (CR, with a non-operational heat exchanger) which were operated at relatively lower and fluctuating temperatures (ΔT=4–20 °C). This study showed that cold recovery influenced the early stages of biofilm development. This was quantified by observing a different pattern of biomass growth (ATP and cell counts) for HT biofilms, whereas REF and CR biofilms showed similar results. From 32 weeks onwards to 99 weeks, the temporal trend for HT biofilms showed 2–3.5 times less biomass compared to REF and CR biofilms. Further, the community diversity indices revealed that all three DWDSs reached to a similar diversity and eveness at week 12 (Shannon: 7.0±0.07, pielou's e: 0.9±0.01) but in system with cold recovery the pattern to reach this diversity was smoother compared to a decrease in diversity observed at week 7 (Shannon: 3.7±0.1, pielou's e: 0.7±0.01) in systems without cold recovery. These results showed that a constant high temperature of water results in an earlier steady state growth in the biofilms, while the biomass activity remains lower as compared with biofilms developed under more variable low drinking water temperature.



**Keywords:** Microbial community and diversity, biofilm development, drinking water distribution system, temperature, biofilm, microbial succession

*This chapter is in preparation for publication as: Ahmad, J.I., Van der Wielen, P.W.J.J., Liu, G., Medema, G. and Van der Hoek, J.P. Temporal development of biofilms within non-chlorinated drinking water distribution systems at high temperature after thermal energy (cold) recovery.*

## 1.1 Introduction

Under the influence of climate change the temperature of the ambient air is increasing (Stocker et al., 2013) and is consequently triggering higher cooling requirements. The greenhouse gas emission related to space cooling accounted for more than 2.4% in United States, which will keep increasing with the changes in climate (US Energy Information Administration, 2016). To reduce the carbon footprint and to use more sustainable sources for cooling, drinking water distribution systems (DWDSs) are providing an opportunity to recover thermal energy in the form of cold during winters by use of a heat exchanger, when the temperature of the water is below 10 °C (Van der Hoek et al., 2018). The recovered cold can be stored underground via aquifer thermal energy storage (ATES) systems, to be used in the upcoming summer for cooling purposes (van der Hoek, 2012). However, cold recovery from distribution systems increases the drinking water temperature and might influence the microbial water quality and biofilm development in the DWDSs downstream of the heat exchanger (Ahmad et al., 2020).



Worldwide, the biological stability of drinking water is maintained either by limiting nutrient concentrations (Prest et al., 2016b; Van der Kooij, 1992) or by applying a disinfectant residual to minimize regrowth during distribution (Berry et al., 2006). Despite these approaches, the presence and regrowth of microbes as well as the seasonal fluctuations in the microbial water quality (in terms of adenosine triphosphate (ATP) concentrations and cell counts) within DWDSs are recognised (Pinto et al., 2014; Prest et al., 2016b; Proctor and Hammes, 2015). DWDSs harbour several micro-environments, namely bulk water (Prest et al., 2016a), biofilms (Chan et al., 2019), suspended solids and loose deposits (Liu et al., 2013). The microbes in these microenvironments may affect the quality and safety of the drinking water from production to customers' tap (Fish et al., 2016a; Liu et al., 2014).

Among all these microenvironments, specifically within unchlorinated systems, biofilms are long residents in DWDSs (days-decades) (Fish et al., 2015; Henne et al., 2012) and constitute more than 80% of the DWDSs microbiome (Liu et al., 2017a). Inside the biofilms, microbial communities are protected from external stress because of formation of extracellular polymeric substance (EPS) (Fish et al., 2016a; Flemming and Wingender, 2010). However, microbes within the biofilms are responsive to changes, e.g. changes in temperature or drinking water quality (Ahmad et al., 2020; Liu et al., 2017c) and are also thought to be the potential reservoirs for opportunistic pathogens (OPs) (Van Der Wende et al., 1989; Wingender and Flemming, 2011). Until now limited knowledge is available on temporal development of biofilms within unchlorinated DWDSs at an increased temperature. Either studies were reported for mature biofilms (20 years) (Henne et al., 2012) or very young biofilms (few days to few months) (Deines et al., 2010; Fish et al., 2015; Van der Kooij et al., 2018; van der Kooij et al., 2005b). There is only one study that has reported long term succession (three years) of biofilms within unchlorinated DWDSs but this research has not investigated the effects of temperature increase on biofilm development (Martiny et al., 2003).

The effects of increase in drinking water temperature were studied previously in water heater systems in relation to their temperature setting and impacts on growth and proliferation of opportunistic

pathogens e.g *Legionella pneumophila* (Dai et al., 2018; Rhoads et al., 2015; Wang et al., 2015). In DWDSs the biofilms formed at an increased temperature were studied in shower hoses (Proctor et al., 2016; Proctor et al., 2018) and water heaters (Proctor et al., 2017; van der Kooij et al., 2005a). According to our knowledge no studies were performed focusing on the effects of instantaneous increase in temperature, as a result of cold recovery, on temporal biofilm development within unchlorinated DWDSs. Therefore, the objective of this study was to investigate the influence of increase in drinking water temperature as a result of cold recovery from unchlorinated DWDSs, on the biofilm development in terms of microbial activity, and community diversity and composition over a longer period of time.

## 1.2 Materials and Methods

### 1.2.1 Pilot distribution facilities with and without cold recovery

Three pilot scale distribution systems (DSs) were designed and operated for almost 99 weeks from May, 2016 till February, 2018. The pilot scale DSs were situated in the laboratory at Water Lab of TU Delft (Figure 4.1), and fed continuously with unchlorinated drinking water (Feed water (FW)). The FW is produced at and distributed from a drinking water treatment plant located in Rotterdam, the Netherlands. The water, originating from surface water (river Meuse), is treated using granular activated carbon filtration and UV disinfection as final treatment steps, and distributed without maintaining a residual chlorine disinfectant during distribution.

Each pilot DS had an internal diameter of 25 mm and a length of 10 meter, and was made of polyvinyl chloride-unplasticised (PVC-U) pipes. For this experiment the flow rate was maintained at 4.5 l/min (0.15 m/s), which is based on normal flow velocities within Dutch drinking water distribution systems. For feed water sampling, a small tap of PVC-U was installed at the beginning of the distribution systems. For biofilm sampling from the pipe surface, 25 cm long PVC-U coupons were designed and inserted in all three pilot DSs: these are sections of pipes with valves on both ends. All the DSs were equipped with flow and temperature sensors, for continuously monitoring of the flow and temperature of the feed water and outgoing water. Dasy Lab software (version 13.0.1) was used for system monitoring and data logging.

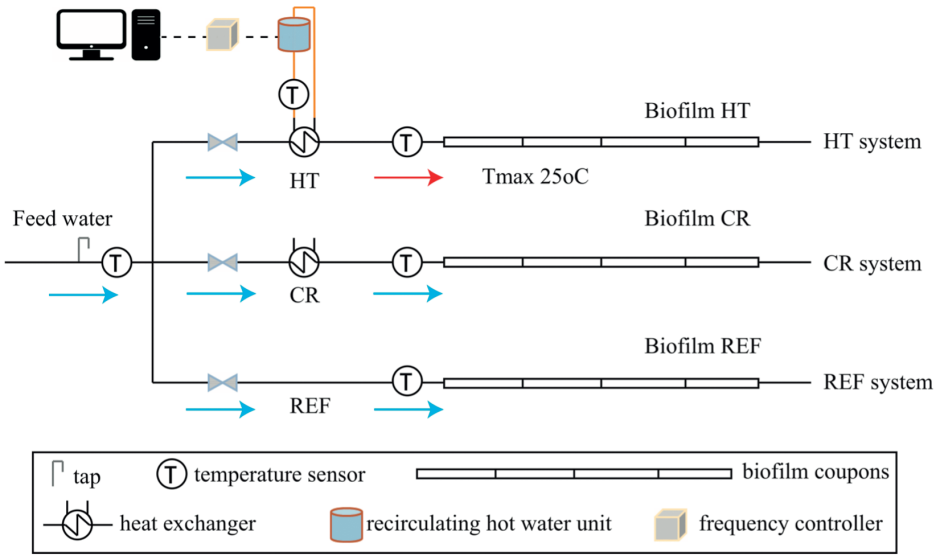


**Figure 4.1:** *Three, 10-meter-long (each), pilot scale distribution systems (DSs) supplied with non-chlorinated feed water, continuously for 24/7 for 99 weeks. All the sampling sites for feed water and biofilm were labelled (Biofilm HT = biofilm formed after cold recovery ($T_{max}$ = 25 °C), Biofilm CR = biofilm formed after non-operational heat exchanger and Biofilm REF = biofilm formed in the reference system).*

Among the three DSs, distribution system 1 is the high temperature (HT) system where temperature of the feed water was increased by using a heat exchanger (HE) to an elevated drinking water temperature of 25 °C, mimicking the cold recovery situation (HE description in Supplementary information). After having passed the HE and having absorbed the heat to gain the set point temperature of 25 °C, heated drinking water flowed further through the pipe and passed the whole length of the HT system. The set point was maintained throughout the entire experimental period, irrespective of changes in the FW temperature based on the seasonal variations. Distribution system 2 is the control system (CR) with a non-operational heat exchanger in which the temperature was not increased. In this system drinking water passed through the heat exchanger without heating, thus water came out of HE without temperature change. This system was operated in order to see if the HE itself had any effects on biofilm development because of the HE plate material (stainless steel, with negligible biomass production potential of <15 pg ATP/cm$^2$ (Tsvetanova and Hoekstra, 2010)), and the additional surface area. Distribution system 3 is the reference system (REF) in which no heat exchanger was installed and also the temperature was not increased, mimicking a Dutch unchlorinated DWDS.

### 1.2.2 Biofilm and feed water sampling

Duplicate biofilm samples were collected during 99 weeks for studying both the biomass formation (ATP and cell concentration) and microbial diversity and composition (next generation gene sequencing) of biofilms. Sampling was done after 1, 2, 4, 7, 12, 20, 32, 52 and 99 weeks of operation. In total 54 biofilm samples (9 times × 3 systems × duplicate samples) were collected from the three

pilot scale DSs. From each system, biofilm sampling was started from the distal end of the system in order to avoid disturbances within the systems related to sampling procedure.

For biofilm analysis, the valves on both sides of the pipe coupons were closed and the coupons were taken out of the systems and filled with DNA-free water. To remove the biofilm from the coupons, the pipe coupons were pretreated in 30 ml water by ultra-sonication, at a frequency of 40 KHz, in a water bath (Ultrasonic 8800, Branson, USA) for two minutes. This sonication procedure was repeated for two additional times (Magic-Knezev and van der Kooij, 2004). The obtained suspension of 90 ml was used for further analysis.

The duplicate FW samples were obtained every two weeks throughout the study period for studying both the biomass activity (ATP and cell concentration) and microbial diversity and composition (next generation gene sequencing) in water phase. In total 104 water samples (52 weeks × duplicate samples) were analysed.

The samples were stored in a refrigerator at a temperature of 4 °C and all microbiological analysis, for both biofilm and water samples, were performed within 24 hours of sampling.

### 1.2.3 Analytical methods

#### 1.2.3.1 Adenosine triphosphate and total cell count

Bacterial cell numbers and active biomass were determined by measuring cell counts and the total adenosine triphosphate (ATP) concentrations from both biofilm (n=54) and feed water (n=104) samples. Cell counts were measured by a flow cytometer (C6-Flowcytometer, Accuri Cytometers, USA) using the same protocol that was previously developed and tested for drinking water samples (Prest et al., 2013). Total and membrane-intact cell counts were distinguished by adding two stains simultaneously as described by Prest et al. (2013). Active biomass was determined by measuring total ATP concentrations from both biofilm and feed water samples using a reagent kit for bacterial ATP and a luminometer (Celsis Advance Luminometer, Charles River, USA), as described previously (Liu et al., 2017b; Magic-Knezev and van der Kooij, 2004).

#### 1.2.3.2 DNA extraction and 16S rRNA gene sequencing

To identify the microbial community composition and diversity of the pilot scale DSs, DNA was extracted using a DNeasy PowerBiofilm kit (Qiagen, USA) from samples of both feed water (n=104) and biofilm (n=54). Each feed water (volume of 2 litres) and biofilm (30 ml suspension) sample was filtered through 47-mm polycarbonate filter (0.22 μm pore size, Sartorius, Germany). The filters were stored at –20 °C and further used for DNA extraction according to the mentioned protocol. For 16S rRNA gene sequencing, the V3-V4 region of the 16S rRNA gene was amplified using primers 341F: 5'-CCTACGGGNGGCWGCAG-3' and 785R: 5'-GACTACHVGGGTATCTAATCC-3' (Thijs et al., 2017). Paired-end sequence reads were generated using the Illumina MiSeq platform. FASTQ sequence files were generated using the Illumina Casava pipeline version 1.8.3. The initial quality assessment was based on data passing the Illumina Chastity filtering. Subsequently, reads

containing the PhiX control signal were removed using an in-house filtering protocol at BaseClear laboratory, Leiden, the Netherlands. In addition, reads containing (partial) adapters were clipped (up to a minimum read length of 50bp). The second quality assessment was based on the remaining reads using the FASTQC quality control tool version 0.10.0, where low quality sequence ends were removed (Quality score=30) and remaining sequences were used further downstream analysis. The duplicate biofilm samples of week 20 and 32 (from all the three systems) and two feed water samples did not generate enough sequences to be included in the results.

#### 1.2.3.3 Data processing and statistical analysis

The obtained sequence libraries after quality control from FASTQC were imported into the Quantitative Insights into Microbial Ecology (QIIME2) (version 2018.11) pipeline (Caporaso et al., 2010). The sequences were further screened (at the maximum length of 281–298 bp), denosied, paired ends were merged and chimeras were removed using the inbuilt, Divisive Amplicon Denoising Algorithm 2 (DADA2) (Callahan et al., 2016). The remaining representative sequences were clustered to operational taxonomic units (OTUs) at an identity of 97%. For taxonomic assignment, feature-classifier plugin in QIIME2 (2018.11) was used against the SILVA database (132 release). The taxa bar plots were generated based on OTUs at different taxonomic levels of Class, Family and Order.



Both alpha (Shannon, Pielou's richness, observed OTUs) and beta (weighted Unifrac) diversity indices were calculated using phylogenetically based rooted tree (generated by aligning sequences using MAFFT plugin for phylogenetic reconstruction in FastTree) and with the sampling depth of 2000 sequences, using QIIME2 diversity plugin. The differences between biofilms formed in the three pilot scale DSs and between various ages, were determined by using permutational analysis of variance (PERMANOVA), with 999 permutations and using pairwise approach. Principal coordinate analysis (PCoA) plots were generated usingweighted distance matrix in emperor plot plugin.

Single factor ANOVA and pearson correlation were performed in Microsoft Excel for mac (version 15.40), to determine the significance of differences between quantitative microbial parameters (ATP, cell counts) and correlation of these parameters with feed water temperature and temperature difference after cold recovery ($\Delta T$ = difference between FW temperature and temperature after cold recovery).

## 1.3 Results

### 1.3.1 Feed water characteristics

As shown in Table 4.1, FW physico-chemical composition remained stable over the period of two years. The dissolved organic carbon (DOC) concentration ranged from 2.00 to 2.20 mg C/l. Other parameters like pH, nitrate, nitrite, ammonium and total hardness were also stable throughout the study.

*Table 4.1: Physico-chemical characteristics of the feed water used for biofilm development within three pilot distribution systems, during 2 years of the study period, starting from May, 2016 till January, 2018.*

| Feed water | |
|---|---|
| Dissolved organic carbon (mg C/l) | 2.15 ± 0.17 |
| Assimilable organic carbon (µg/l ac-C) | 21.83 ± 8.87 |
| Ammonium (mg $NH_4^+$/l) | 0.01 ± 0.01 |
| Nitrate (mg $NO_3^-$/l) | 10.28 ± 1.71 |
| Nitrite (mg $NO_2^-$/l) | 0.01 ± 0.01 |
| pH | 8.04 ± 0.10 |
| Total hardness (mmol/l) | 1.49 ± 0.06 |
| Temperature (°C) | 13.65 ± 6.38 |

During the experimental period, a clear seasonal trend in the temperature of the FW was observed (Figure 4.2). A higher water temperature (≥ 15 °C) was measured in the period from June to October and a lower water temperature (≤ 15 °C) was observed in the months from November till May, in both consecutive years 2016 and 2017 respectively. Overall the temperature ranged between 5.1 to 20.6 °C. The ATP concentration in the FW was between 2 to 7 ng/l (Figure 4.2 a) and cell numbers varied from $2\times10^5$–$5\times10^5$ cells/ml (Figure 4.2 b). Both ATP concentrations and cell numbers concentrations were moderately correlated with the seasonal temperature differences in the feed water ($R^2$ of 0.49 and 0.36, respectively).

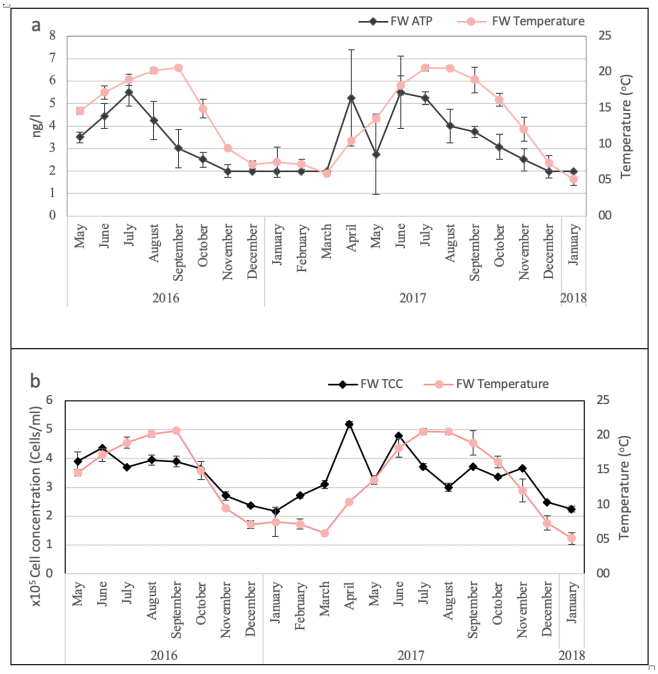


**Figure 4.2:** *Microbiological quality and temperature of the feed water within three pilot distribution systems, measured as, a) ATP and b) cell concentration, over the period of time from May, 2016 to January, 2018.*

Regarding the microbial community composition of the FW, in total, from 102 feed water samples 1,437,113 sequences were generated and assigned to 4,974 operational taxonomic units (OTUs). The taxonomic analysis of the FW samples at phylum level revealed that *Proteobacteria* was the most dominant phylum with relative abundance of 40–67%. The other dominant groups were *Patescibacteria* (6–25%), *Planctomycetes* (5–11%), *Bacteroidetes* (4–14%), *Actinobacteria* (1–17%), *Cyanobacteria* (2–5%), *Chloroflexi* (1–3%) and *Nitrospirae* (0.5–3%) (Figure 4.3a). At Class level (4.3 b), 30-20% of bacterial communities consisted of unknown classes. Six bacterial classes accounted for 70–80% of the remaning community, namely *Alphaproteobacteria* (14–25%), *Gammaproteobacteria* (10–50%), *Deltaproteobacteria* (3–11%), *Parcubacteria* (1–14%), *Planctomycetacia* (4–7%) and *Bacteroidia* (3–15%). At Family level of taxonomic classification (Figure 4.3 c) 50–90% of bacterial groups accounted for unknown families and small proportions were identified as *Parachlamydiaceae* (0.50–1.50%), *Xanthobacteraceae* (0.50–1.50%), *Burkholderiaceae* (2–44%), *Sphingomonadaceae* (1–2%), *Legionellaceae* (0.20–1.50%) *and Pseudomonadaceae* (0.15–1%).



Overall, few variations were observed among the microbial community abundance of the FW samples throughout the experimental period, except for the changes which were seen in the period from June 2017 to January 2018, where a higher relative abundance of *Gammaproteobacteria* (>25%) was observed. Simultaneously, at the family level a higher relative abundance of *Burkholderiaceae* was also observed, its relative abundance was 22–36% higher as compared to June 2016 to January 2017. Overall, no significant correlation was found between temperature and bacterial relative abundance of the feed water.

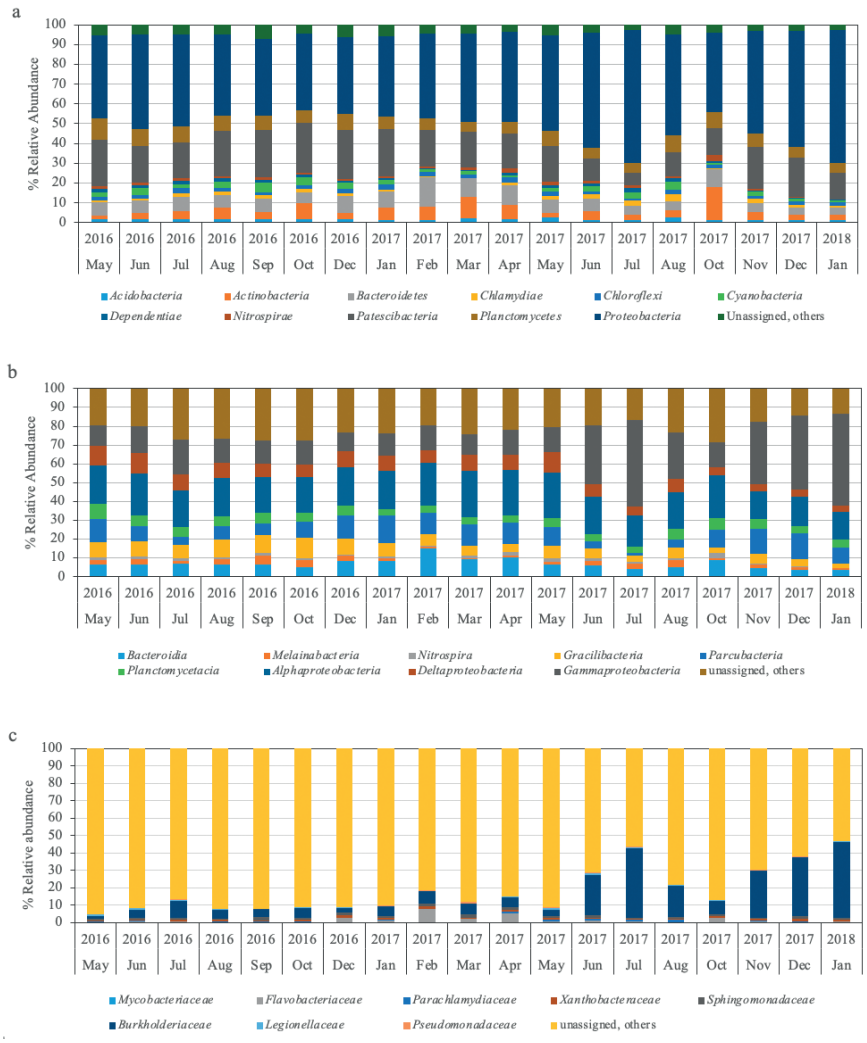


**Figure 4.3:** *Microbial community composition of the feed water, supplied to all the three-pilot distribution systems, at, a) Phylum level, b) Class level, and c) Family level of taxonomic classifications. Identified over the period of 99 weeks, from May 2016 to January 2018.*

## 1.3.2 Quantitiative development of biofilms

### 1.3.2.1 Reference and control systems

Figure 4.4 a shows the ATP concentrations of the biofilm over the period of 99 weeks. The biofilms developed in the reference (REF) and control (CR) systems were fed with the seasonally variable FW temperature. The biofilm development in both REF and CR systems showed similar patterns in the biomass growth starting from week 2 of biofilm sampling: an increase in the beginning, followed by a decrease in biomass and reaching a maximum concentration at the end of the study.

In week 1, a higher ATP concentration (230 pg/cm$^2$) was observed in the REF biofilm compared to a lower ATP concentration in the CR biofilm (10 pg/cm$^2$). After week 2, the ATP concentration in the REF biofilm (60 pg/cm$^2$) decreased, whereas an increase was observed in the CR biofilm (120 pg/cm$^2$). In both systems (REF and CR) ATP concentrations increased from week 2 onwards, and reached a comparable biomass of 300-345 pg/cm$^2$ at week 7. Between week 7 and week 12, a decrease in ATP concentration was observed in both the REF (minimum 76 pg/cm$^2$) and CR (minimum 110 pg/cm$^2$) biofilms. Later on, from week 12 to week 99 the ATP concentrations increased and reached a maximum concentration of 530 pg/cm$^2$ and 580 pg/cm$^2$ in both REF and CR biofilms respectively.

The dynamics in cell counts were comparable to the dynamics in ATP concentration (Figure 4.4 b). Higher cell numbers were observed in REF biofilm (2.9 $\times 10^6$ cells/cm$^2$) after week 1 and decreased to 9.9 $\times 10^5$ after week 2. Cell numbers in CR biofilm increased during this period from 5.3 $\times 10^5$ cells/cm$^2$ to 1.5 $\times 10^6$ cells/cm$^2$. Subsequently, cell numbers increased from week 2 to week 7 in both REF (2.90 $\times 10^6$ cells /cm$^2$) and CR biofilms (3.30 $\times 10^6$ cells /cm$^2$) followed by a decline from week 7 to 12 (week 12: REF 8.7 $\times 10^5$ cells/cm$^2$ and CR 1.5 $\times 10^6$ cells/cm$^2$). An increase in cell numbers was observed in both systems from week 12 onwards and reached to a maximum number at week 99 (REF 1.1 $\times 10^7$cells/cm$^2$ and CR 8.9 $\times 10^6$ cells/cm$^2$).

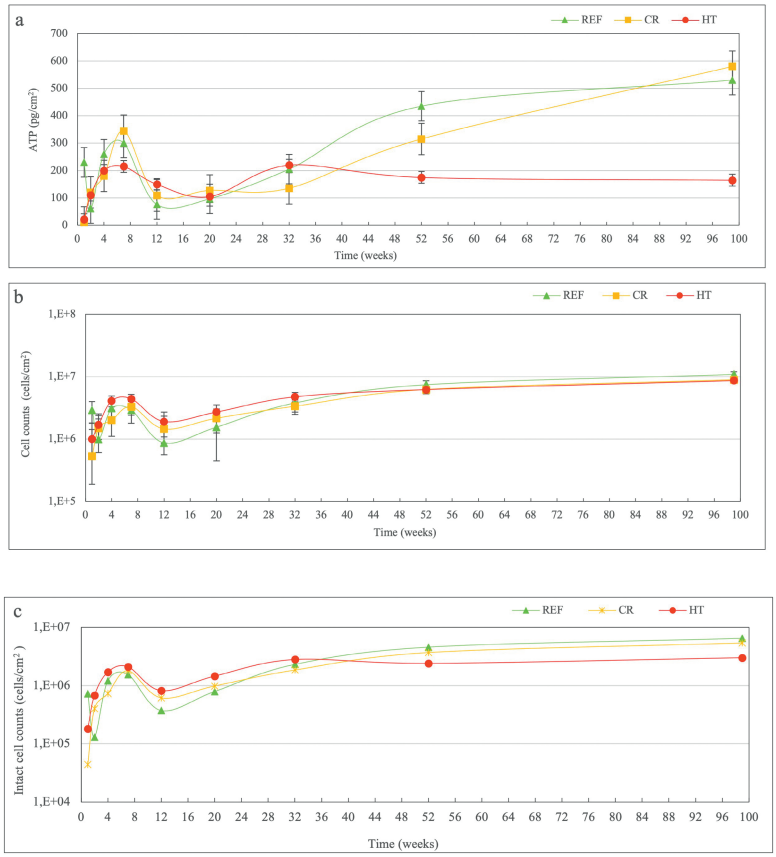


**Figure 4.4:** *Microbial quantification of biofilms developed within three pilot distribution systems (DSs), measured in terms of a) ATP concentration, b) total cell counts and c) intact cell counts. Biofilms were sampled from three systems: Reference (REF), Control (CR) and high temperature (HT) after cold recovery.*

#### 1.3.2.2 High temperature system after cold recovery

The HT biofilms were developed at a constantly stable and higher water temperature (25 °C), as a result of cold recovery, compared to varying FW temperature in the REF and CR systems. The biomass activity in HT biofilms showed a different pattern than in the REF and CR biofilms (Figure 4.4a). First, a steady increase in ATP concentration was observed from week 1 to 7 (from 22 pg/cm$^2$ to 215 pg/cm$^2$, respectively). From week 7 to 20, a decrease in ATP concentration was observed (minimum 105 pg/cm$^2$), followed by an increase between week 20 and 32 (maximum 220 pg/cm$^2$). Finally, from week 32 onwards a decrease in ATP concentration was observed and an ATP concentration of 165 pg/cm$^2$ was measured at week 99. Overall, the ATP concentration of the HT biofilm at week 52 and 99 was 1–3 times and 2–3 times less compared with CR and REF biofilms, respectively.

The HT biofilm showed comparable dynamics in total cell counts as was observed for REF and CR biofilms (Figure 4.4b). An increase in cell numbers was found from week 1 to 7 (1.0 $\times 10^6$ – 4.4 $\times 10^6$ cells/cm$^2$) and a decrease was observed from week 7 to week 12 (minimum 1.9 $\times 10^6$ cells/cm$^2$). In week 99, cell numbers reached a maximum of 8.7 $\times 10^6$ cells/cm$^2$. Similar to the ATP concentration, but in contrast to the total cell count results, the intact cell numbers of all three systems were comparable till week 32. Afterwards, intact cell numbers in REF and CR biofilms increased slightly while in HT biofilms intact cell numbers decreased or stabilized (Figure 4.4c).



### 1.3.3 Microbial communities of biofilm

#### 1.3.3.1 Reference and control systems

From the 42 biofilm samples 493,138 sequences were generated and were assigned to 1,040 operational taxonomic units (OTUs). The microbial diversity of the biofilms in REF and CR systems were characterized by numbers of observed taxonomic units (OTUs) and by measuring the Shannon and pielou's e diversity indices (Figure 4.5). At the begin, in week 1, the REF (41±21) and CR (48±16) biofilms showed a comparable number of OTUs (Figure 4.5a). At week 2 there was a decline in OTUs within REF biofilm (24±4), but an increase was observed in the CR biofilm (54±1). Thereafter, an increase in OTUs was found from week 2 to 4 in both REF (81±6) and CR (76±37) biofilms, followed by a decrease from week 4 to 7 (REF: 47±6; CR:38±2). Later on a continuous increase was observed in the REF biofilm and maximum number of OTUs (206±6) was observed at week 99. On the other hand, in CR biofilm a maximum number of OTUs were observed at week 12 (239±1) followed by a decrease from week 12 onwards, reaching 176±1 OTUs at week 99.

The development of community eveness (pielou's e, Figure 4.5b) and diversity (Shannon diversity, Figure 4.5c) indices showed comparable results as for the development of OTUs. A steady increase was observed in the beginning from week 1 to 7 followed by a decrease in diversity and eveness from week 4 to 7. Later, an increase was observed from week 7 onwards in both REF and CR biofilms. Biofilms in both systems were becoming equally even and diverse around week 12 (pielou's e: 0.9±0.01, Shannon: 7.0±0.07) and minor changes were observed afterwards (from week 12 to 99).

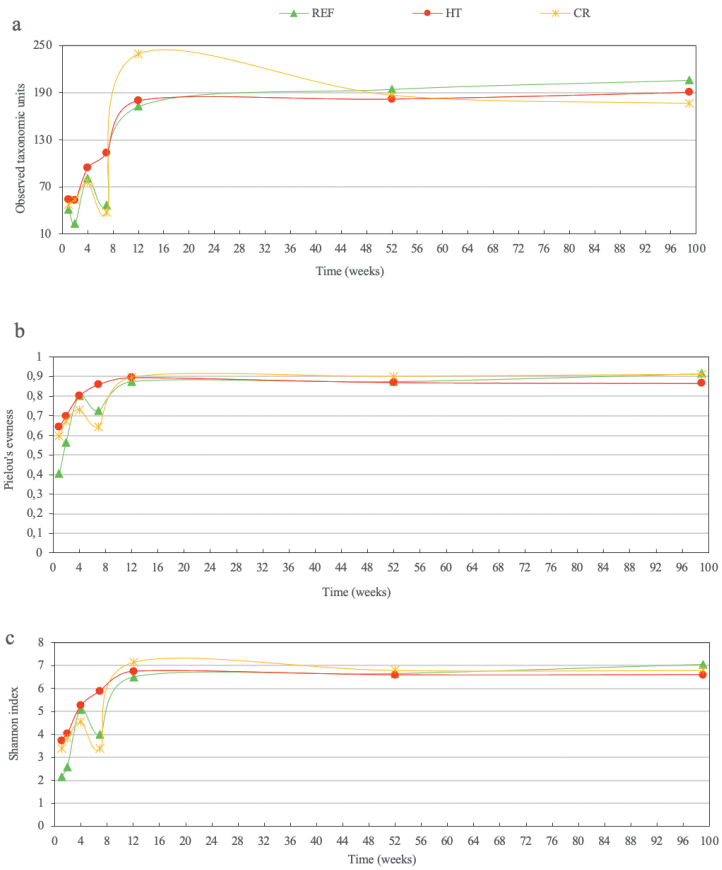


**Figure 4.5:** *Temporal microbial diversity of biofilms, observed in terms of, (a) operational taxonomic units (OTUs), (b) species evenness and (c) Shannon diversity index, from all three pilot scale distribution systems; Reference (REF), Control (CR) and high temperature (HT) after cold recovery.*

During the first 7 weeks the bacterial community composition of both REF and CR biofilms varied considerably. At Family level (Figure 4.6), from week 1 to 2, the bacterial community composition consisted of five major taxa, that constituted 80–90% of the total community and were identified as members of the Family *Burkholderiaceae* (45–75%), *Sphingomonadaceae* (6–16%), *Pseudomonadaceae* (3–11%), *Rhodocyclaceae* (2–5%) and *Xanthobacteraceae* (2–9%). From week 2 to 7, the relative abundance of *Sphingomonadaceae* increased to 45–48% and the relative abudance of *Burkholderiaceae* decreased to 24–26%. Furthermore, between week 7 and 12 a decrease in relative abundance was observed for the three major Family taxa *Burkholderiaceae* (10–15%), *Sphingomonadaceae* (4%) and *Pseudomonadaceae* (0.10–0.30%). This decrease in relative abundance in week 12 was consistent with an increase in abundances of other bacterial groups, which were identified as *Hyphomicrobiaceae* (3.50%), *Xanthobacteraceae* (3%), *Legionellaceae* (1.50%), *Parachlamydiaceae* (1.10%) and *Mycobacteriaceae* (0.80%). The unassigned taxa (68–73%) has the higher relative abundance starting from the age of 12 weeks in both REF and CR biofilms.

Finally, from week 12 to 99 no major changes were observed in terms of differences in relative abundances of major OTUs.

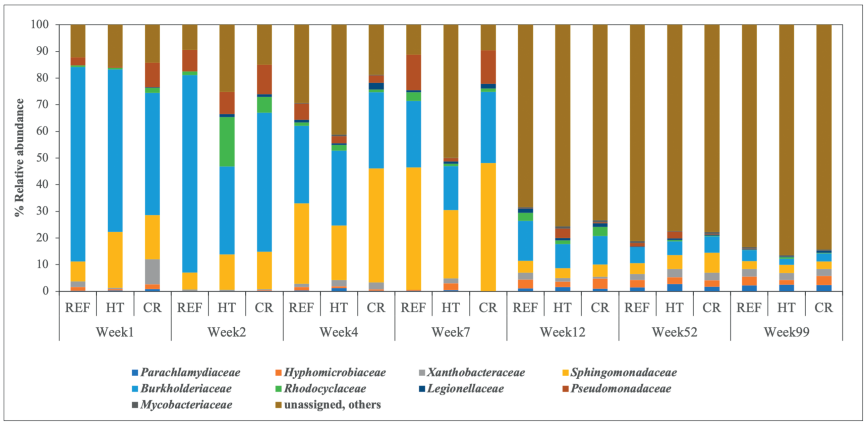


**Figure 4.6:** *Microbial community composition, at Family level of taxonomic classification, of biofilms developed over the period of 99 weeks, within three pilot distribution systems: Reference (REF), Control (CR) and high temperature (HT) after cold recovery.*



### 1.3.3.2 High temperature system after cold recovery

The biofilms grown at high temperature after cold recovery (HT) showed a steady increase in their bacterial diversity indices (Figure 4.5) from week 1 to 99. This is in contrast to the increasing and decreasing patterns of diversity indices as observed in CR and REF biofilms, where a prominent decrease in diversity indices was observed at week 7. The HT biofilm has more OTUs after week 1 (54±4) than the biofilms in the REF and CR systems, and were progressively increasing till it reached a number of 180±6 OTUs at 12 weeks. A stable number of OTUs was observed from week 12 to 99 (190±7) (Figure 4.5 a). Similarly, both pielous' e (Figure 4.5 b) and shannon (Figure 4.5.c) diversity indices showed an even and diverse HT biofilm from the age of 12 to 99 weeks (pielous' e: 0.9±0.0 and 0.9±0.01, Shannon: 7.0±0.0 and 7.0±0.0 respectively).

From microbial community composition perspective at the Family level *Sphingomonadaceae* (21%) and *Burkholderiaceae* (61%) were two most dominant families at week 1 (Figure 4.6). After week 2, diverse bacterial families were observed, such as *Rhodocyclaceae* (19%), *Pseudomonadaceae* (9%) and *Legionellaceae* (1%). At the age of 4 weeks *Xanthobacteraceae* (2.50%) and *Parachlamydiaceae* (1.30%) were also present in the biofilm along with higher relative abundance of unassigned taxa (41%). The increase in these Family taxa was associated with decrease in relative abundances of *Sphingomonadaceae* (13%) and *Burkholderiaceae* (33%) after week 2 and a further decrease in *Pseudomonadaceae* (2.50%) after week 4. Overall, the HT biofilm consisted of more diverse bacterial groups at week 7 (8 major taxa with > 0.5% relative abundance) compared to REF and CR biofilms (5 major taxa with > 0.5% relative abundance).

The beta diversity among the biofilm samples from three DSs and different age groups is shown by Principle coordinate Analysis (PCoA) plot based on Weighted Unifrac distance matrix (Figure 4.7).

No significant differences (PERMANOVA= $p > 0.05$ ) were observed among biofilms from all three DSs and between the age group 12 to 99 weeks. But significant differences (PERMANOVA= $p < 0.05$ ) were observed among the biofilms from 1 to 7 week old within all three studied distribution systems.

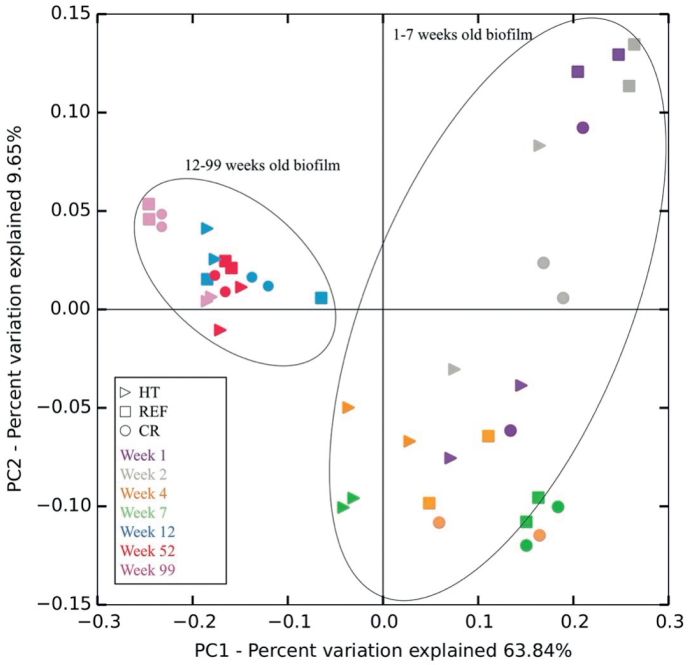


**Figure 4.7** *: Principle coordinate Analysis (PCoA) plot, based on Weighted Unifrac distance matrix; Reference (REF), Control (CR) and high temperature (HT) after cold recovery.*

## 1.4 Discussion

The development of biofilms is a continuous process and consists of various stages and these stages are clearly characterized in the literature (Mathieu et al., 2019). These stages include: 1) initial preconditioning of surface (recruitment of organic substances from bulk water; as soon as (minutes/ hours) surface is exposed to flowing water, on which bacteria will attach), 2) attachment of primary colonizers, 3) growth of attached bacteria, 4) protozoans grazing and 5) finally detachment of bacterial cells from biofilm into the bulk water.

The current study was focused on how an instantaneous increase in temperature (upto 25 °C), as a result of cold recovery, influenced the biofilm development within unchlorinated DWDSs over a long period of time (99 weeks). The development of biofilms was studied, at high temperature and compared with reference and control systems, in terms of microbial quantification (ATP and Total cell count) and microbial community composition.

Mostly feed drinking water bacterial communities are thought to be responsible for initial surface colonization of pipes (Neu et al., 2019). In our study we also observed that certain bacterial groups (*Sphingomonadaceae, Burkholderiaceae* and *Pseudomonadaceae*) were continuously present in the FW (Figure 4.3 c) and also detected in the biofilms during the first two weeks of biofilm development, within all three pilot scale DSs (Figure 4.6).

Along with feed water, temperature is another crucial parameter in controlling the initial biofilm microbial colonization (in this case the first 12 weeks: Figure 4.5) and a higher temperature results into steady and even microbial population within the biofilms (Olsen et al., 2019). It is known that at high temperature more food is being consumed by microbes because of selection and competition for survival within a particular environment (Diaz Villanueva et al., 2011; Lienard et al., 2016; Marañón et al., 2018; Scheikl et al., 2014). In our study as a result of constantly stable and higher water temperature after cold recovery (25 °C) a smooth pattern is observed in HT biofilm to reach to a steady phase of diversity and evenness at the age of 12 weeks, as compared to REF and CR biofilms, which showed a slight decrease in diversity and evenness at the age of 7 weeks before reaching to the similar diversity and evenness, as of HT biofilms, at the age of 12 weeks (Figure 4.5 b and c).



Along with the selection of more diverse microbial communities, a constantly stable and high temperature also results into less active biomass within biofilms (Inkinen et al., 2014). In our experiments, at the end of the study period of 99 weeks, cold recovery at 25 °C (HT biofilms) resulted into a biofilm development that has less biomass activity (ATP and intact cell counts) compared to the biofilms in the REF and CR systems. CR biofilms have 1.8–3.5 times and REF biofilms have 2.5–3.2 times more biomass compared to HT biofilms, between 52 and 99 weeks, respectively (Figure 4.4). The recovery of cold from DWDSs at 25 °C seems not to adversely affect the community composition of biofilms within unchlorinated DWDSs. Further, both the REF and CR systems showed similar behavior in terms of biomass concentration, microbial diversity and composition patterns. This means that the presence of a heat exchanger, as an extra material in contact with drinking water within DWDSs, seems to have limited effect on biofilm development. However, biofilms are thought to be potential reservoirs of opportunistic pathogens (Wingender and Flemming, 2011), and future investigations are required on effects of cold recovery in terms of presence and proliferation of opportunistic pathogenic microbial groups within biofilms to develop further insights. This may be done by targeting microbes of specific concern (e.g *Legionella spp*., *Pseudomonas spp*., *Mycobacterium spp.* ) under different temperatures after recovery of cold.

Recently changes in terms of biomass activity, microbial diversity and composition at high temperature were already observed in the first 12-32 weeks of biofilm development (Ahmad et al., 2021; Ahmad et al., 2020) and the same is observed here within all three studied DSs (CR, REF and HT system). Later, after a period of 32 weeks within all three studied DSs, biofilms become more stable in terms of microbial diversity and composition. Our study covered a period of in total 99 weeks. In contrast, in the past most of the experimental studies that were done to track changes during development of biofilms, only investigated a period less than 32 weeks (Deines et al., 2010; Douterelo et al., 2018; Fish et al., 2016b; Pinel et al., 2021). This time period is not long enough

to establish conclusions about the microbial community structure within biofilms, as biofilms are still in a developing phase during this time period and show varied composition and diversity patterns. Long term biofilm developmental studies (more than 32 weeks) should be performed to better understand the effects of different environmental parameters, such as temperature, on the behavior of microbial community structure and biomass activity within biofilms.

## 1.5 Conclusion

a) The higher water temperature (25 °C) within drinking water distribution system, after cold recovery, results in the formation of 2–3 folds less active biomass (in terms of ATP and intact cell counts).
b) All three DWDSs reached to a similar diversity and eveness at week 12 but at a constant temperature, after cold recovery, the pattern to reach this diversity is smooth compared to a decrease in diversity observed at week 7 in systems without cold recovery.
c) Under the influence of increased water temperature due to cold recovery, the biofilm reached a steady/stable growth phase faster (between 32–52 weeks) as compared to systems without cold recovery (52–99 weeks), in terms of biomass activity.
d) The presence of a heat exchanger itself in a cold recovery system in DWDSs has no effects on biofilm development in terms of biomass activity and community structure, it is the temperature increase that affects biofilm development.
e) Long term investigations are required to study the changes happened during biofilm development at microbial community composition level.

## References

Ahmad, J.I., Dignum, M., Liu, G., Medema, G. and van der Hoek, J.P. (2021) Changes in biofilm composition and microbial water quality in drinking water distribution systems by temperature increase induced through thermal energy recovery. Environmental Research 194, 110648.

Ahmad, J.I., Liu, G., Van der Wielen, P.W.J.J., Medema, G. and Van der Hoek, J.P. (2020) Effects of cold recovery technology on the microbial drinking water quality in unchlorinated distribution systems. Environmental Research 183, 109175.

Berry, D., Xi, C. and Raskin, L. (2006) Microbial ecology of drinking water distribution systems. Current Opinion in Biotechnology 17(3), 297-302.

Callahan, B.J., McMurdie, P.J., Rosen, M.J., Han, A.W., Johnson, A.J.A. and Holmes, S.P. (2016) DADA2: High-resolution sample inference from Illumina amplicon data. Nature Methods 13, 581.

Caporaso, J.G., Kuczynski, J., Stombaugh, J., Bittinger, K., Bushman, F.D., Costello, E.K., Fierer, N., Pẽa, A.G., Goodrich, J.K., Gordon, J.I., Huttley, G.A., Kelley, S.T., Knights, D., Koenig, J.E., Ley, R.E., Lozupone, C.A., McDonald, D., Muegge, B.D., Pirrung, M., Reeder, J., Sevinsky, J.R., Turnbaugh, P.J., Walters, W.A., Widmann, J., Yatsunenko, T., Zaneveld, J. and Knight, R. (2010) QIIME allows analysis of high-throughput community sequencing data. Nature Methods 7(5), 335-336.

Chan, S., Pullerits, K., Keucken, A., Persson, K.M., Paul, C.J. and Rådström, P. (2019) Bacterial release from pipe biofilm in a full-scale drinking water distribution system. npj Biofilms and Microbiomes 5(1), 9.

Dai, D., Rhoads, W.J., Edwards, M.A. and Pruden, A. (2018) Shotgun Metagenomics Reveals Taxonomic and Functional Shifts in Hot Water Microbiome Due to Temperature Setting and Stagnation. Frontiers in Microbiology 9(2695).

Deines, P., Sekar, R., Husband, P.S., Boxall, J.B., Osborn, A.M. and Biggs, C.A. (2010) A new coupon design for simultaneous analysis of in situ microbial biofilm formation and community structure in drinking water distribution systems. Applied Microbiology and Biotechnology 87(2), 749-756.

Diaz Villanueva, V., Font, J., Schwartz, T. and Romani, A.M. (2011) Biofilm formation at warming temperature: acceleration of microbial colonization and microbial interactive effects. Biofouling 27(1), 59-71.

Douterelo, I., Fish, K.E. and Boxall, J.B. (2018) Succession of bacterial and fungal communities within biofilms of a chlorinated drinking water distribution system. Water Research 141, 74-85.

Fish, K.E., Collins, R., Green, N.H., Sharpe, R.L., Douterelo, I., Osborn, A.M. and Boxall, J.B. (2015) Characterisation of the Physical Composition and Microbial Community Structure of Biofilms within a Model Full-Scale Drinking Water Distribution System. PLoS ONE 10(2), e0115824.

Fish, K.E., Osborn, A.M. and Boxall, J. (2016a) Characterising and understanding the impact of microbial biofilms and the extracellular polymeric substance (EPS) matrix in drinking water distribution systems. Environmental science: water research & technology.

Fish, K.E., Osborn, A.M. and Boxall, J. (2016b) Characterising and understanding the impact of microbial biofilms and the extracellular polymeric substance (EPS) matrix in drinking water distribution systems. Environmental science: water research & technology 2(4), 614-630.

Flemming, H.-C. and Wingender, J. (2010) The biofilm matrix. Nature Reviews Microbiology 8(9), 623-633.

Henne, K., Kahlisch, L., Brettar, I. and Hofle, M.G. (2012) Analysis of structure and composition of bacterial core communities in mature drinking water biofilms and bulk water of a citywide network in Germany. Applied and environmental microbiology 78(10), 3530-3538.

Inkinen, J., Kaunisto, T., Pursiainen, A., Miettinen, I.T., Kusnetsov, J., Riihinen, K. and Keinänen-Toivola, M.M. (2014) Drinking water quality and formation of biofilms in an office building during its first year of operation, a full scale study. Water Research 49, 83-91.

Lienard, J., Croxatto, A., Gervaix, A., Lévi, Y., Loret, J.F., Posfay-Barbe, K.M. and Greub, G. (2016) Prevalence and diversity of Chlamydiales and other amoeba-resisting bacteria in domestic drinking water systems. New microbes and new infections 15, 107-116.

Liu, G., Bakker, G.L., Li, S., Vreeburg, J.H.G., Verberk, J.Q.J.C., Medema, G.J., Liu, W.T. and Van Dijk, J.C. (2014) Pyrosequencing Reveals Bacterial Communities in Unchlorinated Drinking Water Distribution System: An Integral Study of Bulk Water, Suspended Solids, Loose Deposits, and Pipe Wall Biofilm. Environmental science & technology 48(10), 5467-5476.

Liu, G., Ling, F.Q., Magic-Knezev, A., Liu, W.T., Verberk, J.Q.J.C. and Van Dijk, J.C. (2013) Quantification and identification of particle-associated bacteria in unchlorinated drinking water from three treatment plants by cultivation-independent methods. Water Research 47(10), 3523-3533.

Liu, G., Tao, Y., Zhang, Y., Lut, M., Knibbe, W.-J., van der Wielen, P., Liu, W., Medema, G. and van der Meer, W. (2017a) Hotspots for selected metal elements and microbes accumulation and the corresponding water quality deterioration potential in an unchlorinated drinking water distribution system. Water Research 124, 435-445.

Liu, G., Tao, Y., Zhang, Y., Lut, M., Knibbe, W.-J., van der Wielen, P., Liu, W., Medema, G. and van der Meer, W. (2017b) Hotspots for selected metal elements and microbes accumulation and the corresponding water quality deterioration potential in an unchlorinated drinking water distribution system. Water Research 124(Supplement C), 435-445.

Liu, G., Zhang, Y., Knibbe, W.-J., Feng, C., Liu, W., Medema, G. and van der Meer, W. (2017c) Potential impacts of changing supply-water quality on drinking water distribution: A review. Water Research 116, 135-148.

Magic-Knezev, A. and van der Kooij, D. (2004) Optimisation and significance of ATP analysis for measuring active biomass in granular activated carbon filters used in water treatment. Water Research 38(18), 3971-3979.

Marañón, E., Lorenzo, M.P., Cermeño, P. and Mouriño-Carballido, B. (2018) Nutrient limitation suppresses the temperature dependence of phytoplankton metabolic rates. The ISME Journal 12(7), 1836-1845.

Martiny, A.C., Jørgensen, T.M., Albrechtsen, H.-J., Arvin, E. and Molin, S. (2003) Long-term succession of structure and diversity of a biofilm formed in a model drinking water distribution system. Applied and environmental microbiology 69(11), 6899-6907.

Mathieu, L., Paris, T. and Block, J.-C. (2019) The Structure and Function of Aquatic Microbial Communities. Hurst, C.J. (ed), pp. 261-311, Springer International Publishing, Cham.

Neu, L., Proctor, C.R., Walser, J.-C. and Hammes, F. (2019) Small-Scale Heterogeneity in Drinking Water Biofilms. Frontiers in Microbiology 10(2446).

Olsen, N.M.C., Røder, H.L., Russel, J., Madsen, J.S., Sørensen, S.J. and Burmølle, M. (2019) Priority of Early Colonizers but No Effect on Cohabitants in a Synergistic Biofilm Community. Frontiers in Microbiology 10(1949).

Pinel, I., Biškauskaitė, R., Pal'ová, E., Vrouwenvelder, H. and van Loosdrecht, M. (2021) Assessment of the Impact of Temperature on Biofilm Composition with a Laboratory Heat Exchanger Module. Microorganisms 9(6), 1185.

Pinto, A.J., Schroeder, J., Lunn, M., Sloan, W. and Raskin, L. (2014) Spatial-Temporal Survey and Occupancy-Abundance Modeling To Predict Bacterial Community Dynamics in the Drinking Water Microbiome. mBio 5(3), e01135-01114.

Prest, E.I., Hammes, F., Kötzsch, S., Van Loosdrecht, M.C.M. and Vrouwenvelder, J.S. (2013) Monitoring microbiological changes in drinking water systems using a fast and reproducible flow cytometric method. Water Research 47(19), 7131-7142.

Prest, E.I., Hammes, F., van Loosdrecht, M.C. and Vrouwenvelder, J.S. (2016a) Biological Stability of Drinking Water: Controlling Factors, Methods, and Challenges. Frontiers in Microbiology 7.

Prest, E.I., Hammes, F., van Loosdrecht, M.C.M. and Vrouwenvelder, J.S. (2016b) Biological Stability of Drinking Water: Controlling Factors, Methods, and Challenges. Frontiers in Microbiology 7, 45.

Proctor, C.R., Dai, D., Edwards, M.A. and Pruden, A. (2017) Interactive effects of temperature, organic carbon, and pipe material on microbiota composition and Legionella pneumophila in hot water plumbing systems. Microbiome 5(1), 130.

Proctor, C.R., Gächter, M., Kötzsch, S., Rölli, F., Sigrist, R. and Walser, J.-C. (2016) Biofilms in shower hoses—choice of pipe material influences bacterial growth and communities. Environ. Sci. Water Res. Technol. 2.

Proctor, C.R. and Hammes, F. (2015) Drinking water microbiology — from measurement to management. Current Opinion in Biotechnology 33, 87-94.

Proctor, C.R., Reimann, M., Vriens, B. and Hammes, F. (2018) Biofilms in shower hoses. Water Research 131, 274-286.

Rhoads, W.J., Ji, P., Pruden, A. and Edwards, M.A. (2015) Water heater temperature set point and water use patterns influence Legionella pneumophila and associated microorganisms at the tap. Microbiome 3(1), 67.

Scheikl, U., Sommer, R., Kirschner, A., Rameder, A., Schrammel, B. and Zweimüller, I. (2014) Free-living amoebae (FLA) co-occurring with Legionellae in industrial waters. Eur J Protistol 50.

Thijs, S., Op De Beeck, M., Beckers, B., Truyens, S., Stevens, V., Van Hamme, J.D., Weyens, N. and Vangronsveld, J. (2017) Comparative Evaluation of Four Bacteria-Specific Primer Pairs for 16S rRNA Gene Surveys. Frontiers in Microbiology 8, 494.

Tsvetanova, Z.G. and Hoekstra, E.J. (2010) The effect of the surface-to-volume contact ratio on the biomass production potential of the pipe products in contact with drinking water, pp. 105-112.

van der Hoek, J.P., Mol, S., Giorgi, S., Ahmad, J.I., Liu, G. and Medema, G. (2018) Energy recovery from the water cycle: Thermal energy from drinking water. Energy 162, 977-987.

van der Kooij, D. (1992) Assimilable organic carbon as an indicator of bacterial regrowth. Journal of American Water Works Association 84(2), 57-65.

van der Kooij, D., Veenendaal, H.R., Italiaander, R., Van der Mark, E.J. and Dignum, M. (2018) Primary Colonizing Betaproteobacteriales Play a Key Role in the Growth of Legionella pneumophila in Biofilms on Surfaces Exposed to Drinking Water Treated by Slow Sand Filtration. Applied and environmental microbiology 84(24), e01732-01718.

van der Kooij, D., Veenendaal, H.R. and Scheffer, W.J.H. (2005a) Biofilm formation and multiplication of Legionella in a model warm water system with pipes of copper, stainless steel and cross-linked polyethylene. Water Research 39(13), 2789-2798.

van der Kooij, D., Veenendaal, H.R. and Scheffer, W.J.H. (2005b) Biofilm formation and multiplication of Legionella in a model warm water system with pipes of copper, stainless steel and cross-linked polyethylene. Water Res 39.

van Der Wende, E., Characklis, W.G. and Smith, D.B. (1989) Biofilms and bacterial drinking water quality. Water Research 23(10), 1313-1322.

Wang, H., Masters, S., Falkinham, J.O., 3rd, Edwards, M.A. and Pruden, A. (2015) Distribution System Water Quality Affects Responses of Opportunistic Pathogen Gene Markers in Household Water Heaters. Environ Sci Technol 49(14), 8416-8424.

Wingender, J. and Flemming, H.-C. (2011) Biofilms in drinking water and their role as reservoir for pathogens. International Journal of Hygiene and Environmental Health 214(6), 417-423.

PART 3

# Microbial drinking water quality from chlorinated distribution systems

Chapter 5

# Thermal energy recovery from chlorinated drinking water distribution systems: effect on chlorine and microbial water and biofilm characteristics

CHAPTER 5


## Abstract

Thermal energy recovery from drinking water has a high potential in the application of sustainable building and industrial cooling. However, drinking water and biofilm microbial qualities should be concerned because the elevated water temperature after cold recovery may influence the microbial activities in water and biofilm phases in drinking water distribution systems (DWDSs). In this study, the effect of cold recovery on microbial qualities was investigated in a chlorinated DWDS. The chlorine decay was slight (1.1%–15.5%) due to a short contact time (~60 s) and was not affected by the cold recovery ($p > 0.05$). The concentrations of cellular ATP and intact cell numbers in the bulk water were partially inactivated by the residual chlorine, with the removal rates of 10.1%-16.2% and 22.4%-29.4%, respectively. The chlorine inactivation was probably promoted by heat exchangers but was not further enhanced by higher temperatures. The higher water temperature (25 °C) enhanced the growth of biofilm biomass on pipelines. Principle coordination analysis (PCoA) showed that the biofilms on the stainless steel plates of HEs and the plastic pipe inner surfaces had totally different community compositions. Elevated temperatures favored the growth of *Pseudomonas* spp. and *Legionella* spp. in the biofilm after cold recovery. Compared with a previous study with a non-chlorinated DWDS, chlorine dramatically reduced the biofilm biomass growth but raised the relative abundances of the chlorine-resistant genera (i.e. *Pseudomonas* and *Sphingomonas*) in bacterial communities.



**Keywords:** Cold recovery; Chlorine; Drinking water microbial activity; Biofilm community structure


*This chapter is based on: Zhou, X., **Ahmad, J.I.,** van der Hoek, J.P., Zhang, K. (2020) Thermal energy recovery from chlorinated drinking water distribution systems: Effect on chlorine and microbial water and biofilm characteristics. Environmental Research, 187, 109655.*

## 1.1 Introduction

Fossil fuels have made up the majority part of the energy resources worldwide in the past decades (Painter, 2020). However, the extensive use of these traditional energy sources poses lots of environment issues, such as global warming (Lelieveld et al., 2019). In 2015, the United Nations Paris Climate Conference reached a consensus that the global temperature rise should be well below 2 °C and efforts should be pursued to limit it to 1.5 °C (Painter, 2020; Rogelj et al., 2016). Therefore, in order to achieve this target, the pursuit of new and clean low-carbon energy resources is necessary (Jiang et al., 2010). Recently energy recovery from the water cycle has been suggested, including thermal energy from surface water, groundwater, wastewater and drinking water (Mol et al., 2011; van der Hoek, 2012). With respect to surface water, energy recovery has already been successfully applied in practice. In the Netherlands, the water from lake "Ouderkerkerplas" is used for office building cooling, and a reduction of greenhouse gas emissions of nearly 20 kton carbon dioxide ($CO_2$)-equivalent/a can be achieved (van der Hoek et al., 2018). In many European countries, groundwater plays a role in the underground thermal energy storage systems and is widely used at full scale (Sanner et al., 2003). In the urban water cycle, heat recovery from wastewater via heat exchangers has been intensively studied (Elias Maxil, 2015; Elías-Maxil et al., 2014), and shower water has also been applied for heat recovery from wastewater in a pilot study (Deng et al., 2016). Recently, the concept of thermal energy recovery from drinking water has been proposed, and researchers have proven its possibility (Bloemendal et al., 2015) and explored the potential technologies in practical use (De Pasquale et al., 2017; Guo and Hendel, 2018; van der Hoek et al., 2018). However, its application still has a long way to go due to several risk concerns (Hofman and van der Wielen, 2015). The most important one is the microbial risk concern of the water quality. Because of the heat exchange, the water temperature in drinking water distribution system (DWDS) will experience an elevation, which may pose effects on microbiological growth and activity in both bulk water and biofilms (Hallam et al., 2001; van der Wielen and van der Kooij, 2010). In our previous study, such effects were evaluated in a pilot-scale non-chlorinated DWDS (Ahmad et al., 2020). However, no research has been conducted in a chlorinated one.



As a key influencing factor in DWDS, temperature can affect both chemical and biological processes (Li et al., 2019). Chlor(am)ine decay rate can be accelerated with increasing temperature (Monteiro et al., 2017; Sathasivan et al., 2009). This can be explained by two major reasons: (i) chlor(am)ine self-decay is a temperature dependent reaction, and the reaction rate is higher at higher temperature (Monteiro et al., 2017); (ii) elevated temperature can change the microbial activities (Ndiongue et al., 2005). Additionally, the efficiency of chlorine disinfection is quite sensitive to temperature (Benarde et al., 1967; Butterfield et al., 1943; Collins, 1955). Collins (1955) studied the chlorine disinfection on a chlorine-resistant species *Pseudomonas fragi*, and found that for equal destruction of *P. fragi* at 4.4 °C and 21 °C, approximately twice as much time was required at 4.4 °C. In another *Mycobacteria gordonae* inactivation study, the chlorine disinfection efficiency doubled when reaction temperature rose from 4 °C to 16 °C, and dramatically increased eight-fold when temperature reached 25 °C (Le Dantec et al., 2002). The microbial water quality in DWDS can be affected by water temperature (Blokker et al., 2013; van der Hoek, 2012). It has been documented

that seasonal temperature changes can result in fluctuations of microbial quantities (e.g. adenosine triphosphate (ATP), heterotrophic plate count, total cell count (TCC) and coliform) (LeChevallier et al., 1996; Prest et al., 2016; van der Wielen and van der Kooij, 2010) and changes of bacterial community dynamics (Pinto et al., 2014) of bulk water. Some researchers have reported that specific opportunistic pathogens favor to be present at relatively higher water temperatures (Dai et al., 2018; van der Wielen and van der Kooij, 2013). Apart from microbes in water phase, biofilm growth in DWDS can also be promoted by high temperatures (Fish et al., 2016). Tsvetanova and Dimitrov (2012) reported that significant correlations between biofilm HPC density and water temperature were detected in plastics pipes. Hallam et al. (2001) found that biofilm activity was approximately 50% lower at a temperature of 7 °C than at 17 °C. In a recent study, differences in both bacterial and fungal community compositions at two different temperatures (16 °C and 24 °C) were observed at family level (Preciado et al., 2019). In conclusion, temperature can regulate various reactions within DWDS.

In our previous study, the effect of cold recovery (with subsequent sudden temperature rise in the distributed drinking water) on microbial characteristics in both water and biofilms were investigated (Ahmad et al., 2020). However, the results were obtained through a non-chlorinated pilot DWDS. As chlorine is still widely used in drinking water disinfection worldwide, a similar study associated with thermal energy recovery is necessary in a chlorinated DWDS. Therefore, the aim of this study is to explore the effect of temperature increase on chlorine, chlorine disinfection and microbial characteristics in a pilot-scale chlorinated DWDS subjected to cold recovery. Specifically, chlorine decay, bulk water microbial activity and biofilm community structure (diversity and composition) were investigated under the influence of cold recovery. The results could promote a better understanding of the effect of cold recovery on microorganisms in chlorinated DWDSs.

## 1.2 Materials and methods

### 1.2.1 *Chemicals*

Sodium hypochlorite (NaClO, 60-185 g active chlorine $L^{-1}$) was purchased from BOOM Lab, the Netherlands. Sodium acetate (NaAc) (500 g) was obtained from Honeywell Research Chemicals, USA. Sodium thiosulfate ($Na_2S_2O_3$) solution (0.1 N) was from Merck KGaA, Germany. Phosphate buffer solution (PBS) tablet was purchased from ThermoFisher Scientific, Sweden.

### 1.2.2 *Experimental set-up*

As displayed in Figure 5.1, the pilot chlorinated system operated in the laboratory of Delft University of Technology consisted of a chemical dosing subsystem (CDS) and three parallel pipelines, which were (i) an experimental pipeline with an operational heat-exchanger (OHE) (Pipe1), (ii) a reference pipeline with a non-operational heat-exchanger (NOHE) (Pipe2), and (iii) a reference pipeline without a HE (Pipe3). The detailed information about the two HEs and the reason of setting two reference pipelines have been discussed in our previous study (Ahmad et al., 2020). The set-up was supplied with drinking water from the treatment plant "Kralingen" of drinking water utility Evides, Rotterdam, the Netherlands, and subsequently dosed with NaClO

solution and NaAc solution (appropriate AOC supplement). This was necessary because in the Netherlands hygienically safe and biologically stable drinking water is produced, without a residual disinfectant and with a very low AOC concentration, below 10 µg acetate C $L^{-1}$ (Van der Kooij et al., 1995; Smeets et al., 2009). In the CDS (Fig. 5.1), NaClO stock solution (80-90 g $Cl_2$ $L^{-1}$) and NaAc stock solution (~ 45 mg acetate C $L^{-1}$) were separately dosed by two peristaltic pumps (Watson-Marlow 504U IP55 Washdown Peristaltic Pump) at a rate of 12 mL $min^{-1}$. At the dosing point, the theoretical chlorine concentration in the bulk water was 0.1 mg $Cl_2$ $L^{-1}$, which is the normal concentration of the residual chlorine in practical DWDSs. Due to the low AOC concentration (< 2 µg acetate C $L^{-1}$) in Dutch drinking water (Ahmad et al., 2019), AOC should be supplemented to mimic the production of biological not stable water in order to avoid limited microbial growth rates on the pipe surface. Thus, according to the relationship between chlorine and AOC displayed in a previous study (Ohkouchi et al., 2013), the AOC concentration in the experimental bulk water was set 50 µg acetate C $L^{-1}$ by dosing NaAc. In order to completely mix the dosed chemicals and feed water, a static mixer (Stock Schedule 80 Threaded PVC Mixer, Koflo Corporation, USA) was installed at the main pipe before the three parallel pipelines. Each parallel pipeline, made of polyvinyl chloride-unplasticised (PVC-U), had an internal diameter of 25 mm and a length of 10 m. For this experiment, the flow rate was set at 3.3-3.8 L $min^{-1}$ (0.11-0.13 m/s), which is within normal flow velocities in Dutch DWDSs. In Pipe 1, the water temperature after the OHE was elevated to 25 °C (the maximum admissible drinking water temperature as mentioned in the Dutch drinking water decree (State Journal, 2011)). All the pipelines were equipped with temperature and flow sensors (Fig. 5.1), to monitor the flow and temperature of bulk water. Dasy Lab software (version 13.0.1) was used for system monitoring and data logging.



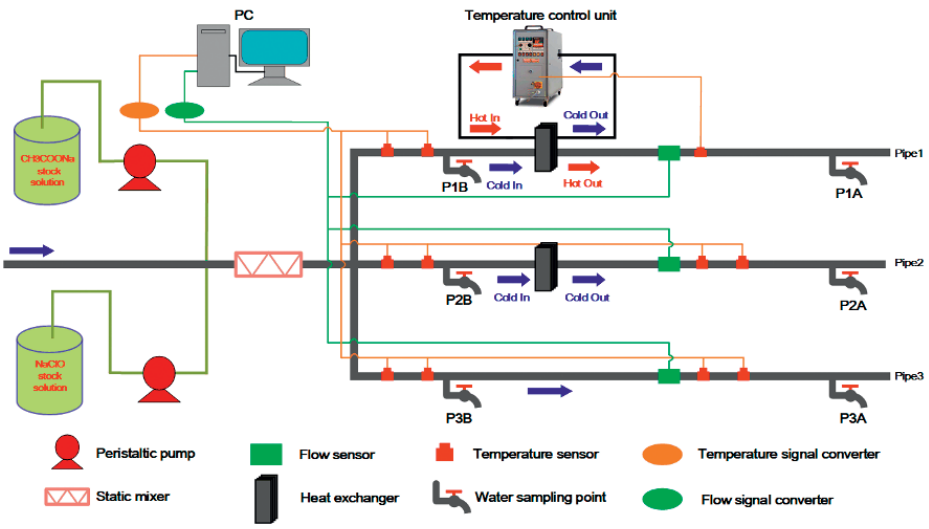


**Figure 5.1:** *Overview of the pilot-scale chlorinated DWDS.*

### 1.2.3 *Sampling*

For water sampling, small PVC-U taps were installed in each pipeline (Fig. 5.1): one was at the front side (P1B, P2B or P3B) and one was at the back side (P1A, P2A or P3A). The water residence time from the front to the back sampling points was around 60s. Feed water and water samples from six taps were taken every seven days during the experimental period (2019 March 15$^{th}$ to 2019 August 9$^{th}$, the data of 6$^{th}$, 7$^{th}$, 9$^{th}$ week were missing). At each tap, after flushing the water for 10 s, 100 mL of water was collected for chlorine determination, and 1 L of water was collected in a sterile glass bottle containing adequate $Na_2S_2O_3$ (quenching residual chlorine) for microbial assay.

For biofilm sampling, 25 cm long PVC-U coupons (pipe sections with valves on both ends) were designed and inserted at the end part of each pipeline. At each biofilm sampling time (1$^{st}$, 2$^{nd}$, 3$^{rd}$, 4$^{th}$, 7$^{th}$, 13$^{th}$ week), biofilms were sampled backwards from the end (p1A, p2A and p3A) of each pipeline in duplicate; and at 21$^{st}$ week, biofilms from both the front sides (p1B, p2B and p3B) and back sides ((p1A, p2A and p3A) of all pipelines were sampled in duplicate and in quadruplicate (two for biomass quantification and two for DNA sequencing), respectively. The two HEs were also disassembled for biofilm collection. To detach the biofilm from the coupons, pipe sections were filled with sterile PBS, placed in a water bath (Ultrasonic 8800, Branson, USA) and treated by ultra-sonication at a frequency of 40 kHz for 2 min. The biofilms grown on the inside plates of each HE were collected in a similar way. The PBS containing detached microbes were subjected to microbial analysis.

### 1.2.4 *Chemical and microbial analysis*

#### *1.2.4.1 Aquatic chemical analysis*

Free chlorine was determined by a chlorine cuvette test kit (LCK 310, HACH LANGE, Germany) and a photometer (DR 3900, HACH LANGE, Germany). Total organic carbon (TOC) was analyzed by a TOC analyzer (TOC-V CPH, SHIMADZU, Japan). pH was determined by a portable pH meter (Multi 3420, WTW, Germany) with a pH-Electrode (SenTix® 940).

#### *1.2.4.2 Biomass quantification*

Bacterial active biomass and cell numbers were quantified by measuring adenosine triphoshpate (ATP) concentration and cell counts of both water samples and biofilm samples (through the PBS containing detached microbes). For water samples, cellular ATP (cATP) concentration was determined to reflect the active biomass using a reagent kit for cATP (QGA™, Luminultra, Canada) and a luminometer (PhotonMaster™, Luminultra, Canada), while to quantify biofilm active biomass, total ATP (tATP) was determined using a reagent kit for tATP (QG21W™, Luminultra, Canada) instead. Cell counts were detected by a flow cytometer (C6-Flowcytometer, Accuri Cytometers, USA) using the same protocol that was previously developed and tested for drinking water samples (Prest et al., 2013). TCC and intact cell counts (ICC) were simultaneously distinguished by adding two stains (SYBR Green I and propidium iodide) as described by Prest et al. (2013).

### 1.2.5 *DNA sequencing and bioinformatics analysis*

#### *1.2.5.1 DNA extraction and 16 S rRNA genes sequencing*

Each PBS containing biofilm sample was filtered by a vacuum pump through a 0.22 μm polycarbonate membrane (25 mm in diameter) to collect biomass for DNA extraction. The total DNA was extracted from the membranes with a FastDNA® SPIN Kit for Soil (Mpbio, Santa Ana, California, USA) according to the manufacturer's protocol. The concentration and purity of the total DNA were measured by a NanoDrop NC2000 spectrophotometry (Thermo Fisher Scientific, Wilmington, Delaware, USA).

Primers 338F (5'-ACTCCTACGGGAGGCAGCA-3') and 806R (5'-GGACTACHVGGG-TWTCTAAT-3') were used to amplify V3 and V4 regions of 16S rRNA gene. PCR amplification was performed using a ABI 2720 PCR (Applied Biosystems, Foster City, California, USA) with a total volume of 25 μL containing 5 μL of 5 × reaction buffer, 5 μL of 5 GC buffer, 2 μL of dNTP (2.5 mM), 1 μL of forward primer (10 μM), 1 μL of reverse primer (10 μM), 2 μL of DNA template, 8.75 μL of ddH2O, 0.25 μL of Q5 DNA polymerase. Thermal cycling conditions were as follows: an initial denaturation at 98 °C for 2 min, and 25-30 cycles at 98 °C for 15 s, 55 °C for 30 s, and 72 °C for 30 s, with a final extension at 72 °C for 5 min. Following amplification, PCR products were purified by VAHTSTM DNA Clean Beads (Vazyme, Nanjing, China), and then quantified using a microplate reader (BIOTEK-FLX800, USA). The high-throughput gene sequencing was performed on the Illumina MiSeq platform by Personal Biotechnology, Co., Ltd. (Shanghai, China).



#### *1.2.5.2 Data analysis*

Raw sequence data were quality filtered and analyzed using QIIME 2 (version 2019.4). Reads were processed by removing tags and primers, and the reads with an average quality score <20 and read lengths <150 bp were discarded. After being processed, reads were assembled by FLASH v 1.2.7 with the overlap between R1 and R2 reads >10 bp. High-quality representative sequences for each operational taxonomic units (OTUs) were assigned using UCLUST with 97% sequence identity. Taxonomic classification was carried out using Greengenes 16S rRNA gene database Release 13.8 (DeSantis et al., 2006). Relative abundance (%) of individual taxa within each community was calculated by comparing the number of sequences of a specific taxon versus the number of total sequences. Alpha diversity of each microbial community was estimated based on Chao1 and Simpson index, respectively. Bray-Curtis dissimilarities were based on individual OTUs, and they were computed for the principal coordinates analyses (PCoA) using PAST 3.

#### *1.2.5.3 Statistical methodologies*

The paired T test was used to determine the significant difference of chlorine, TCC and ICC from the front and the back sampling point of each pipeline. The Wilcoxon signed-rank test was performed to determine the significant difference of cATP from the front and the back sampling point of each pipeline. The Friedmand test was used to determine the significant difference of water quality parameters from different pipelines. Pearson analysis was used to determine the correlation between cATP reduction and chlorine demand. The significant level was set as $p = 0.05$.

## 1.3 Results

### 1.3.1 Bulk water

#### *1.3.1.1 Chemical parameters and temperature of feed water*

During the experimental period, the pH and TOC of the feed water were within the normal value ranges (7.6 ± 0.2 and 3.0 ± 0.7 mg/L, respectively) as displayed in Table 5.1. As shown in Fig. 5.2 (a), the feed water temperature was 9.3 °C at the start of the experiment and increased steadily to 21.4 °C at the end of the experiment, resulting in a temperature difference (□T) in Pipe 1 (the system with cold recovery with a set point of 25 °C after cold recovery) ranging from 3.6 to 15.7 °C. Thus, it can be inferred that the long-term temperature gap in Pipe1 might cause potential microbial difference of bulk water and biofilms at P1A.

*Table 5.1 Microbial and physiochemical parameters of the feed water.*

| Time (week) | cATP (pg/mL) | TCC ($10^5$ cells/mL) | ICC ($10^4$ cells/mL) | pH | TOC (mg/L) |
|---|---|---|---|---|---|
| 0 | 1.91 | / | / | 7.56 | / |
| 1 | 3.11 | / | / | 7.44 | / |
| 2 | 3.05 | 6.96 | 9.54 | / | / |
| 3 | 3.39 | / | / | 7.77 | / |
| 4 | 2.43 | / | / | / | 2.78 |
| 5 | 3.95 | / | / | / | / |
| 8 | 2.00 | 3.61 | 6.69 | / | / |
| 10 | 2.64 | / | / | / | / |
| 11 | 3.64 | / | / | / | 3.88 |
| 12 | 7.54 | / | / | / | / |
| 13 | 4.01 | 4.64 | 10.3 | / | / |
| 14 | 15.7 | / | / | / | / |
| 15 | 2.45 | / | / | / | 2.45 |
| 16 | 7.29 | / | / | / | / |
| 17 | 4.32 | 2.77 | 5.57 | / | / |
| 18 | 6.83 | / | / | / | / |
| 19 | 5.84 | / | / | / | / |
| 20 | 6.47 | / | / | / | / |

#### *1.3.1.2 Free chlorine*

As shown in Fig. 5.2 (b), chlorine experienced slight decreases between two sampling points in all pipelines (1.1%–15.5%). However, paired T-test showed no significant difference of chlorine concentration in Pipe1 and Pipe2 with HEs ($p > 0.05$), and significant difference ($p < 0.05$) only in Pipe3 without a HE. Also, the Friedmand test conducted at the end point of three pipelines showed no significant difference ($p > 0.05$), indicating the residual chlorine at P1A, P2A and P3A were similar.

Furthermore, the chlorine demand (chlorine concentration difference of two sampling points, PA and PB) did not display notable regularity with the change of time in both three pipes (Fig. S5.1).

#### *1.3.1.3 **Biomass***

The microbial activity in the feed water reflected by cATP showed an increasing trend during the experiment from 3.11 to 6.47 pg $mL^{-1}$ (Table 5.1), which was in accordance with the variation patterns of cATP at three front points P1B, P2B and P3B (Fig. S5.2). Fig 5.2(c) showed cATP reductions in all three pipes, but only Pipe1 and Pipe2 showed significant differences ($p < 0.05$) according to the Wilcoxon signed-rank test. Additionally, the cATP concentration decrease in Pipe1 (0.63 pg $mL^{-1}$) and Pipe2 (0.69 pg $mL^{-1}$) were both higher than that in Pipe 3 (0.40 pg $mL^{-1}$). The results showed that the decrease of microbial activity caused by chlorine was more obvious in the two pipes with HEs, but no significant difference could be found between Pipe1 and Pipe2. Moreover, Pearson correlation analysis did not show positive correlation between cATP reduction and chlorine demand ($p > 0.05$).

As shown in Fig. 5.2 (d), there was no significant difference ($p > 0.05$) in TCC among all samples with a narrow average concentration range of 5.51–5.81×$10^5$ cells $mL^{-1}$. Conversely, ICC showed significant decreases in all three pipelines ($p < 0.05$), and the average reduction rates in Pipe1, Pipe2 and Pipe3 were 29.4%, 24.7% and 22.4%, respectively. However, the ICC reductions showed no significant differences among the three pipes ($p > 0.05$).

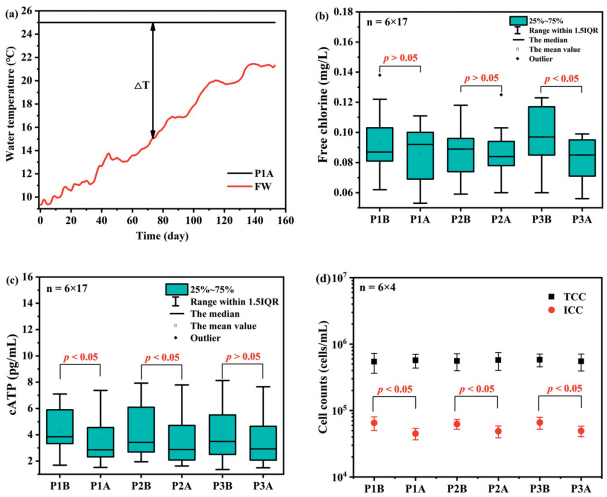


**Figure: 5.2** *(a) Feed water temperature, (b) free chlorine, (c) cATP and (d) cell counts of bulk water samples.*

### 1.3.2 Biofilm

#### *1.3.2.1 **Biomass growth***

The biofilm biomass growth of the back parts of three pipelines was monitored during the whole experiment. As can be seen from Fig. 5.3 (a), the biofilm biomass increased slightly to the values

of 0.91–2.49 pg cm$^{-2}$ during the first 7 weeks, and no significant difference could be found among three pipelines. However, after 7 weeks the biomass rose dramatically in all biofilms, especially for p1A where the biofilm developed at a relatively high temperature of 25 °C. At week 21, the biofilm biomass of p1A, p2A and p3A were 26.5±1.5 ATP pg cm$^{-2}$, 14.6±6.6 ATP pg cm$^{-2}$ and 10.2±1.7 ATP pg cm$^{-2}$, respectively. Additionally, the final biofilm biomass reflected by both ATP and TCC (Fig. 5.3 (b)) showed that the obvious difference between the front and the back biofilm could only be found in Pipe1 (p1B (14.8 ATP pg cm$^{-2}$; 6.2×10$^{4}$ cells cm$^{-2}$) vs. p1A (26.5±1.5 ATP pg cm$^{-2}$; 1.7×10$^{5}$ cells cm$^{-2}$)).

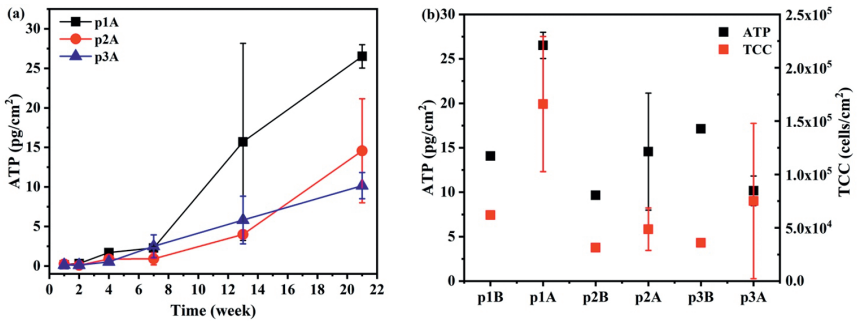


**Figure 5.3:** *Biofilm growth at (a) the back part of three pipelines and (b) comparison of biofilm biomass at week 21 among six sampling points.*

### *1.3.2.2* ***Bacterial community***

In order to explore the bacterial community of different biofilm samples, high-throughput sequencing based on 16S rRNA gens was used. The results of p1A, p2A and p3A were shown as the average values of the duplicate samples, while results of OHE and NOHE were presented as single sample. Two alpha diversity indices including Chao1 (species richness estimator) and Simpson (species diversity index) were used to analyze the biodiversity of the bacterial communities (Fig. S 5.3 (a)). p3A biofilm had the highest Chao1 and Simpson indices, indicating the highest community richness and evenness among all pipeline biofilms. p1A biofilm showed higher community richness than p2A biofilm, while its community diversity was lower than the latter one. Regarding HE samples, the Chao1 index of OHE was less than half of the value of that of NOHE. However, the Simpson index of OHE was more than twice of that of NOHE. This indicates, although the OHE biofilm community had a lower species number compared to NOHE, its species were distributed more evenly. PCoA on the OTU level were plotted to compare the bacterial community compositions of different biofilm samples (Fig. S 5.3(b)). It is clearly shown from the plot that p1A, p2A and p3A biofilms were clustered in one group while the Bray-Curtis distances of NOHE and OHE biofilms were both far away from the pipeline group as well as from each other.

The major bacterial phylum and genus in each biofilm sample are shown by bar plots in Figure 5.4. At the phylum level, *Proteobacteria* (75.6%–87.%) were dominant in all samples, followed by *Bacteroidetes* (3.6%–15.3%) and *Planctomycetes* (0.3%–4.8%). At the genus level, the top three genera in all biofilm communities were *Pseudomonas*, *Sphingomonas* and *Sphingobium*. Regarding

the pipe samples, *Pseudomonas* and *Sphingobium* were found to be more abundant in p1A biofilm (20.2% and 17.4%, respectively) compared to p2A biofilm (2.9% and 5.3%, respectively) and p3A biofilm (2.7% and 12.8%, respectively). The other major genera with the highest relative abundance in p1A biofilm were *Methyloversatilis* (4.4%), *Rhizobacter* (2.7%), *Novosphingobium* (2.3%) and *Legionella* (0.14%). As for the HE samples, OHE biofilm had more *Pseudomonas* (17.3%), *Ralstonia* (7.2%) and *Vibrionimonas* (13.4%) than NOHE biofilm (2.0%, 7.2% and 4.4% for *Pseudomonas*, *Ralstonia*, and *Vibrionimonas*, respectively).

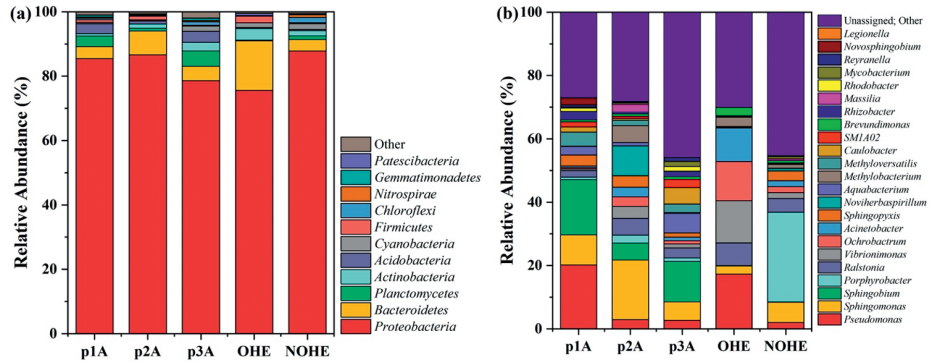


**Figure 5.4:** Bacterial community compositions of biofilm samples at (a) phylum level and (b) genus level.

## 1.4 Discussion

### 1.4.1 Bulk water

Due to the important role residual chlorine plays in controlling microbial regrowth in DWDS, its decay should be carefully investigated. The rate of chlorine decay has been shown to be sensitive to water temperature. Ndiongue et al. (2005) reported that in a simulated DWDS reactor, chlorine demand could rise from 0.5 $Cl_2$ mg $L^{-1}$ to 1.1 $Cl_2$ mg $L^{-1}$ when temperature increased from 6 °C to 18 °C. In another study (Monteiro et al., 2017), authors also proved that the reaction rate coefficient of chlorine decay increased significantly from a water temperature of 10 °C to 30 °C. Additionally, the wall decay coefficient (the rate of wall chlorine decay in pipeline) showed to be related to the specific surface area (SSA) of DWDS (i.e. the pipe-wall area per unit of pipe volume) (Rossman et al., 1994; Vasconcelos and Boulos, 1996), which reasonably leads to a hypothesis that the increasing SSA brought by the HE in the two HE-installed pipelines of this study may affect the reaction rate of chlorine decay. However, the results obtained in this study showed limited chlorine decay in our set-up, and the difference of the decay in three pipelines could not be distinguished clearly as well (Fig. 5.2 (b)). In the previous studies associated with chlorine decay, detectable chlorine concentration reduction was monitored by minutes or hours, but in our experiments the contact time of chlorine and bulk water as well as pipe wall was only ~60 s, which resulted in a slight chlorine decay and insignificant difference among different pipelines.

The detectable decreases of cATP (Fig. 5.2 (c)) and ICC (Fig. 5.2 (d)) in each pipe demonstrated that the chlorine level (0.1 mg $Cl_2$/L) in this study could partially inhibit the microbial activity

in the bulk water within a short contact time. However, such inhibition showed no obvious difference between Pipe1 and Pipe2, indicating limited effect of sudden temperature increase on the chlorine inactivation. The disinfection rate of chlorine is temperature-dependent as discussed above. Nevertheless, as with the absence of a temperature effect on chlorine decay, the absence of a temperature effect on microbial inactivation in this study could also be explained by the short contact time. It should be noted that the pipelines with HE showed larger microbial reduction (Fig. 5.2 (c)) than Pipe3 (without HE). It may be hypothesized that a HE could enhance the disinfection efficiency of chlorine towards microbes, although this could not be confirmed by a chlorine demand increase in this study. A possible explanation for the enhanced disinfection efficiency may be that the closely-aligned plates designed for increasing heat-exchange efficiency in the HE provided several micro-channels for the water flowing through the HE, which enhanced the mixing efficiency of the potential reactants (Li et al., 2007). This might improve the contact frequency between chlorine and microorganisms and subsequently result in a promotion of disinfection efficiency. However, the actual mechanism should be further investigated.

### 1.4.2 Biofilm

In this study, each pipeline biofilm underwent a "lag time", when biomass increased slowly on the pipe surface. This is consistent with a previous study, where detectable biomass was present on the 40$^{th}$ day after the beginning of biofilm formation (Wang et al., 2019). In the lag time, reversible and irreversible attachment of microbial cells successively happen on the pipe surface before the cell proliferation (Liu et al., 2016). Our results showed a much faster biomass growth rate of the biofilm at a higher constant temperature (25 °C) than the ones in the lower fluctuating temperatures (13.3–21.3 °C) after the lag time (Fig. 5.3 (a)). This finding is in accordance with the previously obtained conclusion that an elevated temperature increases biofilm growth, especially in the presence of biodegradable organic matter (Hallam et al., 2001; Tsvetanova and Dimitrov, 2012). Within the common water temperature range, the increase of temperature can promote the microbial cell secretion of extracellular polymeric substances (EPS), a key substance for the microbial early aggregate on the pipe surface (Herald and Zattola, 1988; Yu et al., 2019), and enhance the activity and growth rate of the attached cells (Mayo and Noike, 1996). In contrast, Ndiongue et al. (2005) and Ollos (1998) reported that the temperature effect on biofilm growth became limited when biofilms were in a steady state. Therefore, it can be hypothesized that the biofilm biomass of p2A and p3A might have been closer to that of p1A if the biofilm growth time was long enough to reach a steady state.

Alpha diversity analysis revealed that due to the higher temperature (approximate 27 °C) of the OHE's wall surface than that of NOHE's (Ahmad et al., 2020), the biofilm of OHE had less diverse but more stable community composition than NOHE, which was rewarding to maintain the water quality after the cold recovery. PCoA analysis showed that the community compositions of p1A, p2A and p3A clustered in one group (all on PVC-U surface), compared to OHE and NOHE (both on 316 stainless steel (SS) surface), indicating surface material could shape the biofilm community structure. This could be supported by the former studies which confirmed that pipe materials could affect the diversity and composition of the biofilm community (Norton and LeChevallier, 2000;

Yu et al., 2010). The investigation of community composition showed much higher *Pseudomonas* proportion in the biofilms developing in the higher temperatures (p1A and OHE). It has been reported that *Pseudomonas* spp. favors growing in warmer water under oligotrophic conditions (Proctor et al., 2017). The temperature gap between warm samples (p1A and OHE) and cold samples (p2A, p3A, NOHE) might result in the predominance of *Pseudomonas* in the warm samples. Additionally, the relative abundances of other genera like *Sphingobium*, *Novosphingobium*, *Methyloversatilis*, *Ralstonia* and *Legionella* were also found higher in warmer biofilms (p1A or OHE), and all of them were previously discovered as major inhabitants in the warm environments like hot pipes or geothermal springs (Farhat et al., 2018; Jiang et al., 2016; Mahato et al., 2019; van der Kooij et al., 2017). Because of the likely pathogenic risks brought by *Pseudomonas* and *Legionella* (Hwang et al., 2007), their higher proportions in the biofilms during and after the cold recovery should be heeded.

### 1.4.3 Comparison between chlorinated and non-chlorinated cold recovery DWDSs

In our previous study (Ahmad et al, 2020), the effect of cold recovery on the biofilm formation in a non-chlorinated system was investigated. In that study, after 38 weeks of experimental duration, 5.3 times more biofilm was formed after cold recovery (475 ATP pg $cm^{-2}$) compared to biofilm formed without cold recovery (89 ATP pg $cm^{-2}$). However, in the present chlorinated DWDSs, the biofilm biomass after 21 weeks with and without cold recovery was only 26.5 ATP pg $cm^{-2}$ and 14.6 ATP pg $cm^{-2}$, respectively. This means the biofilm biomass was much lower in the chlorinated system than the non-chlorinated system. Although the total biofilm forming time of the previous study was nearly twice (21 weeks vs. 38 weeks) of that of this study, this could not explain 6 to 18 times more biomass in the former case than this one. Therefore, the main reason for this massive difference could be attributed to the negative effect of chlorine on the biofilm formation. The presence of chlorine could degrade the bacterial cell-membrane functional groups to slow down the microbial depositions onto the pipe wall and, therefore prevented the reversible to irreversible transition of cell attachment to surfaces (Xue and Seo, 2013). Furthermore, chlorine could reduce the microbial growth rate of the attached microbes (Butterfield et al., 2002). It should be noted that the increase in biomass (the ratio of the biomass with and without cold recovery) was also hindered by chlorine in our chlorinated DWDS compared to the previous non-chlorinated one (1.8 and 5.3 times for chlorinated system and non-chlorinated system, respectively). In other words, the cold recovery effect became less obvious in the chlorinated system. This might be due to the promotion of chlorine inactivation towards biofilm when temperature increased.

Regarding the difference of the biofilm community compositions of the two studies, the chlorine-resistant bacteria (CRB) genera *Pseudomonas* and *Sphingomonas* (Butterfield et al., 2002) were more abundant in the chlorinated biofilms (2.7%–20.2% and 5.8%–18.8%, respectively) than the non-chlorinated ones (0.2%–2.3% and <1.0%, respectively). This was in accordance with other studies which reported that the use of chlorination could lead to the selection of CRB, including several opportunistic pathogens (Ingerson-Mahar and Reid, 2013; Sun et al., 2013). Moreover, in this study the abundances of *Pseudomonas* and *Sphingomonas* were both higher in plastic pipe biofilms (*Pseudomonas*: 2.8%–20.2% and *Sphingomonas*: 9.5%–12.3%) than HE biofilms (*Pseudomonas*:

2.0%–17.2% and *Sphingomonas*: 2.5%–6.4%) under the same temperatures (Fig. 5.4), suggesting surface materials could also affect the abundances of CRB in biofilms. Unfortunately, due to the lack of biomass data of HE biofilm, the CRB densities on plastic pipe inner surfaces and HE SS plates could not be compared directly. However, according to a previous biofilm formation study under long-term high chlorine level (Zhu et al., 2014), the biomass density in the stabilized biofilm on SS pipe was lower than that on plastic pipes. Thus, in the consideration of both biomass and CRB abundance, SS pipe material can be recommended to prevent the proliferation of CRB in DWDSs.

### 1.4.4 Outlook for future research

Considering the experimental results obtained in this study, specific topics should attain attention in future research concerning cold recovery from chlorinated DWDSs:

(1) In order to investigate the cold recovery effect on the chlorine decay and microbial inactivation efficiency, prolonged contact time should be achieved by using experimental set-ups with longer pipelines. Also, the effect of initial chlorine concentration should be studied.

(2) The processes that take place between the plates of the HEs should be fully investigated. The interaction between chlorine and microorganisms inside the HE needs to be intensively explored. Chlorine decay inside the HE is of concern, especially for HEs after prolonged running times, when biofouling and corrosion are present on the plate surface (Murthy et al., 2005). Additionally, a proper residual chlorine level should be determined to balance microbial control and chlorine-induced corrosion on the HE plate surface (Martins et al., 2014).

(3) In this work, cATP and ICC showed a decreasing trend in bulk waters, but no quantification of specific species (e.g. pathogens) was conducted. The analysis of microbial community composition and functional prediction showed that there were relatively high risks of pathogenic, antibiotic resistance and human diseases related bacteria in the biofilms after cold recovery. As chlorine can promote the detachment of cells from biofilms (Chen and Stewart, 2000), the potential detachment of the risky bacteria should be monitored after the cold recovery where chlorine becomes more active due to the rising temperature.

(4) In this study, chlorine resulted in higher abundances of CRB in biofilms. To mitigate the risk of CRB, researchers have recently proposed several combined disinfection processes such as UV/$Cl_2$, UV/hydrogen peroxide, UV/peroxymonosulfate, etc. (Zhu et al., 2020; Zeng et al., 2020), although most of these processes were only explored on lab-scale. Future studies may focus on optimizing operation parameters to balance continuous disinfection ability and biofilm CRB control, and large-scale application of these technologies in the practical field.

## 1.5 Conclusion

This study explored the effect of cold recovery on the drinking water microbial quality (as cATP, TCC and ICC), and biofilm growth and composition in a chlorinated DWDSs. Slight chlorine decay was detected in all pipelines, but was not affected by the temperature increase. Chlorine could partially inactivate the microbial activities in bulk water, and the inactivation efficiency was slightly promoted by the HEs. The growth rate of biofilm biomass was significantly enhanced by water temperature. The diversity and composition of biofilm microbial community were both shaped by cold recovery and surface materials. For example, *Pseudomonas* spp. had higher abundances in warm biofilms. Compared to the previous results from a non-chlorinated DWDS, the effect of chlorine in this study led to much lower biomass but higher abundances of chlorine-resistant bacteria in the biofilms.

## References:

Ahmad, J.I., Giorgi, S., Zlatanovic, L., Liu, G., Medema, G., Van Der Hoek, J.P., September, 2019. Drinking water distribution networks: an emerging resource for thermal. 3rd IWA Resource Recovery Conference, Venice, Italy.

Ahmad, J.I., Liu, G., van der Wielen, P.W., Medema, G., van der Hoek, J.P., 2020. Effects of cold recovery technology on the microbial drinking water quality in unchlorinated distribution systems. Environ. Res. 183, 109175.

Benarde, M.A., Snow, W.B., Olivieri, V.P., 1967. Chlorine dioxide disinfection temperature effects. J. Appl. Bacteriol. 30 (1), 159-167.

Bloemendal, M., Moerman, A., Hofman, J., Blokker, M., Agudelo-Vera, C., 2015. Recovery of energy from pipes. Report BTO 2015.001, Nieuwegein, The Netherlands (in Dutch): KWR Watercycle Research Institute.

Blokker, E.J.M., van Osch, A.M., Hogeveen, R., Mudde, C., 2013. Thermal energy from drinking water and cost benefit analysis for an entire city. J. Water Clim. Change 4 (1), 11-16.

Butterfield, C.T., Wattie, E., Megregian, S., Chambers, C.W., 1943. Influence of pH and temperature on the survival of coliforms and enteric pathogens when exposed to free chlorine. Public Health Reports (1896-1970), 1837-1866.

Butterfield, P.W., Camper, A.K., Ellis, B.D., Jones, W.L., 2002. Chlorination of model drinking water biofilm: implications for growth and organic carbon removal. Water Res. 36 (17), 4391-4405.

Chen, X., Stewart, P.S., 2000. Biofilm removal caused by chemical treatments. Water Res. 34 (17), 4229-4233.

Collins, E.B., 1955. Factors involved in the control of gelatinous curd defects of cottage cheese: II. Influence of pH and temperature upon the bactericidal efficiency of chlorine. J. Milk Food Technol. 18 (8), 189-191.

Dai, D., Rhoads, W.J., Edwards, M.A., Pruden, A., 2018. Shotgun metagenomics reveals taxonomic and functional shifts in hot water microbiome due to temperature setting and stagnation. Front. Microbiol. 9, 2695.

De Pasquale, A.M., Giostri, A., Romano, M.C., Chiesa, P., Demeco, T., Tani, S., 2017. District heating by drinking water heat pump: Modelling and energy analysis of a case study in the city of Milan. Energy 118, 246-263.

DeSantis, T.Z., Hugenholtz, P., Larsen, N., Rojas, M., Brodie, E.L., Keller, K., Huber, T., Dalevi, D., Hu, P., Andersen, G.L., 2006. Greengenes, a chimera-checked 16S rRNA gene database and workbench compatible with ARB. Appl. Environ. Microbiol. 72 (7), 5069-5072.

Douglas, G.M., Maffei, V.J., Zaneveld, J., Yurgel, S.N., Brown, J.R., Taylor, C.M., Huttenhower, C., Langille, M.G., 2019. PICRUSt2: An improved and extensible approach for metagenome inference. BioRxiv, 672295.

Douterelo, I., Calero-Preciado, C., Soria-Carrasco, V., Boxall, J.B., 2018. Whole metagenome sequencing of chlorinated drinking water distribution systems. Environ. Sci-Wat. Res. 4 (12), 2080-2091.

Elias Maxil, J.A., 2015. Heat modeling of wastewater in sewer networks: Determination of thermal energy content from sewage with modeling tools. Doctoral Thesis, Department of Water Management, Delft University of Technology, Delft, the Netherlands.

Elías-Maxil, J.A., van der Hoek, J.P., Hofman, J., Rietveld, L., 2014. A bottom-up approach to estimate dry weather flow in minor sewer networks. Water Sci. Technol. 69 (5), 1059-1066.

Farhat, M., Moletta Denat, M., Trouilhé, M.C., Frère, J., Robine, E., 2018. Transitory Change of Bacterial Community Structure in Hot Water Biofilm: Effects of Anti–Legionella Treatments. CLEAN-Soil Air Water 46 (6), 1700203.

Fish, K.E., Osborn, A.M., Boxall, J., 2016. Characterising and understanding the impact of microbial biofilms and the extracellular polymeric substance (EPS) matrix in drinking water distribution systems. Environ. Sci.-Wat. Res., 2 (4), 614-630.

Guo, X., Hendel, M., 2018. Urban water networks as an alternative source for district heating and emergency heat-wave cooling. Energy 145, 79-87.

Hallam, N.B., West, J.R., Forster, C.F., Simms, J., 2001. The potential for biofilm growth in water distribution systems. Water Res. 35 (17), 4063-4071.

Herald, P.J., Zattola, E.A., 1988. Attachment of Listeria monocytogenes to stainless steel surfaces at various temperatures and pH values. J. Food Sci. 53 (5), 1549-1562.

Hofman, J., van der Wielen, P., 2015. Heat and cold from drinking water and sewage system. Report BTO 2015.002, Nieuwegein, The Netherlands (in Dutch): KWR Watercycle Research Institute.

Hwang, M.G., Katayama, H., Ohgaki, S., 2007. Inactivation of Legionella pneumophila and Pseudomonas aeruginosa: Evaluation of the bactericidal ability of silver cations. Water Res. 41 (18), 4097-4104.

Ingerson-Mahar, M., Reid, A., 2013. Microbes in pipes: the microbiology of the water distribution system. American Academy of Microbiology.

Jiang, B., Sun, Z., Liu, M., 2010. China's energy development strategy under the low-carbon economy. Energy 35 (11), 4257-4264.

Jiang, Z., Li, P., Jiang, D., Dai, X., Zhang, R., Wang, Y., Wang, Y., 2016. Microbial community structure and arsenic biogeochemistry in an acid vapor-formed spring in Tengchong geothermal area, China. PLoS One 11 (1).

Kehrer, J.P., Robertson, J.D., Smith, C.V.,2010. 1.14 - Free radicalsand reactive oxygen species, Compr. Toxicol. 1, 277-307.

LeChevallier, M.W., Welch, N.J., Smith, D.B., 1996. Full-scale studies of factors related to coliform regrowth in drinking water. Appl. Environ. Microbiol., 62 (7), 2201-2211.

Le Dantec, C., Duguet, J., Montiel, A., Dumoutier, N., Dubrou, S., Vincent, V., 2002. Chlorine disinfection of atypical mycobacteria isolated from a water distribution system. Appl. Environ. Microbiol. 68 (3), 1025-1032.

Lelieveld, J., Klingmüller, K., Pozzer, A., Burnett, R.T., Haines, A., Ramanathan, V., 2019. Effects of fossil fuel and total anthropogenic emission removal on public health and climate. PNAS 116 (15), 7192-7197.

Li, A., Chen, L., Zhang, Y., Tao, Y., Xie, H., Li, S., Sun, W., Pan, J., He, Z., Mai, C., 2018. Occurrence and distribution of antibiotic resistance genes in the sediments of drinking water sources, urban rivers, and coastal areas in Zhuhai, China. Environ. Sci. Pollut. R. 25 (26), 26209-26217.

Li, R.A., McDonald, J.A., Sathasivan, A., Khan, S.J., 2019. Disinfectant residual stability leading to disinfectant decay and by-product formation in drinking water distribution systems: A systematic review. Water Res. 153, 335-348.

Li, S., Xu, J., Wang, Y., Luo, G., 2007. Mesomixing scale controlling and its effect on micromixing performance. Chem. Eng. Sci. 62 (13), 3620-3626.

Li, W., Tan, Q., Zhou, W., Chen, J., Li, Y., Wang, F., Zhang, J., 2020. Impact of substrate material and chlorine/chloramine on the composition and function of a young biofilm microbial community as revealed by high-throughput 16S rRNA sequencing. Chemosphere 242, 125310.

Liu, S., Gunawan, C., Barraud, N., Rice, S.A., Harry, E.J., Amal, R., 2016. Understanding, monitoring, and controlling biofilm growth in drinking water distribution systems. Environ. Sci. Technol. 50 (17), 8954-8976.

Liu, S., Qu, H., Yang, D., Hu, H., Liu, W., Qiu, Z., Hou, A., Guo, J., Li, J., Shen, Z., 2018. Chlorine disinfection increases both intracellular and extracellular antibiotic resistance genes in a full-scale wastewater treatment plant. Water Res. 136, 131-136.

Mahato, N.K., Sharma, A., Singh, Y., Lal, R., 2019. Comparative metagenomic analyses of a high-altitude Himalayan geothermal spring revealed temperature-constrained habitat-specific microbial community and metabolic dynamics. Arch. Microbiol. 201 (3), 377-388.

Martins, C., Moreira, J.L., Martins, J.I., 2014. Corrosion in water supply pipe stainless steel 304 and a supply line of helium in stainless steel 316. Eng. Fail. Anal. 39, 65-71.

Mayo, A.W., Noike, T., 1996. Effects of temperature and pH on the growth of heterotrophic bacteria in waste stabilization ponds. Water Res. 30 (2), 447-455.

Mol, S., Kornman, J.M., Kerpershoek, A.J., Van Der Helm, A., 2011. Opportunities for public water utilities in the market of energy from water. Water Sci. Technol. 63 (12), 2909-2915.

Monteiro, L., Figueiredo, D., Covas, D., Menaia, J., 2017. Integrating water temperature in chlorine decay modelling: a case study. Urban Water J. 14 (10), 1097-1101.

Murthy, P.S., Venkatesan, R., Nair, K., Inbakandan, D., Jahan, S.S., Peter, D.M., Ravindran, M., 2005. Evaluation of sodium hypochlorite for fouling control in plate heat exchangers for seawater application. Int. Biodeter. Biodegr. 55 (3), 161-170.

Ndiongue, S., Huck, P.M., Slawson, R.M., 2005. Effects of temperature and biodegradable organic matter on control of biofilms by free chlorine in a model drinking water distribution system. Water Res. 39 (6), 953-964.

Norton, C.D., LeChevallier, M.W., 2000. A pilot study of bacteriological population changes through potable water treatment and distribution. Appl. Environ. Microbiol. 66 (1), 268-276.

Ohkouchi, Y., Ly, B.T., Ishikawa, S., Kawano, Y., Itoh, S., 2013. Determination of an acceptable assimilable organic carbon (AOC) level for biological stability in water distribution systems with minimized chlorine residual. Environ. Monit. Assess. 185 (2), 1427-1436.

Ollos, P.J., 1998. Effects of drinking water biodegradability and disinfectant residual on bacterial regrowth. Doctoral Thesis, Department of Civil Engineering, University of Waterloo, Ontario, Canada.

Painter, D.S., 2020. Review of the book Burning Up: A Global History of Fossil Fuel Consumption, by Simon Pirani. Journal of Interdisciplinary History 50 (3), 442-443. https://www.muse.jhu.edu/article/741623.

Pinto, A.J., Schroeder, J., Lunn, M., Sloan, W., Raskin, L., 2014. Spatial-temporal survey and occupancy-abundance modeling to predict bacterial community dynamics in the drinking water microbiome. MBio 5 (3), e01135-14.

Prest, E.I., Hammes, F., Kötzsch, S., Van Loosdrecht, M., Vrouwenvelder, J.S., 2013. Monitoring microbiological changes in drinking water systems using a fast and reproducible flow cytometric method. Water Res. 47 (19), 7131-7142.

Prest, E.I., Weissbrodt, D.G., Hammes, F., Van Loosdrecht, M.C.M., Vrouwenvelder, J.S., 2016. Long-term bacterial dynamics in a full-scale drinking water distribution system. PLoS One 11 (10).

Preciado, C.C., Boxall, J., Soria-Carrasco, V., Douterelo, I., 2019. Effect of temperature increase in bacterial and fungal communities of chlorinated drinking water distribution systems. Access Microbiol. 1 (1A).

Proctor, C.R., Dai, D., Edwards, M.A., Pruden, A., 2017. Interactive effects of temperature, organic carbon, and pipe material on microbiota composition and Legionella pneumophila in hot water plumbing systems. Microbiome 5 (1), 130.

Rogelj, J., Den Elzen, M., Höhne, N., Fransen, T., Fekete, H., Winkler, H., Schaeffer, R., Sha, F., Riahi, K., Meinshausen, M., 2016. Paris Agreement climate proposals need a boost to keep warming well below 2 °C. Nature 534 (7609), 631-639.

Rossman, L.A., Clark, R.M., Grayman, W.M., 1994. Modeling chlorine residuals in drinking-water distribution systems. J. Environ. Eng. 120 (4), 803-820.

Sanner, B., Karytsas, C., Mendrinos, D., Rybach, L., 2003. Current status of ground source heat pumps and underground thermal energy storage in Europe. Geothermics 32 (4-6), 579-588.

Sathasivan, A., Chiang, J., Nolan, P., 2009. Temperature dependence of chemical and microbiological chloramine decay in bulk waters of distribution system. Water Sci. Tech-W Sup. 9 (5), 493-499.

State Journal, 2011. Decree of 23 May 2011 concerning the regulations for the production and distribution of drinking water and the organization of the public drinking water supply. Staatscourant - Official Journal of the Royal Kingdom of The Netherlands No. 293, 23 May 2011 (in Dutch).

Sun, W., Liu, W., Cui, L., Zhang, M., Wang, B., 2013. Characterization and identification of a chlorine-resistant bacterium, *Sphingomonas* TS001, from a model drinking water distribution system. Sci. Total Environ. 458, 169-175.

Smeets, P.W.M.H., Medema, G.J., Van Dijk, J.C., 2009. The Dutch secret: how to provide safe drinking water without chlorine in the Netherlands. Drinking Water Eng. Sci. 2 (1), 1.

Torrens, G., Hernández, S.B., Ayala, J.A., Moya, B., Juan, C., Cava, F., Oliver, A., 2019. Regulation of AmpC-driven β-lactam resistance in *Pseudomonas aeruginosa*: different pathways, different signaling. mSystems 4 (6).

Tsvetanova, Z.G., Dimitrov, D.N., 2012. Biofilms and bacteriological water quality in a domestic installation model simulating daily drinking water consumption. Water Sci. Tech-W Sup. 12 (6), 720-726.

van der Kooij, D., Drost, Y.C., Hijnen, W.A.M., Willemsen-Zwaagstra, J., Nobel, P.J. Schellart, J.A., 1995. Multiple barriers against micro-organisms in water treatment and distribution in The Netherlands. Water Sup. 13 (2), 13–23.

van der Hoek, J.P., 2012. Climate change mitigation by recovery of energy from the water cycle: a new challenge for water management. Water Sci. Technol. 65 (1), 135-141.

van der Hoek, J.P., 2012. Towards a climate neutral water cycle. J. Water Clim. Change 3 (3), 163-170.

van der Hoek, J.P., Mol, S., Giorgi, S., Ahmad, J.I., Liu, G., Medema, G., 2018. Energy recovery from the water cycle: Thermal energy from drinking water. Energy 162, 977-987.

van der Kooij, D., Bakker, G.L., Italiaander, R., Veenendaal, H.R., Wullings, B.A., 2017. Biofilm composition and threshold concentration for growth of *Legionella pneumophila* on surfaces exposed to flowing warm tap water without disinfectant. Appl. Environ. Microbiol. 83 (5), e2716-e2737.

van der Wielen, P.W., van der Kooij, D., 2010. Effect of water composition, distance and season on the adenosine triphosphate concentration in unchlorinated drinking water in the Netherlands. Water Res. 44(17), 4860-4867.

van der Wielen, P.W., van der Kooij, D., 2013. Nontuberculous mycobacteria, fungi, and opportunistic pathogens in unchlorinated drinking water in The Netherlands. Appl. Environ. Microbiol. 79 (3), 825–834.

Vasconcelos, J.J., Boulos, P.F., 1996. Characterization and modeling of chlorine decay in distribution systems, American Water Works Association, USA.

Wang, Y., Zhu, B., Tong, J., Bai, X., 2019. Growth features of water supply pipeline biofilms based on active microorganisms. Chinese J. Environ. Sci. 2 (40), 853-858 (in Chinese).

Xu, L., Ouyang, W., Qian, Y., Su, C., Su, J., Chen, H., 2016. High-throughput profiling of antibiotic resistance genes in drinking water treatment plants and distribution systems. Environ. Pollut. 213, 119-126.

Xue, Z., Seo, Y., 2013. Impact of chlorine disinfection on redistribution of cell clusters from biofilms. Environ. Sci. Technol. 47 (3), 1365-1372.

Yu, J., Kim, D., Lee, T., 2010. Microbial diversity in biofilms on water distribution pipes of different materials. Water Sci. Technol. 61 (1), 163-171.

Yu, R., Liu, Z., Yu, Z., Wu, X., Shen, L., Liu, Y., Li, J., Qin, W., Qiu, G., Zeng, W., 2019. Relationship among the secretion of extracellular polymeric substances, heat resistance, and bioleaching ability of *Metallosphaera sedula*. Int. J. of Min. Met. Mater. 26 (12), 1504-1511.

Zeng, F.Z., Cao, S., Jin, W.B., Zhou, X., Ding, W.Q., Tu, R.J., Han, S.F., Wang, C.P., Jiang, Q.J., Huang, H., Ding, F., 2020. Inactivation of chlorine-resistant bacterial spores in drinking water using UV irradiation, UV/Hydrogen peroxide and UV/Peroxymonosulfate: Efficiency and mechanism. J. Clean. Prod. 243, 118666.

Zhu, Y., Chen, L., Xiao, H., Shen, F., Deng, S.H., Zhang, S.R., He, J.S., Song, C., Wang, X., Zhang, J.H., Gong, L., Hu, C., 2020. Effects of disinfection efficiency on microbial communities and corrosion processes in drinking water distribution systems simulated with actual running conditions. J. Environ. Sci-China 88, 273-282.

Zhu, Z., Wu, C., Zhong, D., Yuan, Y., Shan, L., Zhang, J., 2014. Effects of pipe materials on chlorine-resistant biofilm formation under long-term high chlorine level. Appl. Biochem. Biotechnol. 173(6), 1564-1578.

# Supplementary Information chapter 5

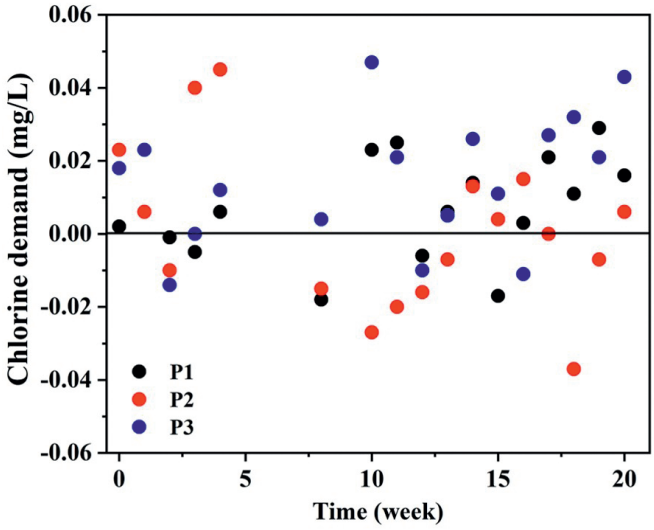


**Figure S** *5.1: The variations of chlorine demand over time.*

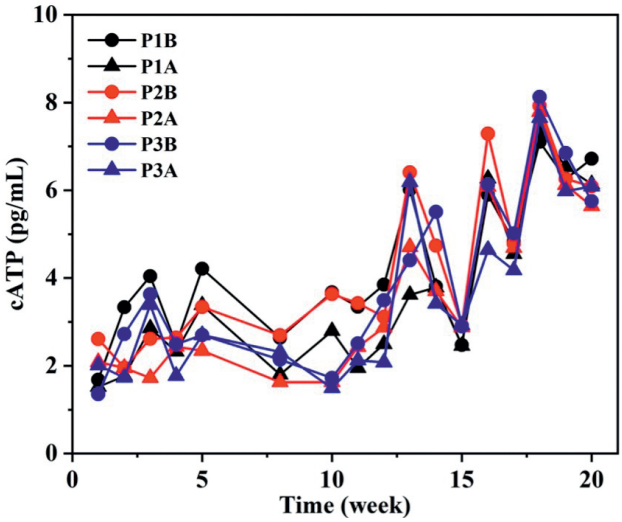


**Figure S** *5.2: The variations of cATP at each sampling point overtime.*

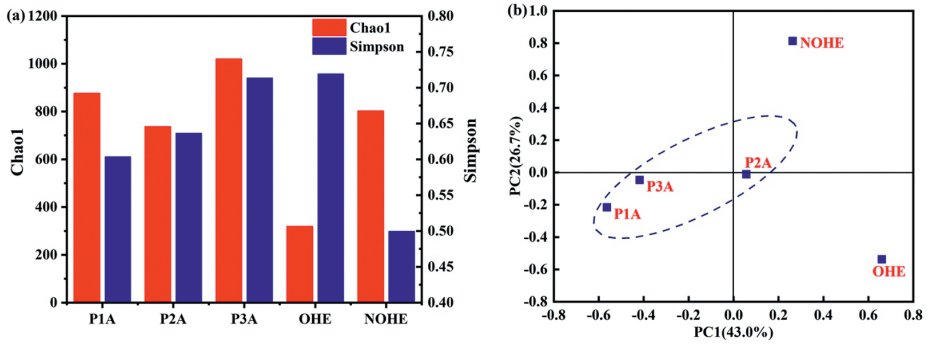


**Figure S** *5.3: (a) Alpha diversity indices (Chao1 and Simpson) and (b) PCoA plot based on Bray-Curtis dissimilarity matrix for all biofilm samples.*

PART 4

# TED POTENTIAL FROM DRINKING WATER DISTRIBUTION SYSTEMS

Chapter 6

# Maximizing Thermal Energy Recovery from Drinking Water for Cooling Purpose

CHAPTER 6


## Abstract

Drinking water distribution networks (DWDNs) have a huge potential for cold thermal energy recovery (TED). TED can provide cooling for buildings and spaces with high cooling requirements as an alternative for traditional cooling, reduce usage of electricity or fossil fuel, and thus TED helps reduce greenhouse gas (GHG) emissions. There is no research on the environmental assessment of TED systems, and no standards are available for the maximum temperature limit ($T_{max}$) after recovery of cold. During cold recovery, the water temperature increases, and water at the customer's tap may be warmer as a result. Previous research showed that increasing $T_{max}$ up to 30 °C is safe in terms of microbiological risks. The present research was carried out to determine what raising $T_{max}$ would entail in terms of energy savings, GHG emission reduction and water temperature dynamics during transport. For this purpose, a full-scale TED system in Amsterdam was used as a benchmark, where $T_{max}$ is currently set at 15 °C. $T_{max}$ was theoretically set at 20, 25 and 30 °C to calculate energy savings and $CO_2$ emission reduction and for water temperature modeling during transport after cold recovery. Results showed that by raising $T_{max}$ from the current 15 °C to 20, 25 and 30 °C, the retrievable cooling energy and GHG emission reduction could be increased by 250, 425 and 600%, respectively. The drinking water temperature model predicted that within a distance of 4 km after TED, water temperature resembles that of the surrounding subsurface soil. Hence, a higher $T_{max}$ will substantially increase the TED potential of DWDN while keeping the same comfort level at the customer's tap.



**Keywords:** energy transition; cold recovery; cooling; carbon footprints reduction; drinking water distribution networks; greenhouse gas emissions

*This Chapter has been published as: Ahmad, J.I., Giorgi, S., Zlatanovic, L., Liu, G., van der Hoek, J.P. (2021) Maximizing Thermal Energy Recovery from Drinking Water for Cooling Purpose. Energies 14, 2413.*

## 1.1 Introduction:

Resource recovery from the water cycle is gaining much attention. The focus is much on materials from wastewater, such as nutrients, carbon, energy in the form of biogas and water itself [1–3]. Resource recovery from drinking water has also been described and is applied in practice, e.g., the recovery of calcite from the pellet softening process in drinking water treatment [4]. The thermal energy from sewage water and wastewater treatment plant effluent has been pointed at as a valuable resource [5,6]. However, at the same time, it is stressed that more research is needed into environmental assessments of thermal energy recovery systems [7]. The potential of thermal energy recovery from the water cycle, including wastewater, surface water, groundwater and drinking water, has been estimated for Amsterdam and its surroundings, focusing on the possibilities to reduce carbon emissions [8–11]. A specific thermal energy source appeared to be the cold water in the drinking water distribution network [12]. Depending on the drinking water temperature in the network, it can be used for both heating and cooling purposes.

Global warming is raising the earth's temperature [13], and therefore, the demand for cooling is growing substantially. In the European Union, the use of central and room air conditioning units for space cooling has increased by 50 times from the 90′s till 2010 [14]. In Amsterdam (the Netherlands), the energy required for space cooling of non-residential spaces amounts to 2162 TJ/y [15,16]. Providing this energy with traditional cooling methods (i.e., mechanical cooling or cooling towers) requires a huge amount of electricity and water and results in a high carbon footprint [17–19]. Hence, there is a need to explore more sustainable cooling resources. Drinking water distribution networks (DWDNs) contain much thermal energy in the form of cold. For example, in Amsterdam, where drinking water is produced from surface water, the temperature within the DWDN is between 4–10 °C in winter and between 15–20 °C in summer [20]. These temperatures offer possibilities to recover thermal energy for cooling by heat exchange during wintertime: drinking water exchanges its cold temperature with a warm carrier medium (e.g., air, water, glycol, etc.) inside a heat exchanger, and the slightly heated water flows back into the DWDN [20–22]. This cold temperature recovery from DWDNs, mostly available during winter time with low drinking water temperatures, is scarcely available during times of high cooling demand (i.e., during summer with high drinking water temperatures). An option to overcome this hurdle is to recover and store the low temperature in aquifer thermal energy storage (ATES) systems for later use in summer. During winter the recovered thermal energy can also be utilized directly without intermediate storage as free available cooling (Figure 6.1).

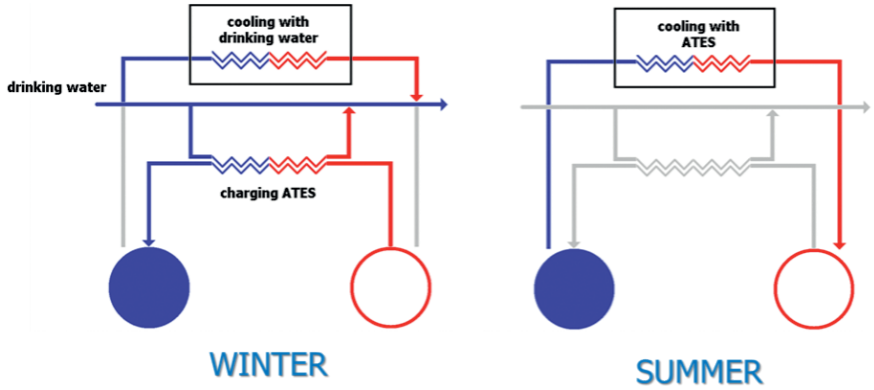


**Figure 6.1.** *Cold drinking water in wintertime (left) is directly utilized in winter periods for places with extensive cooling requirements or is used for charging an aquifer thermal energy storage system (ATES) to provide space cooling in upcoming summer periods (right).*

However, retrieving cold from DWDNs means increasing the temperature of the drinking water during the energy exchange, which means elevated temperatures in the DWDN. After the use of the drinking water by the customers, the drinking water turns into wastewater. Due to the higher temperature of the drinking water after cold recovery, cold recovery does not compete with thermal energy (heat) recovery from wastewater [5,11]. The higher the temperature of the drinking water that can be allowed after cold recovery ($T_{max}$), the higher the temperature difference between the incoming drinking water and drinking water leaving the heat exchanger, and the longer the period in the year the heat exchange can be applied. For example, a $T_{max}$ of 18 °C means that when the incoming water temperature exceeds 18 °C, during that time, the cold recovery cannot be applied. Hence, a high $T_{max}$ is attractive as it increases the energy recovery potential and carbon footprint reduction potential of the system. The $T_{max}$ is determined by the effects an elevated drinking water temperature may have on the microbiological water quality and the standard for the drinking water temperature at the customer's tap.

Concerning an elevated temperature, this may enhance microbial activity and proliferation of temperature-sensitive opportunistic pathogens like *Legionella* spp. [23]. This may occur both in the water and biofilm phase (the layer of microbes attached to the inside of the pipes), with possible negative effects on water quality. Our previous pilot scale studies revealed that, with a drinking water temperature of 25 °C and 30 °C after cold recovery, no negative effects were observed in the water phase in terms of water quality parameters (like microbial activity: total biomass and cell counts) and proliferation of opportunistic pathogens (*Legionella* spp.) [24]. However, the elevated drinking water temperatures, due to cold recovery, did enhance the initial biofilm growth (in terms of biomass) in the first 2–3 months of operation, compared to the biofilm growth in a reference system, in which no cold recovery was applied. Later (after 3–4 months), when the biofilm reached its steady growth phase, comparable biomass was observed in the systems with cold recovery and the reference system. Within the initial three months of applying cold recovery at the pilot plant scale, drinking water quality parameters (biomass activity and cell concentration) increased after

cold recovery compared to the reference system but stayed within the standards of the Dutch drinking water regulation [24].

The concept of cold recovery from drinking water has been of interest to water utilities for the last years. The recovery of cold from DWDNs or from drinking water reservoirs for use in district cooling has been investigated and simulated for potential use in different countries applying chlorinated DWDNs, such as in Italy [25], France [26] and the United Kingdom [27]. However, the cold recovery from drinking water is not yet conceptualized in any of these places because of different reasons. Especially maintaining the drinking water quality after cold recovery was one of the primary concerns. The chlorinated distribution systems are not thoroughly investigated regarding the microbial water quality changes after cold recovery, except one pilot scale study, which observed that the decay of chlorine was not effected by the temperature increase of up to 25 °C, and this higher temperature also had no effect on microbial water quality parameters, such as total cell count and ATP [28]. For full-scale TED application, microbial water quality investigations on chlorinated DWDSs are required.

The feed drinking water that was used at pilot scale in this study and in full-scale studies in the Netherlands for cold recovery, as well as its effect on microbiological water quality, originated from non-chlorinated distribution systems and was of very high quality. Opportunistic pathogens (*Legionella* spp.) were not present in the source drinking water, and the water was microbiologically stable (AOC ≤ 2 µg-C/L). These non-chlorinated drinking water distribution systems have their distinctive micro-environments, where the biological stability of drinking water is maintained by limiting nutrient concentrations [29–33]. Regarding the temperature-sensitive opportunistic pathogens, under the conditions applied ($T_{max}$ of 25 °C and 30 °C) and the non-chlorinated feed water used, cold recovery does not pose a health risk.



The $T_{max}$ after cold recovery also depends on the allowed temperature of the drinking water at the customer's tap in the Netherlands, which is currently 25 °C [34]. However, it is known that the drinking water temperature during transport will balance towards the soil temperature, which is mostly below 25 °C [35], so a $T_{max}$ above 25 °C after cold recovery may be possible without breaching the standard of drinking water temperature at the tap. This means that when the water temperature is being raised for cold recovery purposes, a limit should be set to stay within the temperature threshold of 25 °C at the end users' tap.

More research is required regarding environmental assessment of thermal energy recovery systems, and especially regarding cold recovery from DWDNs and the links between its potential energy, maximum temperature limit and temperature at customers' tap after recovering cold. Hence, the objectives of the current study were (1) to determine the maximum time period within the year to recover cold, related to the drinking water temperature limit after cold recovery ($T_{max}$) and the temperature of incoming drinking water; (2) to evaluate the amount of potential thermal energy and the subsequent carbon footprint savings by recovering cold from drinking water distribution

systems; and (3) to determine the effect of balancing of the drinking water temperature with the soil temperature during transport of the drinking water after cold recovery.

## 1.2 Methodology

For this study, the operational parameters, such as inlet feed water temperature, flow rate, outgoing water temperature after cold recovery, soil temperature and pipe material, of a full-scale cold recovery (TED) plant of Sanquin-Waternet in Amsterdam were used [15]. Based on the results of the previous pilot scale studies [12,24], where no negative effects of cold recovery were observed on the microbial drinking water quality with exit temperatures (after leaving the heat exchanger) up to 30 °C, four values of $T_{max}$ were chosen for this study, 15, 20, 25 and 30 °C, respectively (defined as a threshold for cold recovery). The value of 15 °C is the one currently allowed in the full-scale operational system.

This was done to (1) determine the time span of the year over, which thermal energy in the form of cold can be retrieved, (2) calculate the total amount of retrievable energy and (3) predict the drinking water temperature of water flowing through the mains after cold recovery. The description of the full-scale system is provided in the supplementary information.

### 1.2.1 Cold Recovery Time Period

The incoming feed water temperature ($T_{feed\ water}$), together with the acceptable drinking water temperature after cold recovery ($T_{max}$), was used to determine the time period of the year over which cold can be retrieved. The daily $T_{feed\ water}$ data were collected for the period of January 2018 to December 2019 from the temperature sensors located at the inlet of the Sanquin-Waternet TED unit. The $T_{max}$ values were set at 15, 20, 25 and 30 °C. The viable time period was that in which $T_{feed\ water}$ was at least 1 °C lower than $T_{max}$.

### 1.2.2 Cold Recovery and Carbon Footprint Reduction Potential

Cold recovery potential depends on the available drinking water flow ($F_{feed\ water}$) and the temperature difference ($\Delta T$) between incoming drinking water ($T_{feed\ water}$) and drinking water after the TED installation ($T_{max}$). The maximum theoretical potential is thus directly related to the $T_{max}$. The formulas used to calculate the maximum energy were the following:

Formula for the cooling power (kW)

$$P(cooling) = Q \cdot c_p \cdot \Delta T \qquad (i)$$

Formula for the retrieved energy

$$E = P \cdot \Delta t \qquad (ii)$$

where:
$P$: cooling power (kW);
$Q$: massflow rate of drinking water going through the heat exchanger (kg/s);
$c_p$: heat capacity of water (kJ/kg/K);
$\Delta T$: temperature difference between water before and after the heat exchanger (K);
$E$: energy recovered during a certain period $\Delta t$ (kWh);
$\Delta t$: period in which the energy is recovered (h).

The potential greenhouse gas (GHG) emission reduction from TED was calculated based on the difference between the electricity usage of a TED installation and that of other cooling methods (Table 6.1), multiplied by the GHG factor for the Dutch electricity mix, which is equivalent to 0.475 kg $CO_2$/kWh [36]. For this study, other carbon emissions like $CO_2$ intensive flows (for instance, from chemical substances used in cooling towers) or the $CO_2$ of the materials comprised in the installations were not considered.

$$CO_2\ savings = \left(\frac{1}{COP_{ref}} - \frac{1}{COP_{TED}}\right) \cdot GHG_{el} \cdot \frac{1}{0.0036} \qquad (iii)$$

where:
$CO_2$ savings: GHG potential reduction of TED system (kg $CO_2$/GJ cooling);
$COP_{ref}$: coefficient of performance of the reference cooling method (GJ cooling/GJ electricity);
$COP_{TED}$: coefficient of performance of TED (GJ cooling/GJ electricity);
$GHG_{el}$: $CO_2$ emission factor of electricity (kg $CO_2$/kWh electricity);
1/0.0036: conversion factor between kWh and GJ.



*Table 6.1. Seasonal COP for different cooling methods [37].*

| Cooling Method | Coefficient of Performance (COP) |
|---|---|
| Cooling tower | 80 |
| Dry cooler | 20 |
| Hybrid cooler | 35 |
| Chiller | 7 |
| TED | 100 |

### 1.2.3 Temperature Model

To determine the distance at which the temperature reaches soil temperature, the temperature change after the cold recovery unit was predicted using a temperature model [35]. The network configuration of the Sanquin full-scale system was used to build a hydraulic model (Figure 6.2) in EPANET 2.0, which is a free software package for water distribution network modeling [38]. In the Sanquin system, a portion of the drinking water coming from a 700 mm transport main is being bypassed through a 250 mm pipe towards the heat exchanger unit (HE). After cold recovery, water is being conveyed through a 250 mm pipe to the mixing point (point 4 in Figure 6.2), at which two water streams, one coming from the HE and the other one from the transport main, of different temperatures are mixed. Mixed water is being further transported to a water demand reservoir, which

is located ~3850 m downstream of the mixing point (Figure S 6.1 Supplementary Information). Drinking water temperatures were measured using sensors, which were placed: before the bypass, after the heat exchange process, at the mixing point and before the demand point (point 12 in Figure 6.2).

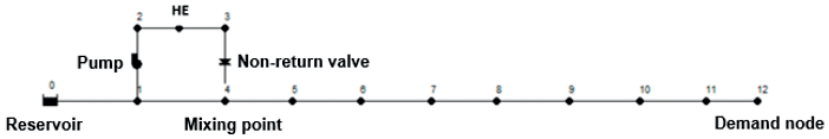


**Figure 6.2.** *Sanquin full-scale model in EPANET. 0—inlet point/reservoir, 1—4 bypass to the Heat exchanger, HE—heat exchanger, 4—mixing point, 5–11 fictitious points, the mixing point (4), and demand node (12) used to assign measured diurnal flow. The distance between the fictitious points is 500 m, except for the distance between fictitious points 11 and 12, which is 350 m.*

$$\frac{dT_{water}}{dt} = \frac{2k}{p_{water}\, rCp, water} (Touter\ wall - Twater) \qquad (iv)$$

Hydraulics within the full-scale Sanquin system was simulated by EPANET 2.0, while an extension to EPANET, multispecies extension, was employed to implement the temperature model equations, shown below.

where $T_{water}$ represents the bulk water temperature (K), $T_{outer\ wall}$ stands for the temperature of the outer wall of the pipe (K), which is assumed to be equal to the temperature of the surrounding soil, $r$ is the pipe radius, $C_{p,water}$ is the heat capacity of water and $k$ is the overall heat transfer coefficient (W/m$^2$ K). The calculation of the overall heat transfer coefficient is further explained in the study of Blokker et al. (2013) [35].

Because the HE unit at the Sanquin plant was operational only during winter days, temperature dynamics in the system were modeled using input parameters for a random winter day. Apart from the $T_{max}$ values (15, 20, 25 and 30 °C), also a reference case ($T_{reference}$) was modeled. This is the water transport main of 700 mm without any HE unit or bypass and transporting water towards the same reservoir at ~3850 m downstream the Sanquin location. On the day that was used for the modeling purposes, $T_{reference}$ was measured to be 11.5 °C. Water flow in the 700 mm main varied between 840 and 940 m$^3$/h, and the flow in the bypass was between 310 and 315 m$^3$/h. A summary of additional input parameters can be found in the supplemental material (Table S 6.1 in Supplementary Information).

## 1.3 Results

### 1.3.1. Operational Period of TED

The daily temperature of the feed water ($T_{feed\ water}$) in the years 2018–2019 is shown in Figure 6.3a. The average daily feed water temperature in the months of January–April was 8 ± 2 °C, in May–August and September–October the temperature remained between 16 ± 2 °C and 12 ± 2 °C, respectively, for both years. Overall, the temperature in the period January–August in the year

2019 was 1 °C higher compared to the year 2018. The average ΔT that can be achieved in specific periods in the year while recovering cold is summarized in Table 6.2. It ranged from 1.8 and 2.1 °C with a $T_{max}$ of 15 °C in the period May–Aug in 2018 and 2019, to 21.2 and 20.4 °C with a $T_{max}$ of 30 °C in the period Jan–April in 2018 and 2019.

Further, in Figure 6.3b, the possible number of days in a year are shown for recovering the cold from drinking water (TED). The results show that with higher $T_{max,}$ the cold recovery period is longer. Compared to 143–193 days of cold recovery for $T_{max}$ of 15 °C, the cold can be recovered throughout the year (354–365 days) with up to 5–15 °C temperature increase when the $T_{max}$ is set at 20, 25 or 30 °C.

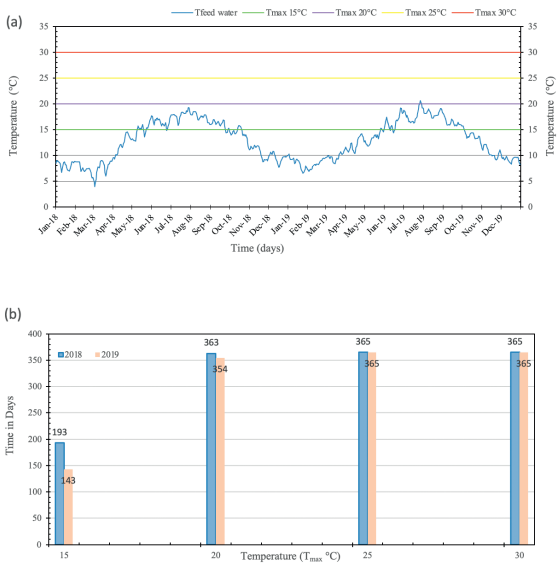


**Figure 6.3.** *(a) Daily temperature over the period of two years (2018–2019) and (b) potential cold recovery time period (total days in a year) based on maximum temperature ($T_{max}$) of 15, 20, 25 and 30 °C after the heat exchanger.*

*Table 6.2. Average seasonal feed water temperature measured over the period of two years and relevant ΔT based on maximum theoretical temperature ($T_{max}$) of 15, 20, 25 and 30 °C after the heat exchanger.*

| Year | Months | Average $T_{feed\,water}$ (°C) ± S.D | $T_{max}$ 15 °C ΔT (°C) ± S.D | $T_{max}$ 20 °C ΔT (°C) ± S.D | $T_{max}$ 25 °C ΔT (°C) ± S.D | $T_{max}$ 30 °C ΔT (°C) ± S.D |
|---|---|---|---|---|---|---|
| | Jan–Apr | 8.8 ± 2.2 | 6.4 ± 2.1 | 11.1 ± 2.3 | 16.1 ± 2.3 | 21.2 ± 2.3 |
| 2018 | May–Aug | 16.6 ± 1.49 | 1.8 ± 1.1 | 3.4 ± 1.5 | 8.3 ± 1.5 | 13.3 ± 1.5 |
| | Sep–Dec | 12.5 ± 2.8 | 4.5 ± 2.1 | 7.4 ± 2.8 | 12.4 ± 2.8 | 17.4 ± 2.8 |
| | Jan–Apr | 9.6 ± 1.8 | 5.4 ± 1.8 | 10.4 ± 1.8 | 15.4 ± 1.8 | 20.4 ± 1.8 |
| 2019 | May–Aug | 16.5 ± 2.3 | 2.1 ± 0.7 | 3.8 ± 2.1 | 8.5 ± 2.2 | 13.5 ± 2.2 |
| | Sep–Dec | 12.5 ± 2.9 | 4.3 ± 1.7 | 7.5 ± 2.9 | 12.5 ± 2.9 | 17.5 ± 2.9 |

### 1.3.2. Theoretical Energy Potential of TED

The retrievable energy from the drinking water can be increased by raising the maximum allowed temperature after cold recovery and the flow rate through the heat exchanger. The thermal energy for cooling that can be recovered is presented in Figure 6.4. This is calculated based on the feed water temperatures in the years 2018 and 2019 and the $T_{max}$ of 15, 20, 25 and 30 °C, which determines the operational period of the heat exchange process. The maximum energy that can be retrieved from the drinking water with flow rates between 150 and 1000 $m^3/h$ ranges from 14 to 630 TJ/year, depending on the $T_{max}$ after cold recovery. By raising the $T_{max}$ from 15 to 20, 25 and 30 °C, the recovered energy for cooling can be increased by 250, 425 and 600%, respectively (Figure 6.4). For this theoretical cooling recovery potential to be applicable, it is required that enough cooling demand is available at such temperature levels.

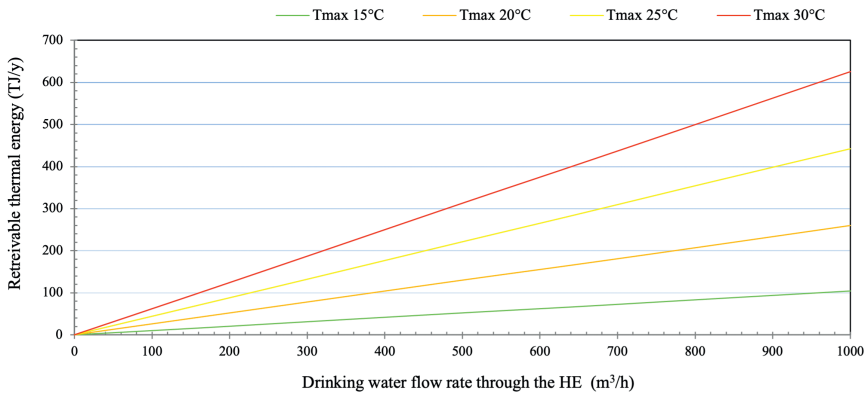


**Figure 6.4.** *Cold recovery potential from drinking water as a function of the drinking water temperature after cold recovery ($T_{max}$) and the drinking water flow rate through the heat exchanger ($m^3/h$).*

This energy recovery from TED, for cooling purposes, will result in the reduction of greenhouse gas (GHG) emissions by avoiding the $CO_2$ emissions when using traditional cooling processes. Table 6.3 shows the results of the GHG emission calculations in $CO_2$-equivalents. Since the latter is based on electricity consumption only, the $CO_2$ savings are linearly related to the difference in COP of the different cooling methods. Further, Table 6.4 shows the same results for a full-scale installation (our case study Sanquin) at an operating flow through the heat exchanger of 250 $m^3/h$ and for $T_{max}$ of 15, 20, 25 and 30 °C. These results show that if the Sanquin system becomes operational throughout the year by gaining the $T_{max}$ of 25 to 30 °C, it can save more than 600% $CO_2$ emissions compared to its current capacity of savings at a $T_{max}$ of 15 °C, 473 ton $CO_2$/y.

*Table 6.3. $CO_2$ emission of different cooling methods and relative $CO_2$ savings of the TED system compared to each method.*

| Cooling Method | COP | $CO_2$ Emission (kg $CO_2$/GJ) | $CO_2$ Savings of TED in Comparison (kg $CO_2$/GJ) | $CO_2$ Savings of TED in Comparison (%) |
|---|---|---|---|---|
| Cooling tower | 80 | 1.6 | 0.3 | 20% |
| Dry cooler | 20 | 6.6 | 5.3 | 80% |
| Hybrid cooler | 35 | 3.8 | 2.5 | 65% |
| Chiller | 7 | 18.8 | 17.5 | 93% |
| TED | 100 | 1.3 | - | - |

*Table 6.4. Potential $CO_2$ reduction of a full-scale (250 $m^3$/h) TED system compared to the other traditional cooling methods.*

| TED System | | Savings $CO_2$ Emission Compared to Alternative Cooling Method (ton $CO_2$/y) | | | |
|---|---|---|---|---|---|
| $T_{max}$ (°C) | Energy Recovered (TJ/y) | Cooling Tower | Dry Cooler | Hybrid Cooler | Chiller |
| 15 | 27 | 9 | 143 | 66 | 473 |
| 20 | 56 | 18 | 296 | 137 | 982 |
| 25 | 113 | 37 | 596 | 277 | 1981 |
| 30 | 157 | 52 | 829 | 385 | 2752 |



### 1.3.3. Effect of Cooling Down Drinking Water during Transport after TED

Based on the flow of the incoming feed water and water flow through the bypass, inlet feed water temperature, pipe material and soil temperature (Table S6.1 Supplementary information) from the Sanquin full-scale system, the drinking water temperature after cold recovery in the water main was modeled (Figure 6.5).

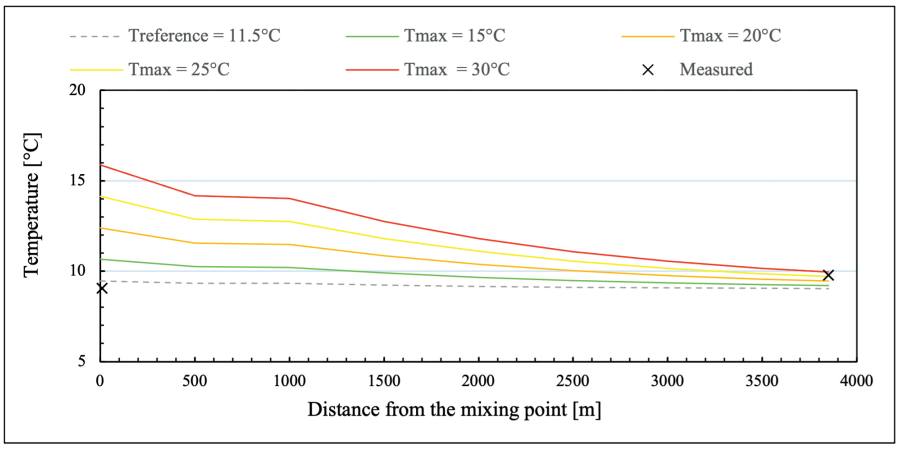


**Figure 6.5.** *Measured drinking water temperature at the mixing point 4 (Figure 6.2) and at point 12 (Figure 6.2), and modeled temperature during transport from mixing point to reservoir entrance.*

Figure 6.5 presents the temperature profile starting from the point where the water, after having passed the heat exchanger in the bypass, is mixed with the cold feed water that is coming from the main transport line, as shown in Figure 6.2 and in Figure S6.1 (Supplementary Information).

The model prediction showed that the water temperature at the mixing point decreased with 2, 4.3, 7.6, 10.9 and 14.1 °C at a $T_{max}$ after the HE of 15, 20, 25 and 30 °C, respectively (Figure 6.5). The temperature at the mixing point was 1.3, 3.0, 4.7 and 6.4 °C above the reference temperature (measured) at the mixing point for $T_{max}$ of 15, 20, 25 and 30 °C, respectively. After a travel distance of 3850 m (to the inlet of the reservoir), the water temperature further decreased by 0.4, 1.5, 3, 4.5 and 6 °C for $T_{max}$ of 15, 20, 25 and 30 °C, respectively. Despite the differences in $T_{max}$, it can be observed that after 3850 m distance, the drinking water temperature in the main approaches the reference temperature, close to the assumed soil temperature of 9 °C.

## 1.4 Discussion

### 1.4.1. Potential Energy and Cooling Down of Drinking Water after Cold Recovery

The cold recovery from drinking water distribution networks (DWDNs) has not been studied broadly in terms of the total amount of available energy and temperature of the drinking water within distribution networks after recovering cold. At the moment, there is only one full-scale system (Sanquin in Amsterdam), where cold is recovered from a DWDN by setting the $T_{max}$ at 15 °C [15] and the retrieved energy equals 30.000 GJ/year [37]. This study revealed that by increasing the $T_{max}$ from 15 to 20, 25 and 30 °C, the time span in which cold can be recovered would be longer (Figure 6.3b), and the retrievable energy at any given moment would be higher due to a higher $\Delta T$ (Figure 6.4). Moreover, a longer recovery period could mean that, for a given continuous cooling demand throughout the year, more recovered thermal energy can be used for cooling directly, allowing for a smaller ATES system.

In addition, the climate change predictions, including more extreme weather conditions (higher temperatures in summer, leading to increase in surface water and soil temperatures and thus higher drinking water temperatures) in upcoming years [13], point at the fact that limiting the $T_{max}$ to 15 °C will not be sustainable both in terms of energy recovery and economics. In addition, the drinking water temperature within the transport mains is affected by the temperature of the subsurface soil, which in turn is influenced by increasing air temperatures [39,40]. With an increasing drinking water temperature, maintaining the $T_{max}$ at 15 °C will reduce the amount of retrievable energy. This increase in temperature stresses the need to set the maximum temperature limit for TED systems higher than 15 °C.

On the other hand, the $T_{max}$ is limited by the effects on the microbiological quality of drinking water and the standard for the drinking water temperature at the customer's tap (25 °C). The former has been already described, and temperatures up to 30 °C have shown no negative impact [12,24]. However, this is specifically the case for non-chlorinated DWDSs with microbiologically stable water and the absence of temperature-sensitive opportunistic pathogens, such as *Legionella* spp.

in the drinking water before cold recovery. With respect to the temperature at the customer's tap, the temperature model (Figure 6.5) predicted that within a distance of 3.8 km, the temperature of the drinking water after $T_{max}$ of 15, 20, 25 and 30 °C resembles the temperature of the surrounding sub-surface soil. Apart from this, various other factors may affect the drinking water temperature in the mains, like heat waves in summer periods, the presence of ATES systems in the subsurface (for district heating/cooling) within the vicinity of the water mains and lastly, the depth of the water mains within the soil (in the Netherlands water pipes are located 1–1.5 m beneath the surface) [39]. It is also important to point out that, for simplification purposes, the burial depth of pipes was assumed to be 1 m beneath the ground surface. Moreover, the soil temperature around the pipes was assumed to be constant throughout the day, and no influence of soil moisture on thermal soil properties was considered. As reported by Blokker et al. (2013) [35], these assumptions may cause a deviation of up to 2 °C between predicted and measured temperatures. Given that one of our objectives was to determine the distance at which the temperature reaches soil temperature after increasing the $T_{max}$ to 20, 25 and 30 °C, the deviation between predicted and measured temperatures of 0.4–0.6 °C is considered to be insignificant.

Furthermore, by increasing the $T_{max}$ to 20, 25 and 30 °C, higher $\Delta T$ and longer periods for energy recovery can be achieved, which results in more cooling capacity on one hand, and a smaller ATES to overcome the period in which $T_{max}$ would be exceeded, and no energy can be recovered, on the other. However, still, it is important to do a case-to-case based extensive environmental and economic assessment before choosing the location of TED systems, to avoid breach of microbial water safety and exceeding the temperature standard at taps (as some transport distance is needed to balance the drinking water temperature with the soil temperature), as well as to match the locations of cold availability and cooling requirements, to make these systems more sustainable and financially viable on the long run.



### 1.4.2. TED as an Innovative and Sustainable Cooling Source

Thermal energy recovered from drinking water for cooling can be used to provide either free cooling (i.e., without using chillers to upgrade the quality of the cooling) or if drinking water is not cold enough to provide the full load and quality of cooling needed, can be used as a pre coolant (for instance, in series with a compression cooling machine) or act as a condensing fluid in chillers to produce higher quality cold with a better chiller COP (coefficient of performance) [25]. The latter will both reduce the energy use of the chiller and requires a smaller electricity connection, which can in some cases be a limiting factor.

Based on the considered drinking water temperature profiles in Amsterdam (for the years 2018–2019), cooling can be recovered from drinking water (TED) throughout the year by setting the $T_{max} \geq 20$ °C (Figure 6.3b).

Free cooling from drinking water is a relatively energy-efficient cooling method. Electricity is only required for the pump, which extracts the water from the drinking water mains and pumps it to the heat exchanger. The required electrical power will, therefore, depend on the size and shape of the

heat exchanger (proportionally with the pressure drop), together with the efficiency of the pump. The achieved cooling power will be, for a heat exchanger of a given shape and running flow rates, proportional to the average temperature difference between hot and cold fluid (LMTD, Logarithmic Medium-Temperature Difference), and therefore, to the efficiency of the heat exchanger. While the exact COP of such systems will thus be dependent on specific conditions, in the examined full-scale installation at Sanquin, it was assessed that such COPs range between 40 and 100 [37].

In any case, the TED system can be installed to (partly) replace less sustainable cooling methods; these can either be too energy-intensive methods (chillers) [19] or possibly methods with intense water spillage (i.e., wet cooling towers) [17,18]. For example, if a TED system replaces fully or partly the cooling provided by a wet cooling tower, electrical energy may be saved (depending on the atmospheric conditions related to the temperature of drinking water; under particularly cold atmospheric temperatures, wet cooling can reach comparably high COPs too [41,42]), and make-up water and the chemicals used to treat the circulating water will be spared. Moreover, the temperature approach (the difference between the exit temperature of the hot fluid and the entry temperature of the cold fluid) for a liquid-to-liquid heat exchanger is in the range of 1 to 2 °C. This means that, for equal drinking water and (wet bulb) outside temperatures, a TED system will be more efficient compared to cooling towers, which have a temperature approach of 4 to 8 °C [19]. If a TED system replaces (fully or partly) the cooling provided by a chiller, energy will for sure be saved (because the COPs of these systems are always by orders of magnitude different, typically ranging between 2.40 and 6.39 [42]).

The exact sustainability gain from TED will depend on the reference situation. To determine the overall sustainability gains from TED, modeling could be done by taking into account the atmospheric conditions (and thus the operation performance of systems operating with outside air), varying cooling loads in time and the temperature of the available drinking water for the cooling [43]. Further, to assess the total environmental benefits of TED systems in addition to $CO_2$ footprint reduction, a life cycle analysis (LCA) should be performed. This takes into account all environmental effects and also includes the construction of the equipment and the yearly material flows [44,45].

### 1.4.3. Practical Implications

Based on this study, it is suggested to install TED units on large flow transport pipes (flow > 250 $m^3/h$) either near the drinking water treatment plant or before the reservoirs. First, the availability of higher flows will linearly increase the retrievable energy. Second, energy recovery close to the drinking water treatment plant or just before the reservoir will have less impact on the water temperature at the customers' tap due to the longer transport distances or longer residence time in the reservoir, which gives time to balance the elevated temperature after the energy recovery to the soil temperature. Third, the larger TED systems with higher flows will become environmentally and economically beneficial because of the higher $CO_2$ emission reductions and because of the economies of scale, reducing the (relative) investment costs for TED installations [37]. Further, where the TED units are not providing direct cooling in winter and are used for storing the cold (for

providing space cooling in summer) or charging the ATES (for underground heat and cold balance), these must be coupled with existing heating/cooling grids (ATES systems) to save the cost further.

The cold recovery potential in this study was calculated based on the days in which the temperature of drinking water is lower than the maximum temperature allowed at the exit of the heat exchanger. It is thus purely theoretical. In practice, operators may want to leave a safety margin (in Sanquin's case, it is 1 °C), and thus, if $T_{max}$ is 15 °C, the cold recovery will not start if drinking water is warmer than 14 °C.

## 1.5. Conclusion

This study examined thermal energy recovery from drinking water in a non-chlorinated drinking water distribution system with a focus on maximizing the recovered energy for cooling purposes. The conclusions are:

- Higher water flows and higher $T_{max}$ (water temperature limit after cold recovery) will allow more energy recovery from drinking water for cooling purposes. In the Sanquin case, increasing $T_{max}$ from 15 °C to 30 °C resulted in an increase in energy recovery from 27 TJ/y to 157 TJ/y.
- The drinking water temperature of the water after cold recovery with $T_{max}$ of 15, 20, 25 and 30 °C will resemble the soil temperature within a distance of approximately 4 km. This means that cold recovery from drinking water hardly affects the temperature of the drinking water at the customers' tap.
- Thermal energy recovered from drinking water, for cooling purposes, can either be used for free cooling or for enhancing the performance and efficiency of cooling units (either used as a pre-coolant in compression cooling machines or as a condensing fluid in chillers).
- TED systems having a higher coefficient of performance (COP) results in a reduction of greenhouse gas emissions by more than 90%, compared to traditional cooling methods, such as chillers, dry coolers, hybrid cooler and cooling towers.

## Nomenclature

| | |
|---|---|
| DWDNs | Drinking water distribution networks |
| DWDSs | Drinking water distribution systems |
| TED | Thermal energy recovery from drinking water |
| ATES | Aquifer thermal energy storage |
| $T_{max}$ | Maximum temperature standard after cold recovery |
| GHG | Greenhouse gas |
| AOC | Assimilable organic carbon |
| $T_{feed\ water}$ | Incoming feed water temperature |
| $\Delta T$ | Temperature difference between $T_{feed\ water}$ and $T_{max}$ |
| COP | Coefficient of performance |
| HE | Heat exchanger |
| $T_{reference}$ | Reference temperature pipeline |
| ATP | Adenosine triphosphate |

## References


1. Li, W.W.; Yu, H.Q.; Rittmann, B.E. Chemistry: Reuse water pollutants. *Nature* **2015**, *528*, 29–31, doi:10.1038/528029a.
2. van der Hoek, J.P.; de Fooij, H.; Struker, A. Wastewater as a resource: Strategies to recover resources from Amsterdam's wastewater. *Resour. Conserv. Recycl.* **2016**, *113*, 53–64, doi:10.1016/j.resconrec.2016.05.012.
3. Wang, X.; McCarty, P.L.; Liu, J.; Ren, N.-Q.; Lee, D.-J.; Yu, H.-Q.; Qian, Y.; Qu, J. Probabilistic evaluation of integrating resource recovery into wastewater treatment to improve environmental sustainability. *Proc. Natl. Acad. Sci. USA* **2015**, *112*, 1630, doi:10.1073/pnas.1410715112.
4. Schetters, M.J.A.; van der Hoek, J.P.; Kramer, O.J.I.; Kors, L.J.; Palmen, L.J.; Hofs, B.; Koppers, H. Circular economy in drinking water treatment: Reuse of ground pellets as seeding material in the pellet softening process. *Water Sci. Technol.* **2014**, *71*, 479–486, doi:10.2166/wst.2014.494.
5. Elías-Maxil, J.A.; Hofman, J.; Wols, B.; Clemens, F.; van der Hoek, J.P.; Rietveld, L. Development and performance of a parsimonious model to estimate temperature in sewer networks. *Urban Water J.* **2017**, *14*, 829–838, doi:10.1080/1573062X.2016.1276811.
6. Kehrein, P.; van Loosdrecht, M.; Osseweijer, P.; Garfí, M.; Dewulf, J.; Posada, J. A critical review of resource recovery from municipal wastewater treatment plants—Market supply potentials, technologies and bottlenecks. *Environ. Sci. Water Res. Technol.* **2020**, *6*, 877–910, doi:10.1039/C9EW00905A.
7. Diaz-Elsayed, N.; Rezaei, N.; Ndiaye, A.; Zhang, Q. Trends in the environmental and economic sustainability of wastewater-based resource recovery: A review. *J. Clean. Prod.* **2020**, *265*, 121598, doi:10.1016/j.jclepro.2020.121598.
8. van der Hoek, J.P. Climate change mitigation by recovery of energy from the water cycle: A new challenge for water management. *Water Sci. Technol.* **2012**, *65*, 135–141, doi:10.2166/wst.2011.820.
9. van der Hoek, J.P.; Mol, S.; Janse, T.; Klaversma, E.; Kappelhof, J. Selection and prioritization of mitigation measures to realize climate neutral operation of a water cycle company. *J. Water Clim. Chang.* **2015**, *7*, 29–38, doi:10.2166/wcc.2015.026.
10. Lam, K.L.; van der Hoek, J.P. Low-Carbon Urban Water Systems: Opportunities beyond Water and Wastewater Utilities? *Environ. Sci. Technol.* **2020**, *54*, 14854–14861, doi:10.1021/acs.est.0c05385.
11. Deng, Z.; Mol, S.; van der Hoek, J.P. Shower heat exchanger: Reuse of energy from heated drinking water for CO2 reduction. Drink. *Water Eng. Sci.* **2016**, *9*, 1–8, doi:10.5194/dwes-9-1-2016.
12. Ahmad, J.I.; Liu, G.; Van der Wielen, P.W.J.J.; Medema, G.; Van der Hoek, J.P. Effects of cold recovery technology on the microbial drinking water quality in unchlorinated distribution systems. *Environ. Res.* **2020**, *183*, 109175, doi:10.1016/j.envres.2020.109175.
13. Stocker, T.; Qin, D.; Plattner, G.; Tignor, M.; Allen, S.; Boschung, J.; Nauels, A.; Xia, Y. IPCC, 2013: Summary for policymakers in climate change 2013: The physical science basis, contribution of working group I to the fifth assessment report of the intergovernmental panel on climate change. *Cambridge University Press Cambridge,* **2013**, doi:10.1017/CBO9781107415324.004
14. Adnot, J. *Energy Efficiency and Certification of Central Air Conditioners (EECCAC)*; Armines: Paris, France, 2003.
15. Van der Hoek, J.P.; Mol, S.; Giorgi, S.; Ahmad, J.I.; Liu, G.; Medema, G. Energy recovery from the water cycle: Thermal energy from drinking water. *Energy* **2018**, *162*, 977–987, doi:10.1016/j.energy.2018.08.097.
16. Mol, S.; Kornman, J.; Kerpershoek, A.; Van Der Helm, A. Opportunities for public water utilities in the market of energy from water. *Water Sci. Technol.* **2011**, *63*, 2909–2915.
17. Kubba, S. Chapter Nine—Impact of Energy and Atmosphere. In *Handbook of Green Building Design and Construction*, 2nd ed.; Kubba, S., Ed.; Butterworth-Heinemann, 50 Hampshire Street, 5th Floor, Cambridge, MA 02139, United States: 2017; pp. 443–571.

18. Wei, X.; Li, N.; Peng, J.; Cheng, J.; Hu, J.; Wang, M. Performance Analyses of Counter-Flow Closed Wet Cooling Towers Based on a Simplified Calculation Method. *Energies* **2017**, *10*, 282, doi:10.3390/en10030282.
19. Chiang, C.-Y.; Yang, R.; Yang, K.-H. The Development and Full-Scale Experimental Validation of an Optimal Water Treatment Solution in Improving Chiller Performances. *Sustainability* **2016**, *8*, 615, doi:10.3390/su8070615.
20. van der Hoek, J.P. Towards a climate neutral water cycle. *J. Water Clim. Chang.* **2012**, *3*, 163–170.
21. Blokker, E.J.M.; van Osch, A.M.; Hogeveen, R.; Mudde, C. Thermal energy from drinking water and cost benefit analysis for an entire city. *J. Water Clim. Chang.* **2013**, *4*, 11–16.
22. van der Hoek, J.P.; Mol, S.; Ahmad, J.I.; Liu , G.; Medema, G. Thermal energy recovery from drinking water. In Proceedings of the 10th International Conference on Sustainable Energy and Environmental Protection: Renewable Energy Sources, Bled, Slovenia, 27–30 June 2017; pp. 23–32.
23. van der Wielen, P.W.J.J.; Italiaander, R.; Wullings, B.A.; Heijnen, L.; van der Kooij, D. Opportunistic pathogens in drinking water in the Netherlands. In *Microbial Growth in Drinking-Water Supplies. Problems, Causes, Control and Research Needs*, 1st ed.; van der Kooij, D., van der Wielen, P.W.J.J., Eds.; IWA Publishing: London, UK, 2013; pp. 177–205.
24. Ahmad, J.I.; Dignum, M.; Liu, G.; Medema, G.; van der Hoek, J.P. Changes in biofilm composition and microbial water quality in drinking water distribution systems by temperature increase induced through thermal energy recovery. *Environ. Res.* **2021**, *194*, 110648, doi:10.1016/j.envres.2020.110648.
25. Pellegrini, M.; Bianchini, A. The Innovative Concept of Cold District Heating Networks: A Literature Review. *Energies* **2018**, *11*, 236.
26. Guo, X.; Hendel, M. Urban water networks as an alternative source for district heating and emergency heat-wave cooling. *Energy* **2018**, *145*, 79–87, doi:10.1016/j.energy.2017.12.108.
27. Liu, F.; Tait, S.; Schellart, A.; Mayfield, M.; Boxall, J. Reducing carbon emissions by integrating urban water systems and renewable energy sources at a community scale. *Renew. Sustain. Energy Rev.* **2020**, *123*, 109767, doi:10.1016/j.rser.2020.109767.
28. Zhou, X.; Ahmad, J.I.; van der Hoek, J.P.; Zhang, K. Thermal energy recovery from chlorinated drinking water distribution systems: Effect on chlorine and microbial water and biofilm characteristics. *Environ. Res.* **2020**, *187*, 109655, doi:10.1016/j.envres.2020.109655.
29. Prest, E.I.; Hammes, F.; van Loosdrecht, M.C.M.; Vrouwenvelder, J.S. Biological Stability of Drinking Water: Controlling Factors, Methods, and Challenges. *Front. Microbiol.* **2016**, *7*, 45, doi:10.3389/fmicb.2016.00045.
30. El-Chakhtoura, J.; Prest, E.; Saikaly, P.; Van Loosdrecht, M.; Hammes, F.; Vrouwenvelder, H. Dynamics of bacterial communities before and after distribution in a full-scale drinking water network. *Water Res.* **2015**, *74*, 180–190.
31. Van der Kooij, D. Assimilable organic carbon as an indicator of bacterial regrowth. *J. Am. Water Work. Assoc.* **1992**, *84*, 57–65.
32. Van der Kooij, D.; Van der Wielen, P.W. Microbial growth in drinking-water supplies: Problems, causes, control and research needs. *Water Intell. Online* **2013**, *12*, 9781780400419.
33. Smeets, P.; Medema, G.; Van Dijk, J. The Dutch secret: How to provide safe drinking water without chlorine in the Netherlands. *Drink. Water Eng. Sci.* **2009**, *2*, 1–14.
34. Staatscourant. *Staatscourant (State Journal in Dutch) 2011 Decree of 23 May 2011 Concerning the Regulations for the Production and Distribution of Drinking Water and the Organisation of the Public Drinking Water Supply. 293*; The Hague, The Netherlands, 2011.
35. Blokker, E.J.M.; Pieterse-Quirijns, E.J. Modeling temperature in the drinking water distribution system. *J. Am. Water Works Assoc.* **2013**, *105*, E19–E28, doi:10.5942/jawwa.2013.105.0011.
36. List Emission Factors (Lijst Emissiefactoren). Available online: https://www.co2emissiefactoren.nl/lijst-emissiefactoren/ (accessed on 6 July, 2020).
37. Reinstra, O.; Mark, R.V.d. *Heating and Cooling Demonstration Monitoring, Drinking Water Cooling, Efficiency Upgrade*; D7.3; European Union: Amsterdam, The Netherlands, 2019; p. 65.

38. Rossman, L.A. *Epanet 2 Users Manual*; U.S. Environmental Protection Agency: Washington, DC, USA, 2000.
39. Visser, P.W.; Kooi, H.; Bense, V.; Boerma, E. Impacts of progressive urban expansion on subsurface temperatures in the city of Amsterdam (The Netherlands). *Hydrogeol. J.* **2020**, *28*, 1755–1772, doi:10.1007/s10040-020-02150-w.
40. Agudelo-Vera, C.; Avvedimento, S.; Boxall, J.; Creaco, E.; de Kater, H.; Di Nardo, A.; Djukic, A.; Douterelo, I.; Fish, E.K.; Iglesias Rey, L.P.; et al. Drinking Water Temperature around the Globe: Understanding, Policies, Challenges and Opportunities. *Water* **2020**, *12*, 1049, doi:10.3390/w12041049.
41. Kojok, F.; Fardoun, F.; Younes, R.; Outbib, R. Hybrid cooling systems: A review and an optimized selection scheme. *Renew. Sustain. Energy Rev.* **2016**, *65*, 57–80, doi:10.1016/j.rser.2016.06.092.
42. Yu, F.W.; Chan, K.T.; Sit, R.K.Y.; Yang, J. Review of Standards for Energy Performance of Chiller Systems Serving Commercial Buildings. *Energy Procedia* **2014**, *61*, 2778–2782, doi:10.1016/j.egypro.2014.12.308.
43. Liberati, P.; De Antonellis, S.; Leone, C.; Joppolo, C.M.; Bawa, Y. Indirect Evaporative cooling systems: Modelling and performance analysis. *Energy Procedia* **2017**, *140*, 475–485, doi:10.1016/j.egypro.2017.11.159.
44. Shah, V.P.; Debella, D.C.; Ries, R.J. Life cycle assessment of residential heating and cooling systems in four regions in the United States. *Energy Build.* **2008**, *40*, 503–513, doi:10.1016/j.enbuild.2007.04.004.
45. Sambito, M.; Freni, G. LCA Methodology for the Quantification of the Carbon Footprint of the Integrated Urban Water System. *Water* **2017**, *9*, 395.

CHAPTER 6

# Supplementary Information chapter 6

## Description of the full-scale cold recovery system

Sanquin produces plasma products from blood and has a huge cooling requirement to cool its processes, round the year. It uses cooling from drinking water in cooperation with Waternet, the water utility that supplies drinking water in Amsterdam. The cold is extracted from a 700 mm large transport main of drinking water, operated by Waternet, by using a double walled heat exchanger (HE). The heat transfer area of the HE is 715.5 $m^2$, the flow rate on the cold side (drinking water) is 500 $m^3/h$ and 552 $m^3/h$ on the hot side (65% water and 35% glycol) of the HE. The doubled walled HE is used to prevent the mixing of drinking water with the hot medium[1]. This system has been in operation already for almost 3 years (2017-2020), to recover cold from DWDN, with the set temperature ($T_{max}$) of drinking water up to 15°C after cold recovery. This limit was set by the health inspectorate as precautionary principle, because at the start of the operation, effects on microbial drinking water quality were not yet investigated. The source of this drinking water is surface water and it results into huge variation in drinking water temperature during summer (maximum 21°C) and winter (minimum 4 °C). Hence the cold is only recovered in winter months when temperature of the drinking water remains lower than 15°C, if temperature is above this limit the cold recovery system is not in operation. The position of heat exchanger, temperature and flow sensors is provided in the scheme below.



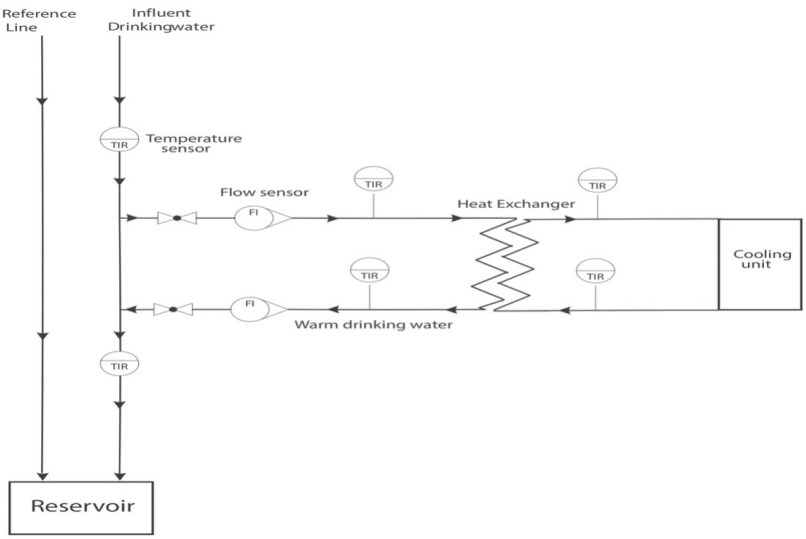


**Figure S6.1:** *Schematic description of Sanquin- full scale cold recovery system in Amsterdam.*

*Table S6.1 Model input parameters*

| Parameter | Symbol | Value | Unit |
|---|---|---|---|
| **Water** | | | |
| Temperature of influent water (measured) | $T_w$ | 7.5 | °C |
| Thermal conductivity at 7.5°C | $\lambda_w$ | 0.584 | $W \cdot m^{-1} \cdot K^{-1}$ |
| Prandtl number at 7.5°C | $Pr_w$ | 9.52 | - |
| Thermal diffusivity 7.5°C | $\alpha$ | $1.42 \times 10^{-7}$ | $m^2 \cdot s^{-1}$ |
| Heat capacity at 7.5°C | $c_{p,water}$ | 4094 | $J \cdot kg^{-1} \cdot K^{-1}$ |
| **Soil** | | | |
| Temperature of the soil* | $T_\infty$ | 9 | °C |
| Thermal conductivity 10°C | $\lambda_s$ | 2.2 | $W \cdot m^{-1} \cdot K^{-1}$ |
| Specific heat of soil 10°C | $c_{p,soil}$ | 1100 | $J \cdot kg^{-1} \cdot K^{-1}$ |
| Thermal expansion coefficient at 10°C | $\beta$ | 0.0035 | $K^{-1}$ |
| Kinematic viscosity at 10°C | $\nu$ | $1.005 \times 10^{-6}$ | $m^2 \cdot s^{-1}$ |
| **Pipes** | | | |
| Pipe wall thickness | $\delta_{wall}$ | 0.1d | m |
| Thermal conductivity of PVC pipes | $\lambda_p$ | 0.19 | $W \cdot m^{-1} \cdot K^{-1}$ |

*- Assumption for the soil temperature is based on the real measurements at the station De Bilt[2] (which was ~9°C on the day used for temperature simulation) and reported difference between temperature in De Bilt and the city of Amsterdam[3](~1°C).


1. van der Hoek, J.P.; Mol, S.; Giorgi, S.; Ahmad, J.I.; Liu, G.; Medema, G. Energy recovery from the water cycle: Thermal energy from drinking water. *Energy* **2018**, *162*, 977-987, doi:https://doi.org/10.1016/j.energy.2018.08.097.
2. KNMI. Ground temperature. Available online: https://www.knmi.nl/nederland-nu/klimatologie/bodemtemperaturen (accessed on 6
3. Visser, P.W.; Kooi, H.; Bense, V.; Boerma, E. Impacts of progressive urban expansion on subsurface temperatures in the city of Amsterdam (The Netherlands). *HYDROGEOLOGY JOURNAL* **2020**.

Chapter 7

# Synthesis

CHAPTER 7

This thesis was initiated with the goal to study the microbiological effects of thermal energy recovery (cold) from drinking water distribution systems (DWDSs). Cold recovery from drinking water will increase the temperature in the drinking water network and hence may change the microbial community, including promoting growth of undesirable micro-organisms, such as *Legionella pneumophila*. Both water and biofilm were extensively investigated for the potential effects of thermal energy recovery from drinking water (TED) on the quantity and community of microbes. In addition, the potential energy recovery and the corresponding reduction in Greenhouse Gas (GHG) emission that can be achieved by TED were determined in a specific case. In the end, the maximum temperature ($T_{max}$) that can be applied without any negative effects on the microbiological water quality under the tested conditions was determined. In this thesis, the focus was on the following four specific research questions:

I.) What are the changes in microbial drinking water quality within unchlorinated DWDSs due to a sudden increase in drinking water temperature after cold recovery?
II.) How does an instantaneous increase in water temperature, as a result of cold recovery, affects the biofilm development within non-chlorinated DWDSs?
III.) How does cold recovery affect the drinking water quality and biofilm development within chlorinated DWDSs?
IV.) What is the maximum allowable temperature ($T_{max}$) after cold recovery, that will not trigger the regrowth or proliferation of opportunistic pathogens within DWDSs with biostable water? And what is the potential of energy recovery and the carbon footprint reductions by recovering cold from drinking water?

To answer these research questions, studies were done at pilot scale unchlorinated and chlorinated DWDSs, which were operated at two locations supplying biostable drinking water in the Netherlands (Delft, AOC ≥ 2 μg C/L; Leiduin, AOC ≤ 2 μg C/L). Two targeted temperatures after cold recovery were studied (25 °C and 30 °C). Based on the experimental study, desk research was conducted to determine the potential of energy recovery and the corresponding reduction in carbon footprints for a specific application.

The detailed results were presented in previous chapters, this chapter is presenting the synthesis of all chapters and the answers to the research questions. The four research questions will be discussed and answered in sections 1.1 to 1.4. Section 1.5 focuses on the effects of AOC concentration on microbiological processes during TED. Section 1.6 discusses the practical implications of TED application for drinking water utilities. Section 1.7 gives a general conclusion and outlook on applying TED in DWDSs.

## 1.1 Effects of TED at 25 °C and 30 °C on water in unchlorinated systems

To answer the first research question, two pilot scale studies were conducted. In the first study, a pilot scale DWDSs with $T_{max}$ of 25 °C after cold recovery was operated for 38 weeks and

compared with two reference systems without cold recovery: one system with a non-operational heat exchanger, and the other system without heat exchanger (chapter 2). The results among three systems showed that cold recovery had no significant effects on the microbial drinking water quality, including cell numbers, ATP concentrations, and the composition and diversity of microbial community. In the TED system with $T_{max}$ of 25 °C, higher relative abundance of *Pseudomonas* spp. and *Chryseobacterium* spp. were observed, but only when the temperature difference (ΔT) caused by TED was higher than 9 °C. It was observed that *Pseudomonas* spp. and *Chryseobacterium* spp. were already present in the feed water, their relative abundance increased only after passing through the TED system because of the high temperature at the heat exchanger surface. This is why monitoring of the (feed) water microbial quality is highly recommended and special attention must be given to the opportunistic pathogens which are more susceptible to changes in the temperature.

In the second pilot study (chapter 3), a $T_{max}$ of 30 °C was investigated for its effects on microbial water quality. A TED system was operated at 25 °C and 30 °C and compared with a reference system with a non-operational heat exchanger, and a control system without any additional equipment. No significant differences were observed in the microbial community composition among effluents of all three systems and the feed water, except the occurrence of the family of *Sphingomonadaceae,* which was observed in the effluent water from all three systems (1–9%), while they were not observed in the feed water (not observed as core OTU or with a relative abundance <1%). The family *Sphingomonadaceae* is relevant to biofilm formation and colonization of bacteria on pipe surface, which possibly caused its presence in the water phase within the pilot scale DWDSs. Chapter 2 and Chapter 3 revealed that the setting of $T_{max}$ after TED at 25 °C and 30 °C does not have significant effects on the microbial quality of drinking water under the conditions tested.



## 1.2 Effects of TED at 25 °C and 30 °C on biofilm in unchlorinated system

To determine the effects and contributions of biofilm on the microbiological quality of water after TED, the effects of TED on biofilm development were investigated. By the end of the 38 weeks' study (one time biofilm sampling), the results obtained for biofilms revealed that TED at 25 °C did lead to a different biofilm with respect to the bacterial quantity and community (chapter 2). In chapter 3, the dynamic of biofilms development were investigated for 32 weeks, with samples taken at 1, 2, 4, 7, 12, 20 and 32 weeks from a TED system (25 °C, 30 °C) and a reference and control system. Quantitatively, similar growth trends were observed for all the systems, but with different timelines, higher temperatures were associated with a faster biofilm development. The biofilm in all systems experienced initial increase of ATP illustrating primary bacterial colonization (e.g. Betaproteobacteriales). Afterwards, there was a decrease of ATP, but increase of relative abundances of some groups (Xanthobacteraceae, Legionellales, Sphingomonadaceae).

It is clear that biofilm is more responsive to TED than the planktonic bacteria in water. The effects of TED ($T_{max}$ 25 °C) on biofilm development was further investigated for a longer period (99 weeks), with the biofilm sampled at 1, 2, 4, 7, 12, 20, 32, 52 and 99 weeks (Chapter 4). As observed

during the 38 weeks' and 32 weeks' study (chapter 2, chapter 3), the 99 weeks' study also found that the early stage of biofilm development was influenced by TED. More specifically, TED induced faster stabilization of biofilm, in terms of biomass activity, at 32-52 weeks compared to reference and control system (52-99 weeks). The curve to reach more even and diverse bacterial community (at week 12) is smooth in TED system compared to a decrease in microbial diversity (week 7) in reference and control system. By 99 weeks, similar bacterial communities were established for all systems regardless of applying TED or not.

When considering the effluent water, it was found that for all systems (TED, reference and control) the formed biofilm (<11weeks) had significant contribution to the bacteria in water (up to 70% according to SourceTracker, Chapter 3). In the same period, higher ATP and high nucleic acid cell numbers were also observed in the effluent compared to the feed water for all systems.

## 1.3 Effects of TED at 25 °C in chlorinated DWDSs

The effects of TED on microbial quality of drinking water and biofilm development were investigated for chlorinated DWDS with an elevated AOC content (50 μg C/L) (chapter 5), which was assessed using the same experimental setup of chapter 2 by dosing chlorine in the influent (0.1 mg $Cl_2$/L). No significant effect was noticed on the chlorine decay by the temperature increase after TED at 25 °C. As observed in unchlorinated systems, the development of biofilm was significantly enhanced by the increased water temperature induced by TED. The diversity and composition of bacterial community within biofilm were shaped by both the elevated temperature and the surface material of heat exchanger. Higher relative abundances of *Pseudomonas* spp. were observed in biofilms formed in the TED system compared to the reference and control systems.

## 1.4 Potential energy recovery and GHG emission reductions as a result of TED application

In this thesis, the extensive microbiological investigations of TED (chapters 2-5) showed that increase in drinking water temperature up to 25 and 30 °C did not affect the microbial drinking water quality. The environmental assessment of TED (chapter 6) showed that a higher $T_{max}$ (temperature limit after cold recovery) will allow recovery of more energy from drinking water for cooling purposes. In this way, the energy can even be recovered throughout the whole year by allowing a $T_{max}$ of 25-30 °C, without having impact on drinking water quality. The temperature modelling study of a full scale TED (chapter 6), operated at $T_{max}$ of 15-30 °C, showed that the drinking water temperature after cold recovery reached to similar temperatures as the surrounding soil temperature after a transport distance of 4 km from the point of the heat exchanger. The results showed that by raising $T_{max}$ from 15 °C to 20, 25 and 30 °C, the retrievable cooling energy and GHG emission reduction could be increased by 250, 425 and 600%, respectively. However, monitoring of the quality of the drinking water is a pre-requisite for TED application within DWDSs to be sure to provide hygienically safe drinking water at customers tap.

## 1.5 TED application and effect of assimilable organic carbon (AOC) within DWDSs

Assimilable organic carbon (AOC) is connected to the regrowth of microbes during drinking water distribution. A maximum level of 10 µg C/L AOC is preferred in order to maintain the biological stability during water distribution (Van der Kooij, 1992), specifically for DWDSs supplying water without a residual disinfectant (as is the case in the Netherlands). In this thesis studies were done at pilot scale unchlorinated DWDSs supplied with two different biostable drinking waters with AOC ≥ 2-10 µg C/L. It was observed that microbiome and biofilm forming potential of both waters were different. It is known that DWDSs with lower AOC have lower biofilm forming potential (Van der Kooij and Van der Wielen, 2013). However, in this thesis the biofilms developed in the DWDSs with higher AOC had less active biomass in terms of ATP and cell counts (chapter 2 and 4) compared to DWDSs with lower AOC in terms of ATP and cell counts (chapter 3). This difference is most possibly observed because of differences in the temperature of the feed water at both locations and seasonal effects on the efficiency of the water treatment methods.

In this research, differences in biofilm development as a result of increased temperature after cold recovery were observed compared to the reference systems. Both for the low (< 2 µg C/L, chapter 3) and higher (> 2 µg C/L, chapter 2 and 4 ) AOC feed waters similar biofilm development curves were observed after TED showing a higher biofilm formation in the beginning followed by stabilization afterwards. Irrespective of the differences in the AOC levels of the incoming feed drinking water, the water quality parameters (ATP, TCC) seems not to be affected by cold recovery at both locations. However, from a global perspective, AOC ≥ 2 10 µg C/L are very low AOC levels. At higher AOC concentrations in feed drinking water, more difference may be expected in the microbial processes after TED.



## 1.6 Practical implications for water utilities

This thesis has extensively studied environmental aspects of TED. Based on the current research, it is concluded that TED is an energy-efficient cooling method. TED could be used as a source of cooling, both as a free cooling (in winters) or to provide partial cooling (by use of ATES) in summer. Application of TED is recommended at a $T_{max}$ of 15-30 °C for unchlorinated and biostable DWDSs. However, more frequent and dedicated microbial drinking water quality monitoring should be done in the first 2-3 months of TED operation, because this study showed initial biofilm formation resulted into frequent changes in community and diversity of microbes within DWDSs. From an economic and sustainability perspective, drinking water utilities should install TED units on large flow transport pipes (flow > 250 $m^3$/h) either near the treatment plant or before the water reservoirs, in order to increase the retrievable energy and to gain higher $CO_2$ emission reductions. In addition, TED application on large flow pipes or before water reservoirs will have less impact on the water temperature at the customers' tap, due to the longer transport distances or longer residence time respectively. In additions, there are no direct household connections to the bigger transport pipes.

## 1.7 General conclusion and future outlook

TED is an innovative and emerging concept and special focus must be given on choosing the location of TED systems, to match the availability of cold (supply) and cooling requirements (demand). If the location of supply and demand do not match, storage and transport of the recovered energy is required which makes the system less attractive. Climate change with shortening the length of the winter period and an overall increase in global air and water temperature could be major concerns for TED. On the other hand, higher air temperatures will increase the demand for space cooling. In addition to cold recovery, the recovery of heat from drinking water is also possible by using the same technology. This may become even more attractive with rising drinking water temperatures: the heat recovery potential increases while after heat recovery the temperature of the drinking water is lower, which offers comfort to the customer and avoids microbial growth in the drinking water transport and distribution system.

With the development of new sanitation concepts, introducing vacuum toilets, rainwater harvesting, and grey water reuse, the drinking water consumption will go down and less drinking water will be transported to the customers. As besides $T_{max}$ also the available volume flow determines the potential of TED (chapter 6), this may limit the effectivity of TED in new urban development projects. Looking at the bigger picture, TED is part of thermal energy recovery from water, including also thermal energy recovery from wastewater and thermal energy recovery from surface water. Taking into account the energy transition and the European Green Deal, focusing on the abandoning of the use of fossil fuel, the combination of these three may be an attractive option: they can feed cooling and heating networks in the urban environment offering a sustainable energy system for heating and cooling purposes, as shown in Figure 7.1.

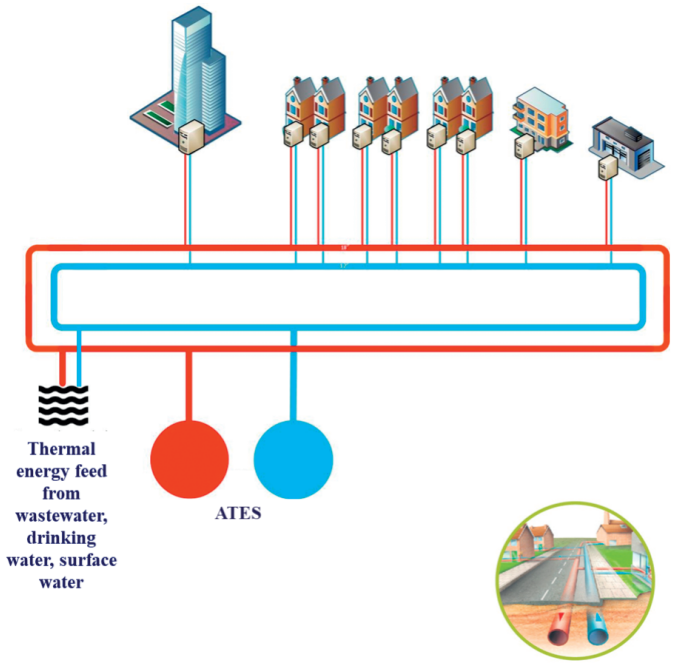


**Figure 7.1.** *A future perspective for aquathermal energy, including TED.*



Based on this thesis, it is recommended to further study the effect of TED on biofilm within DWDSs, from the pipes that are already in operation for a longer time and host mature biofilms. Important topics are how transition to TED will impact the microbial community composition of old biofilms within these DWDSs, and how it may affect the microbial quality of drinking water. There are specific groups of opportunistic pathogens (OPs) that are more sensitive to high temperature and would more likely proliferate after TED or chances of their regrowth will be higher on the surface of the heat exchanger. The OPs were not studied specifically in this research, but it is recommended to study their regrowth and proliferation as a result of TED.

Globally most of the countries are supplying drinking water by maintaining chlorine as a residual disinfectant and there lies an opportunity for the application of TED. For chlorinated DWDSs a preliminary study was done for this thesis. More insight is required in terms of microbiological assessment of TED to further explore the potential within chlorinated systems. Future research is required to study the effects of cold recovery on chlorine decay over longer distances under the influence of high temperature and to study the microbial inactivation efficiency of chlorine within the DWDSs.

## References

van der Kooij, D. (1992) Assimilable organic carbon as an indicator of bacterial regrowth. Journal of American Water Works Association 84(2), 57-65.

van der Kooij, D. and Van der Wielen, P.W. (2013) Microbial growth in drinking-water supplies: problems, causes, control and research needs. Water Intelligence Online 12, 9781780400419.

# Acknowledgements

I would like to express my gratitude to my promotor Prof. Jan Peter van der Hoek for his guidance, encouragement and immense support throughout my research. Apart from a lot of positive feedback and critical review on my research he also supported and understand the fact that I am not only a PhD researcher but also a mother of two daughters. And it was not always possible for me to stick to the deadlines and reaching milestones as had been planned. I really would like to thank him, it was a long journey of seven years and I have learned a lot from him.

I am also thankful to my second Promotor Prof. Gertjan Medema for his critical feedback on my research, Gertjan's comments always helped me to think about my research from a different point of view. It was nice to have him as part of my PhD committee. Many thanks to my co-promotor Prof. Gang liu for his support throughout the first two years. It was a good experience working with him, designing the setups for my lab work and discussions about the sampling.

Apart from my promotors I would like to express my gratitude to Paul van der Wielen from KWR, Marco Dignum and Sara Giorgi from Waternet, Hans Vrouwenvelder from KAUST. They all helped me to design my research and interpret the results. Many thanks to people at TU Deflt Waterlab, without their help setting up a two years lasting 24/7 pilot distribution network was not possible. People at Leiduin Waternet drinking water treatment plant I would like to thank for their help in designing and constructing such a nice setup for my last year of experiments.

Lastly many thanks to all my friends and colleagues at section Sanitary Engineering for their support and encouragement during this research. A lot of thanks to my family back in Pakistan for always listening to my stories of research and their encouragement. I would specially like to thank my husband Shafqat, for tolerating me throughout this period and his unconditional love and support. He was and is always there with me to raise our two beautiful daughters and was encouraging me to complete my experiments on time and offering his support wherever needed. A special thanks to my mother who lets me be who I want to be and what I want to do. A special thanks to my brother Ahtazaz who never stopped me chasing my dreams. A lot of love to my baby sister Siddiqa and my baby brother Afaq for their jokes, love and prayers.

## About the author

Jawairia Imtiaz Ahmad was born in Pakistan on 3rd December 1986. She did her Bachelors in Environmental Sciences from Fatima Jinnah woman university in 2009 and won the silver medal on securing 2nd position in her bachelor studies. She completed her Masters in 2012 from National University of Science and Technology Pakistan and won prestigious President's Gold medal on securing the 1st place in her Master degree. After completing her Master degree, she worked at LEAD (Leadership in Environment and Development) chapter of Pakistan for about one year as a young environment professional. Later in 2013 she joined as Lecturer in Faculty of Meteorology at COMSATS National university, Islamabad, Pakistan. She served there for two years before joining the department Water Management at TU Delft, as a PhD candidate in 2015. During her PhD thesis Jawairia published three first author peer reviewed publications and two co-author publications. She also presented her work globally as speaker at three major international drinking water conferences. Her PhD project "Thermal energy recovery from drinking water: exploitation of a renewable energy source" was selected as Bronze winner of the IWA Project Innovation Award in 2018 under the Category of Performance Improvement and Operational Solutions. From 1st November 2020 Jawairia has started a new position as Program Manager Water at the post academic institute PAOTM, where she is busy developing curriculum for PAOTM Water program by designing new courses, international summer schools and workshops together with Dutch and International partners, such as IWA and CAPTURE-U Ghent, Belgium.

# List of publications

Peer-reviewed publications:

1. Changes in biofilm composition and microbial water quality in drinking water distribution systems by temperature increase induced through thermal energy recovery. **Ahmad, J. I.,** Dignum, M., Liu, G., Medema, G. & van der Hoek, J. P., 2021, In: **Environmental Research**. 194, p. 1-11 11 p., 110648.
2. Maximizing Thermal Energy Recovery from Drinking Water for Cooling Purpose. **Ahmad, J. I.,** Giorgi, S., Zlatanovic, L., Liu, G. & van der Hoek, J. P., 2021, In: **Energies**. 14, 9, p. 1-14 14 p., 2413.
3. Effects of cold recovery technology on the microbial drinking water quality in unchlorinated distribution systems. **Ahmad, J. I.,** Liu, G., van der Wielen, P., Medema, G. & van der Hoek, J. P., 2020, In: **Environmental Research**. 183, 9 p., 109175.
4. Thermal energy recovery from chlorinated drinking water distribution systems: Effect on wchlorine and microbial water and biofilm characteristics. Zhou, X., **Ahmad, J. I.,** van der Hoek, J. P. & Zhang, K., 2020, In: **Environmental Research**. 187, 10 p., 109655.
5. Energy recovery from the water cycle: Thermal energy from drinking water. van der Hoek, J. P., Mol, S., Giorgi, S., **Ahmad, J. I.,** Liu, G. & Medema, G., 1 Nov 2018, In: **Energy**. 162, p. 977-987 11 p.

International conference publications:

1. Drinking water distribution networks: an emerging resource for thermal energy recovery. **Ahmad, J. I.,** Giorgi, S., Zlatanović, L., Liu, G., Medema, G., & van der Hoek, J. P. (2019). Oral presentation at **3rd IWA Resource Recovery Conference**, Venice, Italy.
2. Potential Impacts of Cold Recovery on the Microbial Ecology in Pilot Drinking Water Distribution System. **Ahmad, J. I.,** Liu, G., Medema, G., & van der Hoek, J. P. (2018). Oral presentation at **Water Quality and Technology Conference (WQTC)**, Toronto, Canada.
3. Impacts of cold recovery on the microbial ecology in Drinking Water Distribution Systems: a pilot study. **Ahmad, J. I.**, Liu, G., Medema, G., & van der Hoek, J. P. (2018). Poster presentation at **Biofilms 8 Conference** , Copenhagen , Denmark.